GOVERNMENT OF NEPAL
MINISTRY OF POPULATION AND ENVIRONMENT
DEPARTMENT OF HYDROLOGY AND METEOROLOGY

Final Report:

STUDY OF MAJOR WEATHER EVENTS

Prabhu Engineering consultancy P. Ltd.
Kathmandu, Nepal
June, 2016

Table of Contents

List of Figures: 3
List of Tables: 3
List of Acronyms and Abbreviations 4
ACKNOWLEDGEMENTS 5
1. INTRODUCTION 6
1.1 Background: 6
1.2 Seasons in Nepal: 8
2. LITERATURE REVIEW 10
3. METHODOLOGY 15
3.1 Study Period: 15
3.2 Data collection: 15
3.3 Definition of Major Weather Events: 16
4. RESULT AND DISCUSSION 22
4.1 MWE 1 (July 19): 22
4.2 MWE 2 (August 14 to August 15, 2014): 26
4.3 MWE 3 (11 September,2014): 29
4.4 MWE 4 (14-15 October,2014): 31
4.5 MWE 5 (2-4 January, 2015) 34
4.6 MWE 6 (27 February to March 3) 36
4.7 MWE 7 (March 31) 38
4.8 MWE 8 (May 12): 38
5 CONCLUSION 45
Bibliography 48
ANNEXES 49

List of Figures:

Figure 1: Location map of 15 synoptic stations in Nepal. 15

List of Tables:

Table 1: Human deaths from disasters from 2000 to 2014. 6

Table 2: Hazardous Map with threshold map for RSMC, New Delhi. 11

Table 3 : Details of the 15 synoptic stations. 15

Table 4 : Major Weather Events identified according to the criteria I 19

Table 5 : Major Weather Events identified according to the criteria II 20

Table 6 : Major Weather Events identified for the study. 21

List of Acronyms and Abbreviations

BoB	Bay of Bengal
CAPE	Convective Available Potential Energy
DDG	Deputy Director General
DHM	Department of Hydrology and Meteorology
GPTM or gptm	Geo-potential height in meters
GPM	Global Precipitation Measurement Mission
hpa	Hecto Pascal
ICAO	International Civil Aviation Organization
IMD	India Meteorological Department
JK	Jammu and Kashmir
mb	Milibar
MFD	Meteorological Forecasting Division
mm	Milimeter
MP	Madhya Pradesh
MSLP	Mean Sea level Pressure
MTL	Mid Troposhpheric Level
MWE	Major Weather Events
NMHs	National Meteorological and Hydrological Services
RH	Relative Humidity
RSMC	Regional Sepcialized Meteorological Centre
UP	Uttar Pradesh
UTC	Universal Co-ordinated Time
WMO	World Meteorological Organization

ACKNOWLEDGEMENTS

This study "**STUDY OF MAJOR WEATHER EVENTS"** has been carried out by Prabhu Engineering Consultancy. We would like to thank Department of Hydrology and Meteorology for providing us the valuable opportunity for conducting this research. We wish to express our deepest and most sincere appreciation to respected person, Dr Rishi Ram Sharma, DG, DHM and Dr. Jagadishwor Karmacharya, DDG, DHM, for their co-operation during the study period of this research. Moreover, we would like to thank Ms. Shanti kandel, Mr. Subash Rimal, Mr. Mean Kumar Aryal, Meteorologists, DHM and all the staffs of DHM for their guidance and support.

Prabhu Engineering Consultancy
Baneshwor, Kathmandu

1. INTRODUCTION

1.1 Background:

Nepal is a mountainous country with the Himalayas at its northern boundary, which separates it from China. It is surrounded to the east, south and west by India. Nepal is roughly shaped as a parallelogram having the total area of 147181 sq. km with the east west extension of about 800 km and north south extension of about 200 km. It is located within 26°22' to 30°27' North latitude and 80°40' to 80°12' East longitude. It has large altitudinal variation from 60 m to 8848 m - top of the world (Sagarmatha). The topography of Nepal varies from plain land called Terai in the south to the Himalayan range in the north with numerous folds of mountains and valleys in between. Due to the large altitudinal and topographical variation, the climate of Nepal varies from tropical in the south to alpine type in the north.

Due to the large altitudinal and topographical variations, it is very hard to make site specific and accurate weather forecasts for Nepal. Each year, the hydro-meteorological disasters are responsible for the loss of many lives, live stocks and valuable properties. Such hydro-meteorological disasters are flood, landslides, thunderstorms, gusts, hail, cold waves, heat waves etc. The table below provided by Ministry of Home Affairs shows the deaths of lives due to the fatality of disasters. Flood and landslides is the dominant disaster each year that takes away many lives and properties. Every year more than 100 people lost their lives due to the flood and landslides whereas more than 400 people perished due to the devastating flood and landslide in 2002 alone.

Table 1: Human deaths from disasters from 2000 to 2014.

Human Deaths From Disasters Since 2000 to 2014

Year	Flood & landslide	Thunder-bolt	Fire	Hail-stone	Wind-storm	Avalanche/ snowstorm	Epidemics	Earthquake	Total
2000	173	26	37	1	2	-	141	0	380
2001	196	38	26	1	1	-	154	1	417
2002	441	6	11	0	3	-	0	0	461
2003	232	62	16	0	20	-	0	0	330
2004	131	10	10	0	0	-	0	0	151
2005	141	18	28	0	0	21	41	0	249
2006	141	15	3	1	0	-	34	0	194
2007	216	40	9	18	1	6	0	0	290
2008	134	16	11	0	2	0	3	0	166
2009	135	7	35	0	0	2	10	0	189
2010	240	70	69	0	2	2	462	0	845
2011	263	95	46	2	6	0	36	0	448
2012	123	119	77	0	18	9	9	6	361
2013	219	146	59	NA	3	7	4	0	438
2014	241	96	62	NA	3	38	12	0	452
Total	**3026**	**764**	**499**	**23**	**61**	**85**	**906**	**7**	**5371**

Source: Ministry of Home Affairs

(Source: http://www.drrportal.gov.np/uploads/document/329.pdf)

The various weather events such as heat waves, cold waves, heavy rainfall, extreme temperature, wind gust, etc. could be major weather events depending upon their socio-economic impact. Various weather events have different impact to the public. As it is seen from the above table provided by Ministry of Home affairs that the main hydro-meteorological disaster in Nepal is flood and landslide which takes away more than 100 lives and thousands of properties each year. Flood occurs due to the overflow of water from the water bodies and is caused mainly by heavy rainfall events. Flash flood might occur if heavy rain occurs in short period of time. As rainfall is the main contributor for flood, and the main hydro-meteorological disaster in Nepal is flood and landslides, the major weather events here are identified on the basis of rainfall observed within the synoptic station. If the rainfall monitoring and accurate forecasting could be done with sufficient lead time, the flood forecast could be done with greater lead time and accuracy. This allows for timely dissemination of forecast to affected communities and take preventive measure to save lives and minimize the damage of property and infrastructure. It is very difficult to predict the exact timing and place of the rainfall events, which eventually affect the flood forecast, because of lack of sufficient observation and real time communication, conventional forecasting methods and above all inadequate research endeavors. In this work, atmospheric conditions associated with the heavy rainfall episodes in 2014/2015 are studied. It is anticipated that the findings of the study will be useful for forecasters in predicting the rainfall events, particularly heavy rainfall events, with greater accuracy. This in turn would result in direct societal benefit as improved rainfall forecasts and subsequent improved flood forecast could save many lives and properties in future.

Moreover, different seasons has their own characteristics of the rainfall activities. The same amount of rainfall or snowfall may have different impact in different seasons. Since the total rainfall in monsoon season is almost 80% of the total rainfall amount, the accumulated rainfall is high in monsoon season than in other seasons. Even the form of precipitation in some hilly and Himalaya areas differ with seasons.

The main objective of this study is to articulate the atmospheric conditions and mechanisms associated with major weather events (heavy rainfall events) in Nepal in different seasons. Depending on the weather system and season, different parameters/mechanism might play prominent role for the weather activities. Thus this study will provide us the general idea about the parameters/mechanisms that play important role during different seasons. This study will also help forecasters to anticipate the severity of weather with high level of confidence from the facts revealed by this study.

As dominant mechanism/parameter responsible for major weather event in each season might be distinct, a brief overview of seasons in Nepal is described below.

1.2 Seasons in Nepal:

Nepal has four main seasons. Each season is characterized with different seasonal characteristics, which are described below:

i. **Pre-Monsoon Season (March-May):**

This season starts in March and ends in May. This season is mainly associated with bright sunshine and high temperatures throughout the country with frequent gusty wind and afternoon/evening thundershowers with occasional hail. Thermal convection and instability is the main rain producing mechanism in this season. Westerly wind is dominant at the starting of this season but the south easterly wind is established towards the end of this season. Daily maximum temperature generally attends the annual extreme maximum value in this season. In Terai region of the country, maximum temperature often exceeds 40^0C leading to heat wave condition, which causes deaths of life and live-stocks. In addition, many people loss their life and some people loss their properties due to thunderbolt strike, severe thunderstorms and strong winds.

ii. **Monsoon Season (June- September):**

This season starts in June and ends in September. This season is mainly associated with the monsoon rainfall. The normal monsoon onset date for Nepal is June 10 and the normal monsoon withdrawal date is September 23. Monsoon enters from the eastern region of Nepal and it withdraws from the western part. Many lives and properties are lost each year in this season due to the heavy rainfall causing flood and landslides. Almost 80% of yearly total rainfall occurs in this season. South- easterly wind is dominant in the lower levels with moisture influx mainly from Bay of Bengal. Temperature is relatively high in June, which slowly decreases with the start of monsoon. This season is very important to farmers as well as country's economy as agriculture is mostly rain fade and this is the main rainy season. During the monsoon season, rainfall occurs on majorities of the days over large parts of the country.

iii. Post-Monsoon Season (October- November):

This season starts in October and ends in November. At initial stages, of the season, easterly wind is dominant but at the end of this season, westerly wind becomes dominant. This season is mainly associated with sunny days and bright sunshine. This season is also called harvesting season as farmers harvest paddy planted in the monsoon season. Season wise, this is the most pleasant time in Nepal. Also, main festivals of Nepal viz. Dashain, Tihar and chhath falls in this season. This season is predominently dry but occasional brief rainfall could occur due to the local effect and sometimes due to the effect of the depressions and cyclones developed in Bay of Bengal and Arabian Sea.

iv. Winter (December- February):

This season starts in December and continues up to February of the following year. This is the coldest season in Nepal. Annul extreme minimum temperature mainly occurs in this season. Fog and mist in the morning hours is common in this season. Moreover, this season is associated with occasional rainfall due to the western disturbances. Cold north-westerly wind blowing through the Himalayas brings cold air in Nepal. Dense fog and cold-wave has become a regular phenomenon in Terai region of Nepal in recent years, which takes away many lives each year.

2. LITERATURE REVIEW

The main weather events that make any remarkable socio-economic effect are considered as the major weather events. The major weather events could be of temperature, rainfall, wind gust, heat waves, cold waves, drought, etc. Every weather events are directly or indirectly related to the society and economy.so, each weather events have their own distinct features and importance with reference to the country and their topography. Some weather events may have greater effect to one country but the same weather event could be unimportant to the other country. Moreover, the intensity or the definition of the major and extreme weather events could be different depending on their impact to each country. For example, the same amount of rainfall could lead to heavy flooding and landslide with significant impact to the society for one country but the same amount of rainfall could be of less important to the other country. The same amount of precipitation may have different impact on the society. So, the definition of major weather events may vary between the countries. There are many studies and researches on the studies of the extreme and major weather events. Since the flood and landslides are the main hydro-meteorological disasters in Nepal, the literature on heavy rainfall are mainly focused here.

Regional subproject implementation plan for Severe Weather Forecasting Demonstration Project for Bay of Bengal states that each country has its own thresholds for extremes based on good, historical reasons. The guidance forecasts provided by RSMC (Regional Specialized Meteorological Centre) uses a representative threshold for each hazard designed in such a way to draw the attention of forecasters of all NMHSs to potential hazards threatening their region which helps the National Meteorological and Hydrological Service Centers to decide the threat and monitor it for proper advisory or warning actions as determined in their particular countries. The following hazards are monitored by RSMC, New Delhi.

Table 2: Hazardous Map with threshold map for RSMC, New Delhi.

HAZARD	THRESHOLD	COMMENTS
Heavy Rain	≥ 50 mm in 24 hours ≥ 100 mm in 24 hours (the risk over 200mm/24 should be described in discussion in the Regional Guidance)	The operational country-thresholds may differ widely among participating countries of SWFDP-Bay of Bengal. NMHSs may translate the heavy rain into potential flooding in areas likely to be affected by heavy rain depending upon the soil condition, topography and drainage systems in respective areas
Strong winds	≥ 17 knots (over land and Sea) ≥ 34 knots (over Sea)	Affecting oceanic and coastal areas especially. Gusts on land from severe convective systems are not predictable on this time scale effectively
High Waves	≥ 2.5 m	NMHSs may use the information contained in the RSMC Guidance Product to generate impact-based forecasts and risk-based warnings for use by the coastal communities, fisheries, disaster managers etc. at national levels.
Storm Surge	≥ 1m	

(Source: http://www.wmo.int/pages/prog/www/DPFS/SWFDP/RAII-BoB/BoB-RSIP.html)
Since the weather, climate and topography are closely related between Nepal and India, we could use the same threshold values for Nepal too. Greater than or equal to 50mm of rain or greater than or equal to 100 mm of rain in 24 hours period is considered as the heavy rainfall event in India. We could use the same value for Nepal too. It is clearly stated in the table prepared by RMSC that the threshold for the heavy rainfall may differ among the countries and the NMHs could translate the heavy rain into potential flooding depending upon the soil condition, topography, and drainage systems in the areas. In this study, while identifying the major weather events, the total accumulated rainfall greater than or equal to 100 mm in 24 hours period is considered for the major weather event.

As the criteria of heavy and extreme rainfall events vary among the countries, the India Meteorological Department also classifies rain in basis as heavy, very heavy and extremely heavy. IMD defines the rain as heavy if it lies between 64.5 mm to 115.5 mm within 24 hours period. The rain is considered to be very heavy if it lies between 115.6 mm -204.4 mm. Similarly, IMD classifies extremely heavy rain if the 24 hours accumulated rain is greater than 204.6 mm. Similarly, Indonesian Meteorological services define heavy precipitation as the 24 hour accumulated rainfall of 50 mm and the extreme rainfall in Jakarta is 100 mm per day. To study those heavy and extreme rainfall events, the researchers (SISWANTO, OLDENBORGH, SCHRIER, LENDERINK, HURK (2015)) study the synoptic analysis of wind and relative humidity anomalies at 850 hpa from the NCEP/NCAR Reanalysis-1 which shows an intensified monsoon with the northerly component penetrating more to the south than usual, especially over South China Sea resulting in flooding in Jakarta. In this research, two separate criteria are defined for identifying the major weather events. The different synoptic features of the major weather events are then studied to find the driving mechanism for the happening of the major weather event.

After the identification of the major or the extreme weather events, different synoptic patterns of different levels and other lifting mechanisms should be studied to find out the cause of the occurrence of the events. Supply of moisture, deepening of trough, wind movement, lifting, CAPE, relative humidity, reative vorticity are some parameters that contribute for the occurrence of the event. Different literatures are available for the study of such major and extreme weather events. According to Pfahl (2014) extreme weather events on Europe are closely related with the anomalies of atmospheric circulations and to the particular atmospheric conditions like cyclone and atmospheric blocking. They noted that the precipitation extremes over the ocean and over flat terrain are closely related with cyclones in the vicinity and the associated dynamical lifting. They concluded that cyclonic anomalies at remote locations provide favorable conditions for extreme precipitation over complex terrain through the flow of moist air towards topography.

Forecasting is itself a challenging job and accurate forecasting is another challenge. Due to the chaotic nature of atmosphere, the synoptic features changes rapidly making the forecasting very complex. Deswell III (1980) also highlighted that it is always a great challenge to make accurate forecasts of occurrence of thunderstorm activities. Moreover, he stated that there is a great need to identify the reason behind the occurrence of such severe thunderstorm activities. He showed some linkage between severe thunderstorms in the high plains and specific synoptic scale pattern. He further noted that severe storms tend to occur on several consecutive days until the passage of a major upper level system over the region, which sweeps the moisture out of the area, followed by establishment of a stronger ridge.

However, there are very few studies on the extreme and major weather events in Nepal. The main major weather events in Nepal are- heavy rainfall, flooding, wind gust, thunderstorms, etc. and the main major weather event is the heavy rainfall. One of the study carried out by Chalise and Khanal (2002) shows that extreme weather events associated with heavy rainfall are the principal cause of natural disasters in Nepal. They cited a paper (Khanal, 1995) that reported more than 19 extreme precipitation events exceeding 400 mm of rainfall in 24 hours in different parts of the country between 1959 to 1993 out of which three events exceeded 500 mm rainfall in 24 hour. Furthermore, they found increasing trend in hazardous rainfall events in Nepal from the analysis of heavy rainfall events (exceeding 100 mm in 24 hour) during monsoon in 1981-1990 compared to 1971-1980. They concluded that the improved knowledge of the frequency, magnitude, causes and consequences of the extreme events is essential to develop the short and long term mitigation measures.

Nepal is highly dominated by summer monsoon and its circulation arising from Bay of Bengal. It is estimated that the summer monsoon accounts for 80 % of the annual rainfall in Nepal. The mean rainfall for Nepal during monsoon season amounts to about 1422.8 mm with a standard deviation of 132.6 mm and coefficient of variation 9.3 % (Shrestha, 2000). Since the flooding and landslide are highest during the monsoon season and the economic as well as social damage is highest during the monsoon season, we also give much importance to monsoon season. Among the studied eight MWEs, three MWE are of the monsoon Season. According to Pokhrel, (2003), summer precipitation is highest over middle mountains i.e. Mahabharata range; and decreased slightly over Terai and decreased rapidly over the Himalayan range. The monsoon oscillation is stronger in the northern hemisphere than southern hemisphere especially over south east Asia because of the Himalayas (Kelkat 2007). The Himalayas range forms an orographic barrier forcing the moist air to ascend and precipitate in the southern slope while hampering migration of moist air towards northern leeward side creating a prominent rain shadow region (Singh and Kumar 1997, Wulf et al. 2010). The research carried out by S.D Kotal, S.S Roy and S.K R Bhowmik (current Science, July 2014) from IMD revealed that forecasting of heavy rainfall, particularly over high complex terrain, is one of the most challenging task for forecasters. This is attributed to the complexity of the orography, lack of understanding of interaction between synoptic scale and meso-scale weather systems, sparse good quality data over remote areas and large spatial and temporal variation of rainfall, which is equally valid in case of Nepal as well. The interaction between the complex topography and moisture is not easy to comprehend.

3. METHODOLOGY

3.1 Study Period:

The Study period is for one year as specified in Terms Of Reference. This study is carried out from the start of monsoon season (June) of 2014 to the end of the pre-monsoon season (May) of 2015. The eight major weather events within the study period as specified in TOR are identified on the basis of the 24 hrs.' accumulated rainfall as described below.

3.2 Data collection:

All the meteorological data needed to complete this research are collected from Department of Hydrology and Meteorology if DHM owns the data. To identify the eight major weather events, the daily accumulated rainfall of the 15 synoptic stations are used as specified in the TOR. Moreover, the seasonal normal values as well as extreme values of rainfall are also collected from DHM as required. Below is the map of 15 synoptic stations.

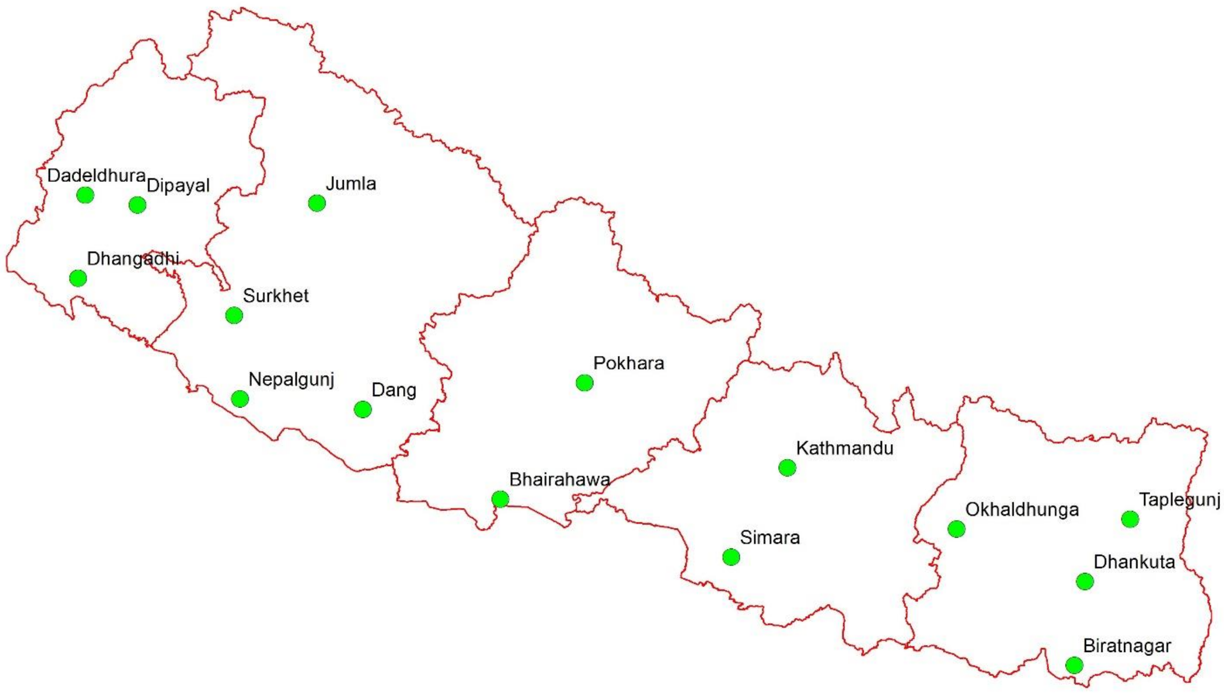

(Source: DHM)

Figure 1: Location map of 15 synoptic stations in Nepal.

Addition details of the 15 synoptic stations used in this study is listed in the table below.

Table 3 : Details of the 15 synoptic stations.

S.N.	Station ID	Station Name	District	Longitude (degree)	Latitude (degree)	Elevation (m)
1	44404	Dadeldhura	Dadeldhura	80.58	29.30	1848
2	44406	Dipayal (Doti)	Doti	80.93	29.23	720
3	44409	Dhangadhi(Atariya)	Kaliali	80.55	28.80	187
4	44416	Surkhet(Birendra Nagar)	Surkhet	81.63	28.59	720
5	44418	Nepalgunj Airport	Banke	81.67	28.10	165
6	44424	Jumla	Jumla	82.18	29.27	2366
7	44429	Ghorai (Dang)	Dang	82.48	28.04	634
8	44434	Pokhara Airport	Kaski	83.98	28.20	827
9	44438	Bhairahawa Airport	Rupandehi	83.42	27.51	109
10	44449	Simara Airport	Bara	84.98	27.16	137
11	44454	Kathmandu Airport	Kathmandu	85.37	27.70	1337
12	44462	Okhaldhunga	Okhaldhunga	86.50	27.31	1720
13	44474	Taplejung	Taplejung	87.67	27.36	1744
14	44477	Dhankuta	Dhankuta	87.35	26.98	1187
15	44478	Biratnagar Airport	Morang	87.26	26.48	72

(Source: DHM)

Available satellite images covering the extreme events are collected from Meteorological Forecasting Division of the Department of Hydrology and Meteorology. As DHM lacks upper air data, these surface and upper air re analysis data are gathered from ERA-Interim reanalysis data (http://apps.ecmwf.int/datasets/data/interim-full-daily/levtype=sfc/) from European Centre for Medium Range Weather Forecast (ECMWF) are used to study the synoptic features of each event. Moreover, satellite estimated rainfall from Global Precipitation Mission (Level-3 IMERG algorithm) is used to compare against the rain gauge observations. For this purpose, graphical display that can be viewed in Google earth (http://giovanni.gsfc.nasa.gov/giovanni/#service=AcMp) is used. Moreover, Grid Analysis and Display System (GrADS) is used to visualize the data in binary or netcdf format as required.

3.3 Definition of Major Weather Events:

The formulation of criteria for the identification of Major Weather Events is really a challenging task. After the collection of necessary rainfall data from DHM, efforts were made to identify major weather events using a number of test criteria. For this daily rainfall data of all the 15 synoptic stations were utilized. After testing various criteria, two criteria were finally adopted in order to identify the major weather events in this study, which are as follows:

Criteria I: An event (day) is considered as Major Weather Event (MWE) if the cumulative daily precipitation in any five or more stations (out of 15 stations) exceed 25% of their respective seasonal normal precipitation values.

Criteria II: It is based on the heavy precipitation events .If the daily accumulated rainfall of any two stations (out of 15 stations) exceed 100 mm, then the day is considered as the day of major weather event.

More than eight major weather events were identified from the above mentioned criteria, so, the eight major weather events were selected such that at least one major weather event falls in each season as defined in TOR and on the basis of the impact to the public. The major events common to both the criteria are also included in the eight major weather events.

Above criteria are chosen in order to focus on events that are of synoptic scale rather than extreme events with limited spatial coverage as it is almost impossible to find strong association between large scale atmospheric conditions and extremes that affect only small areas. However, coarse resolution datasets (such as reanalysis data) does not provide the details of the atmospheric conditions at local level, so it is difficult to study local scale extremes and associated atmospheric conditions that is responsible for the occurrence of the event unless such data are gathered through say a field campaign Another important reason for choosing large scale events rather than the local scale ones is that the large scale events have much greater impacts on the public as they affect large number of people and property than the local scale phenomenon. So, it can be said that selection criteria is set on the basis of societal impacts. Finally, above two criteria are set after testing a range of criteria in order to identify the major weather events on the basis of rainfall.

After the identification of eight major weather events, the detail study for the occurrence of each major weather event is carried out. The detail study for each major weather event spans a period of 2 days prior to the MWE and 1 day after the event. This provides a clear picture of genesis and decay, or trajectory of the events. Following fields are analyzed in each case study:

a. Mean Sea Level Pressure.

b. Upper atmospheric conditions (e.g. geo-potential height, wind and other derived parameters (e.g. CAPE, relative vorticity, etc. on basis of necessity and availability)) at standard pressure levels (850, 700, 500, 300 hpa).

c. Relative humidity at 600 hpa.

d. Satellite image for the cloud development, movement and dissipation.

e. Satellite estimated rainfall.

Though the MWEs were identified being based on the rainfall of 15 synoptic stations, the rainfall of more than 300 stations were studied for the detail analysis of the events. To compare the 11 KM grid data from GPM with the observed gauge rainfall, more than 300 stations are used so that the comparison would be reliable. The detail study of each event helps to identify typical atmospheric conditions during the occurrence of heavy rainfall in the country. It is hoped that this would provide a valuable reference to forecast precipitation induced by MWE over Nepal in future.

3.4 Identification of Major Weather Events:

Two stage analysis is carried out to identify the eight major weather events. Firstly different schemes were designed to identify the major weather events of the year according to the terms and conditions defined in TOR. From the detailed analysis and discussion among our staffs and among the staffs of Meteorological Forecasting Division, above mentioned two criteria were set. From the criteria I mentioned in Methodology above, the following major weather events were identified.

Table 4 : Major Weather Events identified according to the criteria I

Year- 2014/2015				
S.N.	**Month**	**Date**	**Season**	**No. of MWE (per season)**
1	August	14-15	Monsoon	1
2	October	14-15	post-Monsoon	1
3	December	14	Winter	5
4	December	16		
5	January	2-4		
6	January	23		
7	February	27		
8	March	2-3	Pre-Monsoon	3
9	March	31		
10	May	12		

There are altogether ten major weather events identified according to the criteria I. Five major weather events are identified in the winter season, three major weather events are identified in the pre-monsoon season, and one MWE is identified in monsoon and pre-monsoon season each. Though there are ten MWE identified according to the criteria I and we need eight MWE to complete this research, we set other criteria too to choose the MWE because there is just one MWE identified in monsoon season according to the criteria I. However, monsoon season is very important in terms of its contribution to annual rainfall, frequent occurrence of rainfall induced disaster such as floods and landslides in this season and heavy dependency of the agro economy on good monsoon. We need to study more events on the monsoon season. Moreover, the daily accumulated rainfall in monsoon season is greater compared to other seasons. So it is decided that out of eight MWEs few events should be in the monsoon season. So a second criterion is formulated as described above, From the criteria II, following five major weather events are identified.

Table 5 : Major Weather Events identified according to the criteria II

Year- 2014/2015				
S.N.	**Month**	**Date**	**Season**	**No. of MWE (per season)**
1	July	7	Monsoon	4
2	July	19		
3	August	14-15		
4	September	11		
5	October	15	Post-monsoon	1

According to the second criteria, there are altogether five major weather events identified; four in the monsoon season and one in the post-monsoon season.

To choose eight major weather events out of the 13 independent major weather events identified from the above mentioned two criteria (Both criteria gives the identical MWEs in the month of August and October), the terms and conditions in TOR and the impact of the event to the public was considered. The eight major weather events are identified such that at least one major weather event falls in each season. The overlapped two MWE are also included being common to both criteria. The two major weather events, identified according to criteria I, that occur in late winter (27 February) and early pre-monsoon (2-3 March) are combined as a single major weather event occurring in winter season (27 February- 3 March) because they are separated by only a few days and rainfall in early March is often associated with western disturbance rather than pre-monsoon activities.

With above consideration, following eight major weather events are identified in the year 2014-2015 (monsoon to pre-monsoon), which are studied in detail in the next chapter

.

Table 6 : Major Weather Events identified for the study.

Year- 2014/2015				
MWE no.	**Month**	**Duration**	**Season**	**No. of MWE (per season)**
1	July	19	Monsoon	3
2	August	14-15		
3	September	11		
4	October	14-15	post-Monsoon	1
5	January	2-4	Winter	2
6	February and March	Feb 27- March 3		
7	March	31	Pre-Monsoon	2
8	May	12		

4. RESULT AND DISCUSSION

The eight Major weather events are studied separately on detail. The common features of the event are also discussed conclusion.

4.1 MWE 1 (July 19):

During this event, almost all synoptic stations received rainfall on 19 July including heavy rainfall in the western hilly region (e.g. 126 mm in Dadheldhura and 123.8 mm in nearby Dhodhara station within 24 hours.) and central southern part of the country (e.g. Bharatpur, Rampur and Bhairahawa recorded 80, 101.2 and 84.2 mm respectively). . Being the monsoon season, the rainfall activities throughout the country was fairly widespread, however in some stations didnot record the rainfall because of the rain shadow areas and in the bank of the river facing opposite to the monsoonal wind. Nevertheless, from the record of rainfall in the country over the four days from 17 to 20 July, it can be concluded that almost all parts of the country received moderate amount of rainfall including heavy rainfall in some parts of western hilly and central Terai regions (Fig 1.1 to 1.4).

A comparison of the GPM satellite estimated rainfall with observed rainfall shows a high correlation in far western middle hilly region of Nepal and satisfactory correlation in the central and the eastern hilly regions. For example, GPM satellite estimated rainfall in the western hilly region was 90 mm to 125 mm whereas the observed rainfall was 125 mm in Dhadeldhura synoptic station and a nearby station (Dhodhara) recorded 123.8 mm and moderate amount of rain was observed in the central and eastern hilly regions.

The satellite image shows a huge and dense cloud mass in the far western hilly and Terai region at 12 UTC of 18 July (Fig 1.10) where heavy rainfall occurred. Small patches of cloud were observed in the low rainfall areas (Fig 1.11). After 12:45 UTC of 19 July it starts dissipating and the system was weakening then after. The cape vale of 1500-1800 J/kg was observed in the western hilly region of Nepal at 09 UTC of 18 July, which helped to intensify the cloud amounts by convective phenomena as well as supported the monsoon system for heavy rainfall (Fig 1.14). On 19 and 20 July the cape value was not very supportive for heavy rainfall (Fig 1.15 to 1.16).

On 17 July, 90 % relative humidity was observed at 600 hpa in eastern and central Nepal and 80% in the western Terai belt (fig 1.65). At 00 UTC of 18 July, almost all part of Nepal was covered by 90 % relative humidity at 600 hpa and the central southern part was covered by 100% relative humidity (fig 1.67), which was favorable for the heavy rainfall over central to western part of Nepal and moderate type of rain to eastern part but at 12 UTC of 18 July, western Terai had lesser relative humidity at 600 hpa compared to other regions of Nepal (Fig 1.68). The humidity percentage available in the morning of 19 July was high comparatively in the evening time of the same day .Its percentage in western terai was around 70% in 12 UTC of 19 July. Likewise at 00 UTC of 20 July humidity percentage was in the range of 70-80% and its percentage go on decreasing at 12 UTC of the same day.. Overall analysis shows that in the mid tropospheric level (600 hpa) adequate amount of moisture was supplied for the heavy rainfall events on 19 July in the western hilly region and central Terai regions.

For this event the relative vorticity at 12 UTC of 17 July and 00 UTC of the 19 July at 500hpa was more supportive for convergence from low level to develop the system. (Fig 1.58 and 1.61). It was strongly positive in the heavy rainfall areas especially in the western hilly regions and central region and then after it became negative, which means it was not favorable for the heavy rainfall (Fig 1.63).

Synoptic sequences

On 17 July the position of monsoon trough at MSL was north of its normal position in the western part than the eastern part of Nepal and the position of the trough was clearly observed from Multan of Pakistan to BOB. In the same way at 00 UTC of 850 hpa in 17 July the position of trough was observed in central India with the extending trough line passes from Chhattisgarh, Orissa and northern part of Andra Pradesh followed by the wind patterns. The trough line at 12 UTC of 17 July was shifting north in the western Nepal from its normal position (Fig 1.26). At 700 hpa level the monsoon trough passes from the Arabian Sea to east Madhya Pradesh where low pressure system was observed and elongated up to Gangatic west Bengal. The wind pattern follows the cyclonic circulation in the low pressure region at 700 hpa level in the same day. The low pressure system in the Rajasthan area captures the moisture from the Arabian Sea for giving the rainfall in the Northern part of India and Nepal. The position of the trough was a bit shifted in the western part of Nepal with the strong low pressure system was observed (Fig 1.33). Similarly at 500 hpa on 17 July the upper air trough was observed in Arabian sea and passes to central India . The mid tropospheric cyclonic circulation was observed in the northern part of Arabian Sea along with upper air trough passes to east Rajasthan,west Madya Pradesh and end to the Orissa followed by upper wind chart of 500 hpa but at 300hpa the anticyclonic circulation (high) was observed in Nepal and its pheriphery (Fig 1.50).The upper air circulation of wind exactly followed the wind pattern in the areas of Nepal in clockwise directions. The divergence in the upper level (300 hpa) over the heavy rainfall areas provided favourable condition for the low level convergence and development of system for heavy rainfall. On 18 July, the position of monsoon trough at MSL was more or less in same position but more elongated than the previous day in eastern side and at 850 hpa trough was extending from north western part of India to north of Orissa and ending at central BOB where the low pressure was observed in the periphery of West Bengal. The circulation pattern of wind was clearly observed in Uttaranchal and its periphery (Fig 1.28). Like wise at 00 UTC and 12 UTC of 18 July at 700 hpa the position of the trough was almost in the same place but the low pressure system was more stronger and elongated more in the north western part of UP to JK and wind pattern closely followed the circulation patterns which helped the supply of moisture from the Bay of Bengal in the heavy rainfall areas. Similarly at 500 hpa of 18 July also the extended trough was clearly observed with its position near to the western border than the eastern border of Nepal and ended in the central BOB. But in the eastern hilly region from 00 UTC to 12 UTC of 18 July high pressure system was observed (Fig 1.43 and 1.44). At 300 hpa of 18 July high pressure systerm was clearly observed in Nepal which helps to converge the moisture from the low level for heavy rainfall. In the 00 UTC of 19 July MSL pressure was observed north of normal position and at 12 UTC of the same day the trough was almost in same position but more elongated in the eastern part. While observing at 850 hpa at 00 UTC the position of trough was near the border of western Nepal covering some part of middle hill and Terai region. At 12 UTC of the same day trough position shifts towards east but below its normal position ended over central BoB (Fig 1.30). The position of monsoon trough at 700 hpa at 00 UTC and 12 UTC of 19 July? was clearly observed in the northern part of west Nepal covering almost all part of western region, where the heavy rainfall was occurred. Its position is quite southwards in the eastern region of Nepal. The strong cyclonic wind flow originating from BoB supplied sufficient moisture over eastern Nepal (Fig 1.37). Similarly on 19 July also the position of the upper air trough was not so much shifted but strong circulation was observed in the Chhattisgarh and its pheriphery (Fig 1.46). Easterly wind was observed in the eastern and central part of Nepal and south easterly wind in the western part of Nepal that brings sufficient moisture for the rainfall. The wind flow at 500 hpa clearly followed the patterns of low pressure area developed in the West Bengal. Likewise at 300 hpa, there was no significant change in high pressure system on 19 July but the wind patterns was strongly diverse in the West (Fig 1.54). On 20 July at 00 UTC and 12 UTC the monsoon trough was observed near normal position in west and in normal position in the eastern part of north India. High pressure system was clearly observed from the Maharastha coast to north western side of Rajasthan (Fig 1.23 to 2.24). which signals the fair weather thanafter. At 850 hpa at 00 UTC the monsoon trough was elongated from western border of Nepal to north of Odissa, west Bangal and ended to central BOB but at 12 UTC of the same day the strong circulation was observed in the pheriphery of west Bengal with the extended trough almost in the same place as in 00 UTC. On 20 July at 700 hpa the position of the trough was very close to the western part of Nepal and far from the eastern part of Nepal. The wind pattern at 700 hpa closely follow the system. The wind flowing from the Bay of Bengal to the north western part of India and Nepal carry sufficient amount of moisture to the heavy rainfall areas. Strong circulation being quite below from its normal position of monsoon trough, may suck up the humid air passing in the eastern part of Nepal leading to less pricipitation over the region (Fig 1.40). In the same way at 500 hpa the circulation was observed in the pheriphary of west Bengal and in the north western side of JK with clearly shows shifting of the trough south of its normal position. The ridge elongated from eastern Nepal to south western part of Nepal signals the weakning of the events in the study areas. (fig 1.47). The flow of wind was easterly in the eastern region and southwesterly to southerly in the mid western to far western regions of Nepal clearly in agreement with the pattern of the low pressure area. At 300 hpa, on 20 July at 00 UTC and 12 UTC distinct high pressure system was observed in the central India to Nepal which clarly indicates the weakning the major system.

Conclusion:

The monsoon trough in the MSL was very near to the boarder of western Nepal. The pressure falls to 996 hpa in the periphery of western border of Nepal. (Fig 1.20). Vertical extend of the trough was clearly observed from MSL to 500 hpa and was near to the western part than eastern part of Nepal. The wind pattern follows the pressure pattern and helps to supply the moisture from the Arabian Sea and the BOB branch up to 500 hpa. The relative humidity at 600 hpa at 00 UTC of 18 July shows that the adequate amount of moisture was available for heavy rainfall in the far western part and southern central part as well. The relative vorticity was strongly positive from 12 UTC of 18 July to 00 UTC of 19 July, which helps to support the heavy rainfall on 19 July. Satellite image shows huge mass of cloud at 18 UTC of 18 July, which also supports for the heavy rainfall on 19 July. Finally it was concluded that strong positive vorticity, sufficient moisture supply, position of monsoon trough, route of the wind flow aligned with system, accumulation of cloud masses in the heavy rainfall areas results the heavy rainfall in Dadeldhura synoptic station and its periphery and to the central southern border of Nepal and their adjacent areas. The supply of the moisture was mainly from Arabian Sea and BoB for this event.

4.2 MWE 2 (August 14 to August 15, 2014):

MWE 2 is the weather event of August 14 and August 15. From August 12 to August 16, almost all the stations received rainfall except a few stations. While analyzing the rainfall we found that mostly the rainfall amount increases day by day from 12 August to 15 August and then decreases slowly. Both the number of stations receiving daily rainfall of 100 mm or more and the nationwide highest daily rainfall increased each day from 12 to 15 August. Out of 360 station, on 12, 13, 14, 14 and 16 August, 7, 18, 60, 87 and 11 stations recorded 100 mm or more rainfall respectively. While the highest amount of daily rainfall across the nation was 220.4 mm, 200.4 mm, 300.9 mm, 442.3 mm, and 145 mm on 12, 13, 14, 15 and 16 August respectively. On 15 August, 5 stations recorded 400 mm or more rainfall. Although most of the stations in Nepal received rainfall on those five days, the highest rainfall occurred in central hilly and Himalayan region of Nepal on the 13th, central and western Terai and Siwalik region on the 14th, mid-western Terai and Tiwalik region on the 15th, mid-western and far western Terai on the 16th and Siwalik region and eastern Terai region on the 17th August respectively. Moreover, two of the synoptic stations viz. Birendranagar and Dang received the record breaking extreme rainfall of 423.1 mm and 294.4 mm respectively in 24 hours period observed at 03 UTC of 15 August for the month of August with the previous record of 169 mm and 155.6 mm of rainfall respectively. Heavy rainfall mainly occurred in Terai and Siwalik region of the country than the hills and mountains. Many people died and thousands of properties were lost during this episode of heavy rainfall event which triggered one of the extreme flood events in Nepal.

A comparison of the observed gauge rainfall with the GPM estimated rainfall shows that the estimated rainfall is highly co-related with the station rainfall but there are some disagreements between the two. For example, observed rainfall is greater than 80 mm in the border of central and western region of the country on August 16 (Fig. 2.4) but the GPM estimated less than 50 mm of rainfall (Fig 2.9).

The satellite imageries clearly follow the rainfall pattern (Fig. 2.11 to 2.15). Since this is the monsoon season, and the rainfall is widespread throughout the country, the satellite imagery shows scattered to broken amount of cloud masses throughout the country during the study period. The cloud masses are dense with overcast cloud amount in the region where the rainfall is high. More intensified cloud masses precipitate heavily in the ground. For example, a comparison of observed rainfall (Fig 2.4) and satellite image (Fig 2.14) show that rainfall is highest in the mid- and far-western Terai and Siwalik regions, where cloud patches are more dense and brighter.

Moreover, from a comparison of observed rainfall with relative vorticity, it is seen that 850 hpa relative vorticity matches well with the rainfall during this MWE with higher value of relative vorticity in the areas where rainfall is also high. For example, comparison of Fig 2.71 and 2.72 with Fig 2.8 shows that the relative vorticity is highest in western terai region of Nepal and the rainfall is also high in the same areas.

Relative humidity at 600 hpa is generally higher in the low level low pressure areas and lower in the low level high pressure areas, and higher in eastern Nepal than in western Nepal (Fig 2.76 to 2.85). The relative humidity slowly increases all over Nepal from 12 August onwards. The relative humidity is higher in most parts of UP, Bihar, Jharkahnda, west Bengal, Orissa and adjoining parts of Andhra Pradesh on the MWE days of 14th and 15th August (Fig 2.80 to 2.83). But the relative humidity decreased over the region after 12 UTC of 15th August.

Synoptic features analysis shows monsoon trough at the surface on the first day, ie. 00 UTC of the 12th August, which extends from north- central Pakistan to Punjab, Haryana, Uttar Pradesh, and the adjoining parts of Bihar and Jharkhanda. The trough then extends downward from Bihar and Jharkhanda to west Bengal, coastal part of Orissa and Andhra Pradesh ie. the monsoon trough is in its normal Position. Another branch of trough extends from North-central Pakistan to Arabia Sea. The position of the monsoon trough from central Pakistan to Haryana, UP and Bihar is almost same up to 850 hpa but the trough extends downward from Bihar to West Bengal, a little bit west than the position of trough in MSL, and lies from the adjoining Part of UP and Bihar to Chhatishgarh and Andhra Pradesh. At 700 hpa, the trough from North-central Pakistan extends to Punjab, Haryana, and UP. The trough is then divided into two branches from UP. One branch of which extends from adjoining parts of UP and Bihar to Chhatishgarh and Andhra Pradesh while the other branch of the trough extends to Arabian Sea via UP, adjoining parts of Rajasthan and Madhya Pradesh and Gujarat. The trough lies closer from western Nepal than from eastern Nepal. Also, pressure is lowest in western Nepal than in other parts of the country at 700 hpa (Fig 2.36). High is dominant over Nepal at 500 hpa and 300 hpa. Moreover, at 500 hpa, low pressure area persists in Mahrashtra and adjoining areas. From 12 UTC of 12th August, the pressure values at Pakistan decreases slowly with time and the trough shifts slowly upward towards Nepal up to 850 hpa. Also, the trough at 700 hpa that extends from adjoining areas of UP and Bihar to Chhatishgarh and Andhra Pradesh intensifies and deepens, and slowly moves northward while the other trough extending from UP to Arabian Sea remains stationary. At 500 hpa, the low pressure area at Arabian Sea weakens slowly and the high at Nepal also starts weakening. High pressure area is dominant over Nepal at 300 hpa. On 13th August, both at 00 UTC and 12 UTC, the monsoon trough at MSL lies north of its normal position i.e. close to foothills of Himalayas but the pressure is slightly lower in western Nepal than in the central and eastern Nepal. At the same time, the trough at 850 hpa also shifts northwards and lies close to the foothills of Himalayas while the branch of the trough extending from Bihar to southwards shifts east and lies in the coastal part of Orissa and Andhra Pradesh. At 00 UTC of 13th August, a circulation extends from western Nepal to UP, Madhya Pradesh, Chhatishgarh and Orissa resulting in the wind flows from Bay of Bengal to western part of Nepal while the high is dominant in the central Pakistan and adjoining India (Fig 2.48). The high at 300 hpa slowly shifts westward. On 14th August, both at 00 UTC and 12 UTC and up to 00 UTC of 15th August, the monsoon trough lies in the foothills of Himalayas (Fig 2.20, 2.21). At 850 hpa, the trough extending from Bihar to southwards is similar to previous days but other branch of the trough intensifies, move northwards and lies in the foothills of Himalayas with the pressure minima over western part of Nepal. The wind flow becomes south westerly as seen in fig 2.38. The wind both from Arabian Sea and BoB contribute for the sufficient moisture supply in Nepal which can be seen from fig 2.40 and fig 2.50. The associated trough extends up to 500 hpa with the extension of trough from Northern Pakistan to Punjab, Nepal and then to adjoining part of MP and chhatishgarh, and adjoining part of Orissa and Andhra Pradesh. At 500 hpa also, the trough is close to western Nepal. At the same time, at 300 hpa, the high is displaced westward and lies in central Pakistan while a small trough exists in western Nepal. The wind speed decreases in Nepal than in the previous day (fig 2.59 and fig 2.60). From 12 UTC of

15th August onwards, the trough at MSL weakens slowly. The trough at 850 hpa, 700 hpa and 500 hpa also weakens slowly with time while the high starts to strengthen in 300 hpa thereafter.

To conclude, the major cause of the heavy precipitation event is the location of trough at the foothills of Himalayas and the extension of the trough up to 700 hpa. Moreover, the associated trough was developed in 500 hpa to support the feature at the surface. The development of slight trough in western part of Nepal at 300 hpa also shows the instability up to 300 hpa .The trough was closer from the western Nepal; as a result precipitation was heavier in western Nepal. Moreover, sustained supply of moisture was maintained by the strong wind flow towards the Himalaya from the BoB and Arabian Sea while the monsoon trough was located near the Himalayan foothills and this provided conducive condition for cloud formation leading to heavy precipitation. In addition, rainfall activities are found greater in the high vorticity (cyclonic circulation) areas and low in low relative vorticity areas. Finally, rainfall activities decreased from the 16th onwards as the trough shifts to its normal position.

4.3 MWE 3 (11 September,2014):

Synoptic sequences:

As seen in Fig. 3.3, on 11 September 2014, observed rainfall was heavier in western Terai and Siwalik region in comparison to the other parts of the country .The 700 hpa chart revealed the isolated low over Pokhara areas at the meantime station recorded significant rainfall in 9 and 10 September. Moisture distribution at 600 hpa also indicated the dense cloud development over the UP, MP and neighbourhood. Satellite estimated rainfall also shows heaviest precipitation over the same region in the whole of South Asia on that day (Fig. 3.7). Satellite imagery of 10 and 11 September also depicted dense cloud mass concentrated over the south western regions of Nepal (Fig 3.10 and 3.11). At 12 UTC of 9 September western end of monsoon trough at the surface was located north of its normal position (Fig3.14) and in the same time low pressure was developed over MP with vertical extension up to 700 hpa. Moreover strong divergence and negative vorticity at 500 hpa marked the strong low level convection over the western plains of Nepal and Up areas .At the same level feeble westerly trough was also located over the Uttarakhand areas and was extended up to 300 hpa. The Lower tropospheric level (upto 850 hpa) shifted slightly northwards and was located over UP at 12 UTC of 10 September (Fig 3.24 and 3.32). At the meantime the surface low was found to merge with the monsoon trough (Fig 3.16). Converging wind circulation at LTL supports moisture influx toward UP and west Nepal from both Arabian sea and BoB (Fig 3.24 and 3.32). The trough observed at 300 hpa gradually propagated eastward and situated over the western Nepal at 12 UTC of 10 September. The strong divergence and negative vorticity at 500 hpa marked the strong low level convection over UP and adjoining western plains gave rise to abundant low level moisture supply, which in turn created the moist instability for development of dense convective cloud over UP and neighbourhood as depicted by satellite imagery of 10 September (Fig 3.10).The feeble westerly trough observed at 300 hpa and distinct westerly trough at 500hpa over north west Nepal created cold air advection from higher latitudes and warm moist air drew by wind from Arabian sea and BoB at lower atmosphere helps in accumulating abundant moisture which triggered dense cloud yielding heavy precipitation over the western plains of Nepal. The upper air westerly trough at 300hpa and 500 hpa propagated eastwards gradually but ridge developed over eastern region curbed its movement .The LTL low weaken by 00 UTC of the 11^{th} however it again intensified by 12 UTC of 11th September and shifted north eastwards yielding light to moderate rain in central and eastern region of Nepal. Then after monsoon trough shifted southwards. Despite the southward shifting of the monsoon trough, sufficient moisture get accumulated leading to development of dense cloud mass over the UP, central and eastern region of Nepal because of distinct low persisted over MP and adjoining east UP. The low over UP and positive vorticity at 500 hpa over UP on 12 September (Fig 3.59 and 3.60) yielded moderate rain over central and eastern Terai (Fig3.4). Besides that the isolated low pressure was observed in the 700 hpa chart over western hilly regions rain was observed widespread over the Nepal in 11th September the reason was due to the closely approaching monsoon trough towards the south Nepal. Synoptic analysis based on the reanalysis data explored the fact that the shifting of monsoon trough towards the north to its normal position and the persistence of low over the south UP and adjoining north MP created the conducive environment to yield rain over the Nepal

Summary

The approaching monsoon trough towards the southern plains of Nepal drew the abundant amount of moisture from BoB due to which substantial rainfall occurred in the country. South easterly current from BOB and south westerly current from the Arabian sea entrained the moisture towards the UP and adjoining areas .The low level low pressure areas mainly over 850 and 700 hpa developed over UP and adjoining promoted the moisture flux throughout the country yielding the moderate to heavy rainfall depending upon the topography. Besides that the isolated low pressure was observed in the 700 hpa chart over western hilly regions. The 700 hpa chart revealed the isolated low over Pokhara areas at the meantime station recorded significant rainfall on 10th and 11th September. Mainly the moisture accumulation in the periphery of mountains increases the moisture instability, which in turn triggered the dense precipitable cloud and give rise to brief to continuous downpour depending upon the moisture quantity and supply. The moisture coalition from BoB and Arabian sea yielded significant rainfall on 10 September mainly over western Nepal whereas shifting of Low over east UP get intensified and moisture flux only from BoB couldn't produce significant rainfall in eastern and central Nepal. Thus we can conclude that the development of cloud in the merger of abundant moisture from BoB and Arabian Sea is more precipitable.

4.4 MWE 4 (14-15 October,2014):

Synoptic features and consequences

Cyclonic storm formed on 8 October over Bay of Bengal (BoB) deepened and became severe cyclonic storm on the 9th and further intensified due to immense moisture supply,negligible wind shear and less friction over the BoB and finally became very severe cyclonic storm. Surface weather charts, satellite imageries, circulation and geopotential analysis of different levels revealed that the very severe cyclonic storm HudHud, formed over BoB, moved in northwest direction towards the landmass. In theafternoon of 12 October, Hudhud made landfall over Visakhapatnam of Andhra Pradesh with surface pressure of less than 990 hpa at the center. But it slightly weaken into Severe Cyclonic Storm soon after the landfall with the core pressure of 996 hpa. Fig 4.17, 4.27, 4.37 and 4.47 depict well organized cyclonic circulations near the time of landfall from surface to MTL with north westward tilted core with height. Feeble cyclonic circulation is seen even up to UTL (Fig 4.57). The positive vorticity drained from throughout the sub Indian continent and accumulated over the coastal AP. At 12 UTC of 12 September, UTL wind flow was westerly over the North west India and adjoining Pakistan areas without any trace of trough in there(Fig 4.57). But the UTL wind flow over Nepal was south westerly and strong.

With the advent of time,by00UTC of the 13th, feeble trough emerged over Pakistan and adjoining Afghanistan at 300 hpa and the converging wind pattern shifted slightly north westwards over AP and weakened. At 500 hpa the strong converging wind flow shifted north northwestwards with decreasing intensity but the feeble trough started developing over west Pakistan areas at 00 UTC of the 13th. In the same way, cyclonic circulation observed at 700 and 850 hpa shifted north north westwards with slightly diminishing intensity. The organized converging wind pattern lost its vigour and diminished into severe cyclonic storm after some time of landfall and gradually became cyclonic storm at 00 UTC of 13. It further re-curved northwards at 00 UTC of 13 (Fig 4.18) and converted into deep depression and was located over south Chhattisgarh with central pressure of 996 hpa at the surface. The deep depression further weakened into depression with its core pressure 998 hpa at the surface and was situated over central Chhattisgarh and neighborhood at 12 UTC of 13 September. At the same time distinct westerly trough developed over the central Pakistan at 300 and 500 hpa (Fig 4.49 and 4.59) with associated feeble trough at 700 hpa. The depression was extended up to 500 hpa tilting northwards with height. Moisture distribution was not concentrated about the depression but spatially distributed throughout Chhattisgarh, MP and UP areas whereas dry atmosphere was noted over NW India at 600 hpa (Fig 4.79). On the other hand, high moisture content was observed over the central Pakistan and neighbourhood at low levels at the same time. The depression drifted northwards and located over the east Madhya Pradesh with its vertical extension up to the 500 hpa at 00 UTC of the 14th. At the same time deep trough observed at 300 hpa propagated eastwards towards NW India and adjoining Pakistan which ultimately combined with the remnants of cyclone where the ridge was observed over north east India. The depression in the course of shifting northwards interacted with the trough observed at 500 hpa over NW India as illustrated in Fig 4.50. In the lower atmosphere the depression is approached with the circulation developed over central Pakistan. Moisture contents of depression combined with the moisture observed over NW India. By 12 UTC of 14 October, depression had shifted north northwards towards east Uttar Pradesh and weakened to well marked low pressure, which merge with the westerly trough at 500 hpa. Also, the low coupled with the 700 hpa low developed over north west India as illustrated by fig 4.51 and 4.41. In the same time dense cloud mass was observed over east UP, central Nepal and neighbourhood where significant rainfall was also observed. The converging wind circulation is located over east UP at 700 and 850 hpa. Upper level westerly trough is located over the NW India. Significant rainfall was observed over Nepal under the influence of mid latitude westerly trough and low level circulation. The short wave trough collide with the well marked low pushed the moisture north eastwards causing the blizzards over the Himalayas due to the orographic lift and rainfall over central and western regions of Nepal where the high moisture content was observed at mid troposphere(at 600 hpa,Fig 4.81). Cold air mass dragged by upper air trough from higher latitude and warm moist air accumulated by well marked low created moist instability which in turn gave rise to dense cloud mass with high moisture content.

At 00 UTC of the 15th, the upper air trough at 300 hpa and 500 hpa weakened, and shifted only slightly eastwards due to the high pressure over the east Nepal. However weak cyclonic circulation is observed at 700 and 850 hpa and moisture content at 600 hpa decreased rapidly and the atmosphere appeared to be nearly dry resulting in only isolated rain over one or two places. Upper and mid troposphere Trough further propagated only a bit eastwards and seems to be locked at 12 UTC of 15 September (Fig 4.53 and 4.63). The trough observed at 700 and 850 hpa receded in the same way atmosphere seems dry over many parts of Nepal and India. At 00 and 12 UTC of 16 September, upper air trough remained over NW India but it did not play any significant role in weather pattern as there was not support from the lower atmosphere. Slight trough is observed at 00 UTC over Uttarakhand areas in 700 hpa causing light rain over there and at 850 hpa trough is observed over east Nepal and neighborhood. At 12 UTC trough vanished from NW India and strong westerly prevailed at 700 hpa and 850 hpa, which marked the end of cyclone's influence.

summary

Shortly before landfall near Andhra Pradesh (AP) , on October 12, Hudhud reached its peak strength with three-minute average wind speeds of 175 km/h (109 mph) and a minimum central pressure of 990 hpa. After two days, the system then drifted northwards towards south Chhattisgarh, east UP and Nepal causing widespread rains in both areas and heavy snowfall in the latter.On 14 October 2014, sudden weather changes from Cyclone Hud-Hud in Nepal reportedly caused an avalanche and blizzard on Mount Dhaulagiri, in the Annapurna region and Mustang- Jomsom areas. The avalanche and heavy snowfall killed at least 43 hikers and guides in Nepal. Regarding the synoptic features the eastward propagating higher latitude westerly trough in the upper atmosphere merged with the remnants of cyclone HudHud which is manifested in the 300 hpa and 500 hpa chart in the 13 and 14 October .The well-marked low remained from cyclone in the course of shifting northwestward direction encountered with the eastward propagating westerly trough. The well-marked low with organized cyclonic circulation up to the 500hpa is situated over the east U.P and adjoining west plain of Nepal generated heavy precipitation. However that organized cyclonic circulation extended up to the 300 hpa where feeble trough can be seen. The geopotential and wind pattern analysis revealed the clear picture of coupling of two moisture laden air masses. This is also ascertained from the 600hpa relative humidity analysis. The vigor of the remnants is due to the unification of the two moisture rich air mass.

4.5 MWE 5 (2-4 January, 2015)

Synoptic Sequences

Quick glance over the system cued that the rainfall is due to the eastward propagating upper air trough which penetrated to the lower atmosphere, generated the conducive ambience for the supply of moisture in turn created vast pool of moisture from Arabian Sea. The north south trough originated from the central Pakistan towards the Arabian sea via Rajasthan is observed in the 300 and 500 hpa level at 12 UTC of 31 December 2014 as illustrated in Fig 5.49 and 5.59. At the same time at the 850 and 700 hpa ,easterly wind is blowing over the Nepal and core low was observed over the Arabian sea and adjoining Maharashtra coasts which is elongated towards the north west India(Fig 5.29 and 5.39). Likewise low was observed over peninsular India in mean sea level. Broken cloud was observed over Madhya Pradesh(MP), Uttar Pradesh(UP) and west Nepal areas (Fig 5.13). Rainfall was also observed in those corresponding places(Fig 5.7) whereas rain was more pronounced over western hilly region of Nepal as shown by Fig 5.1. According to the relative humidity map, there was substantial relatively humidity at 600 hpa over the west MP. In the 300 hpa chart trough observed in the previous day was nearly stationary but deepened at 12 UTC of 1 January 2015(Fig 5.61). Similarly the trough at 500 hpa became more pronounced at 12 UTC of 1 January. In the meantime strong southerly wind blew over the Nepal in such a way that moisture from Arabian sea is drained towards the north west India and Nepal. Likewise on the same day at 700 and 850 hpa the low over Arabian sea became less intensified, however the moisture pool from BoB towards Nepal is paved due to favourable wind flow pattern(Fig 5.41 and 5.31). On the same day Banke station recorded 40.2mm, Gorkha station recorded 59.1mm, Doti recorded 79mm rain and Kaski recorded 40mm rain which was significant amount of rain in winter season. Cloud oriented towards MP and UP from Arabian sea as seen in Fig 5.14 indicates significant upper air moisture flow from 500 hpa. 500 hpa vorticity and streamlines also manifested the higher vorticity values originated from Arabian sea towards MP,UP and west Nepal. The wind flow indicated the low level moisture flow was from BoB and Arabian sea although upper air moisture flow was from Arabian sea. In the upper atmosphere the observed trough further deepened and shifted slightly northwards at 12 UTC of 2 January (Fig 5.63). On the same day at 300 and 500 hpa trough further deepened and propagated slightly north east towards Nepal and wind flow is southerly. Trough can also be observed in mean sea level chart in the UP areas. Similarly trough and flow pattern established over 850 hpa directed towards Nepal and at 12 UTC of 2 January 700 hpa trough is more directed towards west Nepal originating from Arabian sea and oriented like the conveyer belt to transport the moisture. Rainfall was more pronounced over west Nepal as shown by Fig 5.3 and 5.9 which is also revealed by satellite imagery where dense cloud can be observed over west Nepal. The approaching trough yielded significant rain over the western hilly areas where 98mm rain occurred over Humla,52 mm in Achham, 40 mm in Bajhang,46.2 mm in Baitadi, 49.7mm in Kalikot, 77 mm inBajhang, 76 mm inBajura,72 mm in Mustang, 84.6 mm in Achham and 66.7 mm in Gorkha. Thus steeped upper air tough triggered heavy to medium rain mainly over the western mountainous regions supported by the lower level moisture incursion mainly from Arabian sea.At 00 UTC and 12 UTC of 3 January upper air trough propagated eastwards and was located over west Nepal and south India via MP. At 00 UTC of 3 January steep trough approached west Nepal whereas at 12 UTC the trough receded at 500 hpa as illustrated in Fig 5.55. Likewise at 700 hpa at 00 UTC weak converging circulation is established over western hilly region and trough seemedto be abated by 12 UTC of 3January. Upper air trough approached nearer to Nepal but not significant rain occurred, this is because the lower level trough weakened. On4 January at the 300 and 500 hpa the trough further shifted eastward and reached eastern Nepal whereas high pressure was established over Arabian sea by 12 UTC as illustrated by Fig 5.67 and 5.57. Likewise the upper atmospheric low situated over east and central Nepalweakened. Satellite imagery revealed mainly fair weather however broken amount of cloud was over the western hilly region (Fig 5.17), which yielded moderate rain over one or two places in there. On 5 January upper air trough crossed Nepal and strong westerly prevailed. In the similar way high was observed over Arabian sea in mid tropospheric level and lower level. Fair weather prevailed throughout the Nepal and most parts of India.

Summary

On2 January 2015, 78mm rain was occurred in the Dadedhura which exceeds the extreme rainfall of January for the station. Dipayal station recorded 58 mm rainfall. Similarly, Nepalgunj, Jumla and Pokhara recorded above 20 mm rainfall which is significant rain in the context of dry and winter month of January. Likewise 72 mm rain in mustang, 98mm in Humla,84.6mm in Achham occurred which indicated the westerly trough yielded significant rain over western hilly areas in comparison to plains. Similarly light to moderate rain also occurred on 1 January over western hilly regions. Analysis of the synoptic features associated with the rain causing system revealed that the system is an extra tropical disturbance dipping from the Mediterranean sea, which propagated eastwards from the upper atmosphere. Westerly trough at upper atmosphere propagated from the Central Pakistan towards the Rajasthanon31st December, 2014. With the advent of time it penetrated towards the lower atmosphere. On1st January 2015 it intensified and continued shifting eastwards. As it approached west Nepal on 2nd January, a distinct trough also observed drifting towards northwest India in the lower atmosphere and wind is oriented from Arabian sea to UP and west Nepal. As a result substantial amount of moisture is transported towards western Nepal. This moisture yielded light to moderate rain in the plains; and due to the rugged terrain over the hilly regions, it triggered the denser rain bearing clouds and yields heavy rain and snow over the high altitude areas on the 2nd January. The upper atmospheric trough quickly shifts eastward and its intensity diminished at the same time. On 3rd January, the system yielding light rain at a few places and on 4th January it further became fragile paving way for strong westerly wind and high pressure centre in the central India. On 5th January it totally vanished and stronger westerly winds dominated the whole nation and over the Indian peninsula. The westerly system is steered by the upper atmospheric trough. Finally, we can conclude that the lower atmospheric trough is induced, shifted and disappeared in tune with upper air trough.

4.6 MWE 6 (27 February to March 3)

Two major rainfall event occurred in Nepal from 27 February to 3 March 2015. One event occured on 27 February and the other event occurred on 2 to 3 March. On 27 February, 12, out of 15, synoptic stations in Nepal received rainfall (Fig 6.2). Among those highest amount of rain fell in Dadeldhura (33 mm[1]). But on the next day only 0.2 mm of rain fell there. On 1st March, eight synoptic stations in western Nepal received rainfall, out of which highest amount of rainfall was recorded in Surkhet (10 mm). On 2nd and 3rd March, all the fifteen synoptic stations received rainfall (Fig 6.5 and 6.6). Among those, maximum amount of rainfall was observed at Dadeldhura (54 mm) and Dipayal (71 mm) on 2 and 3 March respectively. These are significant amount of rainfall for this season.

A comparison of the station rainfall with the GPM estimated rainfall shows that the GPM rainfall estimated rainfall matches well with the observed station rainfall in most cases (Compare Fig 6.1 to 6.8 with Fig 6.9 to 6.16). However, in some cases GPM estimated less rainfall than the observed station rainfall (fig 6.3 and fig 6.11) and (fig 6.8 and fig 6.16); in particular, GPM underestimated rainfall in the far western region of the country. Cloudy condition depicted in the satellite images are generally in good agreement with the observed rainfall as rainfall is higher in the areas with dense cloud mass and low in areas with few cloud (Fig 6.2 and fig 6.19).

Weather charts show the extension of westerly trough from west central Pakistan to SE Pakistan, Gujarat and adjoining Arabian Sea throughout the troposphere (From surface up to 300 hpa) with westward tilt with height. The trough shifts eastward with time and the intensity of trough decreases at 300 hpa and 500 hpa and the intensity of trough increases at 700 mb and 850 mb and the trough is divided into two branches from north central Pakistan. One branch of the trough extends from central Pakistan to central Arabian Sea via Rajasthan, Gujarat and adjoining areas whereas the other branch of trough extends from north central Pakistan to Punjab, Haryana, and southern border of Nepal at 00 UTC of 27th February (Fig 6.57 and 6.41). Under the influence of elongated trough at LTL (850 and 700 mb) moisture laden wind flows from Arabian Sea to Nepal. The trough at LTL weakens after 12 UTC of 27th February.

At 00 UTC of 28th February, another westerly trough is seen at 300 hpa and the trough extends from central Afghanistan to South-central Pakistan, Gujarat and adjoining Arabian Sea (Fig 6.91). The associated trough extends down to 500 hpa and is tilted westward with decreasing altitude (Fig 6.75). Moreover, the associated circulation is seen at 700 hpa and 850 hpa with the centre of the circulation at Rajasthan, Gujarat, South eastern Pakistan and adjoining areas. The trough deepens and shifts eastward with time and lies in central Pakistan to Rajasthan, Madhya Pradesh, Maharashtra and adjoining areas at 12 UTC of

[1] Here and at other places this refers to last 24 hour accumulated precipitation measured at 03 UTC of the given day.

March 1st (Fig 6.94). The associated circulation at 700 hpa and 850 hpa move eastward, and by 12 UTC of 2 March it weaken and develops into trough, which lies close to western Nepal (Fig 6.48 and 6.64) . Moreover, a trough is developed at 700 mb as seen in fig 6.60 and with its extension from NE Pakistan to Haryana, Punjab, UP, Bihar and adjoining Punjab. Both the trough at LTL slowly dissipates after 00 UTC of March 4.

The Vorticity at 300h pa co-relate well with the precipitation events as precipitation occurs in the areas where the vorticity is positive (Compare Fig 6.2 and 6.104). Moreover, precipitation is higher in the areas of high relative vorticity and there is no precipitation in the areas of negative relative vorticity. It is seen that if the relative vorticity at 300 hpa is greater than $3*10^{-5}$ s^{-1}, there is greater chance of precipitation.

The 600 hpa RH charts clearly show the moisture influx from Arabian Sea with the movement of trough as can be inferred from comparison of the RH plot (Fig 6.125) with 300 hpa and 500 hpa circulations (Fig 6.93 and 6.77) at 00 UTC of March 1st. Moreover, the rainfall is greater in high humid areas and less in less humid areas.

The extension of trough from 300 mb to 850 mb and the development of trough from central Pakistan to Haryana, UP, Bihar and adjoining southern Pakistan is the main cause of precipitation for this MWE ie. the precipitation occurs due to the influence of the westerly trough and its extension downward. As the trough is approaches Nepal, the precipitation is high in Nepal. Also, the trough is deeper in western Nepal than that in eastern Nepal; as a result precipitation is higher in western Nepal than in eastern Nepal. One of the most important results that came out from the study of this MWE is that the relative vorticity at 300 hpa is well corelated with the precipitation at surface.

4.7 MWE 7 (March 31)

Study of this event spans from 29 March to 01 April with moderate to heavy rainfall received throughout the country on 30 and 31 March. On 30 March, under the influence of the westerly trough, moisture laden wind originating from Mediterranean sea brought heavy rainfall (30 to 45 mm) in the western hilly and mountain regions (e.g. in Dheldhura, Darchula, Dhaulatiya,Bijayapur, Koisabas ,Mangelsen etc.) of Nepal. On 31 March, the upper air westerly trough shifted eastwards bringing central and eastern Nepal under its influence (Fig 7.40 and 7.48), and the supply of the warm moist air from Arabian sea likely to have resulted in moderate to heavy rainfall in most of central and eastern (?) Nepal as depicted by the rainfall records of some synoptic stations like Biratnagar (53.9 mm) and

Janakpur (40.6 mm) and other stations (rainfall, climatic station etc.) such as Ilam tea state (31 mm), Gharedhaunga (25 mm), Ghorepani (40 mm), Garkot (25.3 mm), Kabre (28 mm), Kanyam Tea state (30.2 mm), Siraha (28.2 mm), Syamga (43.1 mm).

A comparison of the GPM satellite estimated rainfall with the observed rainfall shows good agreement in isolated places of eastern hilly and Terai regions of Nepal and satisfactory agreement in the isolated places of the central hilly and Terai region on 31 March. But little agreement is seen in the western hilly and Terai region on both 30 March and 01 April. The agreement is somehow better on 02 April, though GPM underestimated the observed rainfall. Similarly, comparison of satellite image with observed rainfall and GPM satellite estimated rainfall shows good agreement between the location of cloud mass and areas of rainfall on 29and 30 March (Fig 7.9 and 7.10) as scattered to broken amount of cloud was observed in the heavy rainfall areas. On 31 March and 01 April, few amount of cloud was observed, which indicates the fair weather (Fig 7.11 and 7.12).

The 600 hpa relative humidity at 00 UTC of 29 march was 70-80 % in the eastern and western Himalayan region and at 12 UTC of the same day it was higher over hilly to high mountain region throughout the country (Fig 7.61 and 7.62) which is supportive for the rainfall in the western hilly to mountain regions. On 30 March, at 00 UTC the relative humidity increased to 80-90 % in western part of the country. By 12 UTC the relative humidity reached about 80-90 % in the eastern and central regions while it was 100 % in the isolated areas of the western and far western high mountainous areas, which was favorable for moderate to heavy rainfall over those areas. However western Terai remains much drier with the relative humidity of only 20-30 % (Fig 7.64). On 00 UTC of 31 March, almost all part of the country was drier with 40-60 % relative humidity and from 12 UTC of 31 March onwards, Terai regions of Nepal along with the Gangetic plains remained much drier compared to hilly regions, which indicates the lack of sufficient moisture for the formation of rain bearing clouds. Overall analysis indicates that in the mid tropospheric level (600 hpa) adequate amount of moisture was supplied for the heavy rainfall events in 30 and 31 March from western Nepal to Eastern Nepal.

The 500 hpa relative vorticity at 00 UTC of 29 March was negative in the central Terai and isolated places of far western hilly region (Fig 7.53) but at 12 UTC of the same day the vorticity was strongly positive in the central hilly region and supportive in the western and eastern hilly to mountain regions. This is conducive for the development of the convective phenomena over those regions leading to heavy rainfall in those areas (Fig 7.54). At 00 UTC of 30 March, vorticity was positive almost all part of the country but strongly positive in the eastern, central and western hilly to mountain regions of Nepal and at 12 UTC it was strongly positive in the western hilly to mountain regions and slightly positive in the far eastern hilly regions of Nepal (Fig 7.55 and 7.56). Similarly at 00 UTC of 31 March it was positive throughout the country but stronger in the middle hilly region; likewise at 12 UTC of the same day it was positive throughout the country except central and western Terai regions but stronger in eastern and central hilly regions (Fig 7.58). Then after vorticity became negative in the country. Finally it was concluded that the strong positive vorticity in the isolated places of western, central and eastern hilly and Terai regions help develop the convective phenomena for orographic rainfall in the isolated areas of the country.

Synoptic sequence:

On 29th March the elongated MSL trough with strong low was observed in west Rajasthan and its periphery. The trough line extended up to Chhattisgarh and it seems to be close to eastern part of Nepal than the western part. At 00 UTC of 29 March a low pressure system was observed in the northern part of Pakistan and its periphery at 850 hpa. But at the same time, a ridge was observed from north west parts of India to the northern part of Madhya Maharashtra at 700 hpa. But by 12 UTC, low pressure system was clearly observed in north Pakistan at 700 hpa, which was elongated in north south direction and extends up to northern part of Arabian Sea (Fig 7.30) with an associated upper air trough at 500 hpa, which was elongated in north south direction from north part of Pakistan to north part of Arabian Sea (Fig 7.38). The upper air trough is positioned such that mid tropospheric wind flow over the Arabian Sea is directed to the central and eastern Nepal, which is conducive for rainfall over those regions. At the higher level of 300 hpa, on 29 March, a ridge was observed from the eastern Nepal covering east central India to coastal Andra Pradesh and its periphery but at 12 UTC the north south extending upper air trough was observed from central Pakistan to north part of Arabian Sea (Fig 7.45 to 7.46), which gradually shifted northwestwards towards Nepal. At 00 UTC of 30 March at MSL no distinct trough with low was observed but the trough line was very near to central Terai of Nepal than eastern and western parts (Fig 7.15) but the system observed was isolated from 12 UTC of the 30 March but very near and concentrated below the eastern border of Nepal. The other isolated lows were in central India and the central western part of India covering the central part of Sindh (Pakistan) (Fig 7.16). At the same time a distinct low was observed in Punjab and West Rajasthan at 850 hpa with elongated trough that extended up to Gangetic West Bengal via southern border of Nepal.

Associated upper air low is noted over north Pakistan at 700 hpa (Fig 7.24) and trough at 500 hpa that extends from Uttaranchal to Madhya Pradesh (Fig. 7.32). At the same time a distinct low is seen over Himanchal Pradesh at 300 hpa with a trough extended southward (Fig 7.48). This supports the advection of moisture carrying wind from north Arabian Sea towards the eastern side of Nepal. Overall, these charts clearly show rather rapid eastward migration of the westerly trough. From 31 March at MSL the system became weak but a low lies just south of the east and central Terai region (Fig 7.17 and 7.18). Likewise, at 850 hpa the system seems to have weakened in the morning of 31 March but slightly regain strength at 12 UTC (Fig 7.25 and 7.26). From 00 to 12 UTC on 31 March, the system completely passes from Nepal at 700 hpa and became weak (Fig 7.33 to 7.34). By 00 UTC of 31 March the westerly upper air trough at 500 hpa has clearly weakened and shifted eastward and was located over eastern hilly region of Nepal (Fig 7.41); and by 12 UTC it has completely dissipated from the eastern region and a feeble high pressure system was observed over western part of Nepal (Fig 7.42) which is conducive for commencement of the fair weather in the country from the western parts. In the same manner, at 00 UTC on 31 March a distinct upper air low was located over Tibet at 300 hpa with associated trough reaching up to eastern Nepal. Another feeble trough extends from west UP to north Arabian Sea, but by 12 UTC the weak trough had shifted eastwards. At 00 UTC on 1 April an isolated low pressure system was observed just south of eastern Terai but it became weak by 12 UTC (Fig 7.19 and 7.20). And at 850 hpa, at 00 UTC of 1 April an elongated ridge extends from J and K to central India, which shifted slightly eastwards at 12 UTC; a strong high was also observed over Bhutan (Fig 7.28). At 700 hpa, at 00 UTC of 1 April the system has dissipated from Nepal and strong westerly wind prevail just south of Nepal (Fig 7.35 and 7.36), which indicates the fair weather conditions. Likewise at 500 hpa a very weak upper air trough was seen from central Nepal to Orissa but by 12 UTC the trough has shifted eastwards and smoothly running westerly wind was observed over Nepal and Gangetic plain, which confirms the fair-weather condition (Fig 7.43). At 300 hpa, at 00 UTC westerly trough was seen over central Nepal which extends up to Orissa but by 12 UTC the trough was completely dissipated from Nepal (Fig 7.51 to 7.52).

Conclusion

The rainfall event of 31 March 2015 was caused by upper air westerly trough coming from the Mediterranean Sea. Western disturbances reached western Nepal by 12 UTC of 29 March and covered the whole country at 12 UTC of 30 March. The vertical extent of the trough was clearly observed from MSL to 300 hpa in the western Terai region and small part of eastern Terai region. The system was strong over Nepal and its vicinity at 12 UTC of 30 March, but it became weak from 12 UTC of 31 March and completely dissipated from 01 April, which can be inferred from the flow of strong westerly wind from MSL to 500 hpa. Moreover, convective activities over isolated area of the eastern region, especially in the eastern hilly and Terai regions was supported by the lower level system i.e. moisture carrying wind flowing from the Arabian Sea to central and eastern parts of Nepal. Maximum rainfall was recorded in eastern parts of Nepal (e.g. 53.9 mm in Biratnagar, 43.2 mm in Syamga) on 31 March likely due to merger of upper and lower level systems over there. As the westerly system propagated further eastwards from western Nepal from 12 UTC of 29 March, almost all part of the country received moderate type of rainfall, with imbedded isolated heavy rainfalls on 30 and 31 March, which was supported by the adequate supply of moisture in the western region and the isolated places of the central and eastern regions. Further relative vorticity played a strong supportive in the hilly region of the country than the Terai region for the development of the convective phenomena leading to orographic rainfall. Taking consideration of its contribution in the rainfall in the country, it can be concluded that the upper air westerly trough has crucial role in the western and central region and has influence in the eastern region as well by supplying the moisture carrying wind from low level system of Arabian Sea. The huge, dense cloud mass over most parts of Nepal, as seen in satellite image at 12:46 UTC of 30 March, supports moderate rainfall in the country including isolated the heavy rainfall on 31 March. Since the system was large, almost all parts of the country received moderate amount of rain. The correlation of the GPM estimated rainfall and observation rainfall was also relatively strong in the eastern Terai region and satisfactory in the eastern hilly region and isolated places of the central region but the relation was rather weak in the western region.

Finally, it was concluded that the flow of moisture was from Mediterranean sea with the driving wind of 50 Knots in upper level (300 hpa) in the western region and central region as a westerly trough but in case of the isolated places of the eastern hilly and Terai region the rainfall activities was more supportive by the convective phenomena from lower level on 30 and 31 March and no trough was observed from the of 01 April which indicates the fair weather in the country.

4.8 MWE 8 (May 12):

During this episode, thirteen out of fifteen synoptic stations received rainfall with the higher rainfall in eastern region of the country compared to western region. More than 10 mm of rainfall was recorded in the nine stations over the 24 hour period ending at 03 UTC of 12th May (Fig 8.2). This amount of rainfall in a day during pre-monsoon season can be considered relatively high when compared against the normal seasonal totals.

A comparison of the observed station rainfall with the estimated rainfall from GPM shows that the GPM estimated rainfall generally correlates well with the observed rainfall (Fig 8.2 and 8.6), however there are some disagreements between the two on few days. For example, comparison of Fig 8.4 and 8.8 shows that the observed rainfall is higher in mid- western hilly and the Himalayan regions than that estimated by GPM.

The satellite images shows the dense and overcast cloud masses in the high rainfall areas but small patches of scattered cloud masses in low rainfall areas and clear sky over the areas with no rainfall. Hence, there is a good agreement between spatio-temporal distribution of cloud and rainfall (fig 8.2 and fig 8.11).

Analysis of CAPE values shows its increment in Nepal form 10 to 11 May followed by its decrease thereafter. Rainfall is higher in the areas where the CAPE values are greater than 1000 J/kg. The CAPE value increases up to 2500 J/kg in some parts of central and western region of the country at 09 UTC of 11th May. Moreover, the CAPE values are highest in the monsoon trough areas i.e. over parts of UP, Bihar, Jharkhanda, West Bengal, Orissa, and Andhra Pradesh (Fig 8.14).

At MSL, a trough extends form central Pakistan to Delhi and west Bengal up to 12 UTC of 11th May. Although position of the trough remains almost stationary its magnitude shows noticeable diurnal variation (i.e. it deepens (intensifies) in the evening and weaken in the morning). The trough dissipates slowly after 00 UTC of 12th May. The associated trough extends up to 850 mb with the position shifting northward towards Nepal. At 00 UTC of 10th May, a deep trough extends from Northern Pakistan to adjoining parts of Rajasthan and Madhya Pradesh and to Arabian Sea via Maharashtra at 300 hpa. The associated trough extends down to 850 mb but it progressively weaken and till westwards with decreasing altitude. The trough at 300 hpa slowly moves eastward and lies over western Nepal at 12 UTC of 11th May (Fig 8.52) while the associated trough, which extends down to 850 mb, gradually weakens with the eastward movement. However, another trough is gradually developed over western parts of Tibet at mid-tropospheric level (MTL, 500 hpa), which extends to eastern Nepal and adjoining areas. This MTL trough attends its peak at 12 UTC of 11^{th} May and gradually weakens then after.

Due to the influence of the westerly trough, the associated trough exists almost up to MSL, moisture laden wind is directed towards Nepal from Arabian Sea. The moisture enters Nepal from surface to around 3km above the surface (700 hpa) as seen in fig 8.28, fig 8.29 in 850 hpa and 8.36, fig 8.37 in 700 hpa . Due to the extension of the trough extending from Tibet to adjoining eastern Nepal at MTL, and the shifting of trough to west Nepal (fig 8.52) and east Nepal fig (8.53) at upper troposhperic level, (300 hpa) , the heavy rainfall is reported throughout throughout the country on May 12. The trough dissipates 00 UTC of 12 May. From 12 UTC of 12 May, as seen in fig 8.54, 8.46, 8.38, another western disturbance extending from Pakistan to Arabian Sea exists and the associated trough extends to 850 hpa. The trough moves slightly eastward with time.

Relative vorticity at 500 hpa is generally well correlated with the observed rainfall, as. in most of the cases, the rainfall is high in the areas where the relative vorticity is also high. In particular, precipitation is high in the areas where the relative vorticity is greater than $8 * 10^{-5} S^{-1}$.

The relative humidity chart at 600 hpa shows that the relative humidity is 70- 80 % in most parts of Nepal except in western Terai region of Nepal at 00 UTC of 10^{th} May fig (8.65). The relative humidity at Nepal increases with time and it is more than 90% at most places of eastern region and central and western hilly regions up to 12 UTC of 11^{th} May. The humidity decreases slowly after 00 UTC of 12^{th} May.

To conclude, the influence of the westerly trough up to the surface and the additional moisture supply from Arabian Sea due to the influence of the trough is the main cause of Precipitation all over Nepal on May 12. Moreover, higher the relative vorticity at 500 hpa, higher is the rainfall observed.

5 CONCLUSION

While studying the synoptic features and other parameters, it is observed that there are some common features among the different major weather events. These common features are listed below:

1. During the monsoon Season, it is observed that widespread rainfall occurs in Nepal due to the shifting of monsoon trough to the north of its normal position. When the monsoon trough lies in foothills of Himalayas, heavy rainfall occurs in Nepal.
2. Moisture supply from both Bay of Bengal and Arabian Sea contributes to widespread rain in Nepal with heavy rain at a few places. Also moisture supply from Arabian Sea generally causes heavy rainfall in Nepal.
3. Westerly trough contributes for the rainfall in winter Season.
4. The interaction of westerly trough with low pressure systems migrated from BoB triggers the development of dense cloud masses with the potential for heavy rainfall.
5. Upper level system (UTL) is highly co-related with the upper level vorticity while the lower level system is highly co-related with the lower level Vorticity
6. High CAPE values (>1500 J/kg) are associated with rainfall in Nepal.

Moreover, the synoptic patterns in the same season are generally similar. The following conclusions are drawn from each of the eight major weather events.

a) The shifting of monsoon trough to the foothills of Himalayas, the extension of trough up to 500 mb is the main reason for the major weather event in August. Moreover, development of slight trough in mid-western and far western hilly regions of the country and the deeper trough in the western part of Nepal is the main reason for the heavy rainfall event in western Nepal on 14^{th} and 15^{th} August.

b) The westerly trough extending from 300 hpa to surface and the moisture supply from Arabian Sea along with high cape values and high vorticity at all levels is the cause of heavy precipitation during the May 12 major weather event.

c) The vertical extension of trough from 850 mb to 300 mb is the main cause of precipitation for the MWE in February. As the trough is situated near Nepal, precipitation is high in Nepal. As the trough is deeper in western Nepal than that in eastern Nepal, precipitation is higher in western Nepal than in eastern Nepal. One interesting feature noted is that vorticity at 300 hpa is well co-relate with the precipitation at the surface.

d) The widespread rain over Nepal on 11th and 12th September was caused by proximity of the monsoon trough from southern parts of Nepal. Synoptic analysis based on the reanalysis data reveals that northward shifting of the monsoon trough from its normal position and the persistence of low over north U.P and adjoining north M.P create the conducive environment for yielding rain over Nepal. Besides that the southeasterly wind triggered rain bearing clouds over the hilly region due to which significant rain was observed mainly over the eastern hilly region. Moreover streamlines analysis of 700 hpa chart reveals a low pressure system over Pokhara region on 10th and 11th September when significant isolated rainfall was recorded in the MWE of September 11.

e) Upper air charts (300 and 500 hpa) of 13th October show that the MWE of 14th and 15th October is caused by the interaction of eastward propagating upper air westerly trough with a northwestward propagating well marked low at lower level, which is the remnants of cyclone Hud Hud. The well-marked low, with organized cyclonic circulation up to the 700 hpa, is situated over U.P and the adjoining west plain of Nepal, it and was coupled with a feeble upper air trough at 300 hpa. The system generated heavy precipitation mainly over the western region of the country and widespread rainfall throughout the country Apart from the geopotential and wind analysis, the clear picture of coupling of two air masses is also revealed by the analysis of 600 hpa relative humidity. The vigor of the remnants is due to the unification of the two air masses.

f) The MWE in January is caused by the proximity of the trough from west Nepal on 2nd January 2015. The trough is clearly seen drifting towards northwest India in the lower atmosphere and wind is oriented from Arabian Sea to U.P and west Nepal. As a result, substantial amount of moisture is transported towards the western Nepal and the supply of moisture yielded light to moderate rain in the plains but heavy rain and snow fall over the high altitude areas because of the orographic affects on 2nd January.

g) During MWE of March, the vertical extent of the trough was clearly observed from MSL to 300 hpa, which was stronger in the western region than the eastern region. The relative humidity was more than 80% - 90% in the western region and the isolated places of the central and eastern regions, which was favorable for heavy rainfall. The relative vorticity was also positive, which supports the heavy rainfall.

h) The MWE on 19th July was caused by a deep trough situated near west Nepal, which is extended vertically from MSL to 500 hpa, The wind pattern, which follows the pressure pattern, helped the moisture supply from the Arabian Sea and the BOB branches up to 500 hpa. The relative humidity of 600 hpa at 00 UTC of 18th July shows that the adequate amount of moisture was available for heavy rainfall in the far western and southern central parts of Nepal. The relative vorticity was strongly positive at 12 UTC of 18th and 00 UTC of 19th July, which supported heavy rainfall on 19th July.

Bibliography

Bharti, V. (2015). *Investigation of the Extreme Rainfall Events Over the NorthWest Himalaya Region Using Satellite Data.*

Christidis Nikolaos, S. P. (2015). Extreme Rainfall in the United Kingdom during winter 2013/14:the role of Atmospheeric Circulation and climate change DOI.

Daniel G Huber, J. G. (2011). Exteme Weather and Climate Change:Understanding the Link and Managing the Risk. *Science*.

Doswell III, A. C. (1980). Synoptic scale environments associated with high plains severe thunderstorms. *American Meteorological Society*.

Government of Nepal, M. o. (2015). *Nepal Disaster report 2015.*

Krishnamurthy, V. (2011). Extreme Events and Trends in Indian Monsoon.

Nickel, E. M. (2009). *The impact of Extreme Weather Events on Budget Balance and implication for Fiscal Policy.*

O.S.R.U. Bhanu Kumar, P. S. (2012). Simulation of Heavy rainfall events during retreat phase of Summer Monsoon Season over Parts of Andhra Pradesh. *International Journal of Geo- Science*.

Olivier Deschenes, E. M. (2007). *Extreme Weather Events, Mortality, and Migration.*

Pfahl, S. (2014). Characterising the relationship between weather extremes in Europe and synoptic scale circulation patterns.

R Vautard, G.-J. O.-M. (n.d.). Extreme fall 2014 Precipitaion in the cevennes Mountains. *2015*.

S. D. Kotal, S. S. (2014). Catastrophic heavy rainfall episode over Uttarakhand during 16–18 June 2013 –Observational Aspects. *Current science*.

S.D kotal, S. S. (2014). Catastrophic heavy rainfall episode over Uttarakhanda during 16-18 june 2013 Observational aspects.

Schneider, M. (n.d.). Investigation pf Heavy Rainfall Events in the Sau Paulo region After the Peak of the Severe Drought of 2014 -2015 .

Siswanto Oldenborgh, G. J. (2014). Trends in high-daily precipation precipitaion events in Jakarta and the flooding of january . *Agency of Meteorology*.

Suresh raj Chalise, N. R. (2002). Recent Extreme Weather events in Nepal and Himalayas. *The Extreme of Extremes: Extra Ordinary Floods*.

ANNEXES

Annex 1: Charts used for the study of MWE 1 (17-20 July 2014)

24 hour accumulated gauge rainfall ending at 03 UTC **Unit: mm**	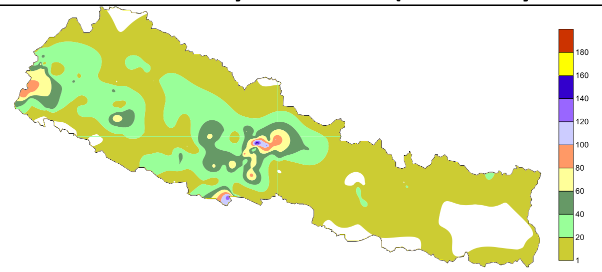 Fig 1.1 18 July	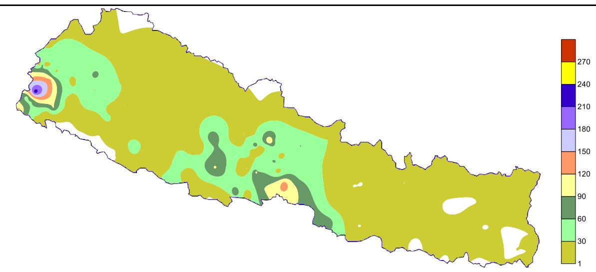 Fig 1.2 19 July	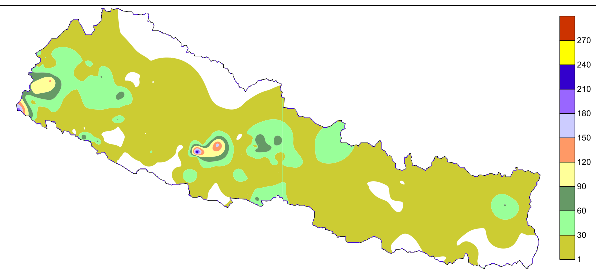 Fig 1.3 20 July	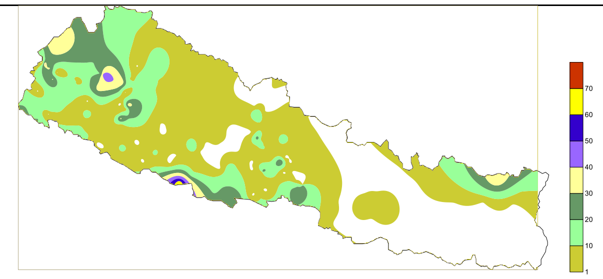 Fig 1.4 21 July
24 hour accumulated estimated rainfall from GPM ending at 03 UTC **Unit: mm**	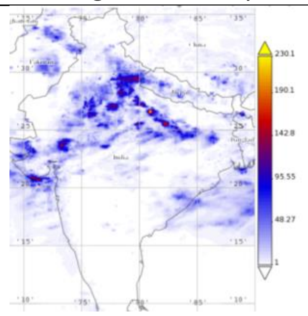 Fig 1.5 18 July	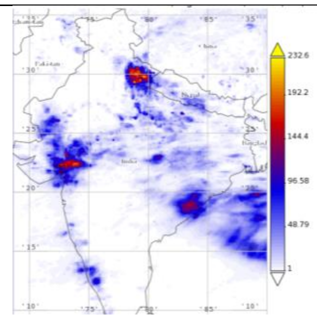 Fig 1.6 19 July	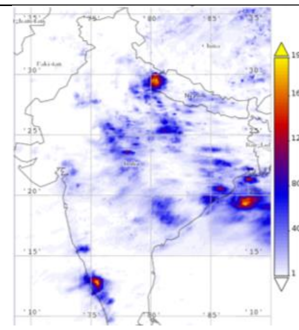 Fig 1.7 20 July	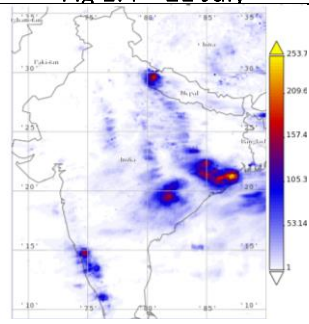 Fig 1.8 21 July
Infra-Red Satellite images **Unit: Unit less**	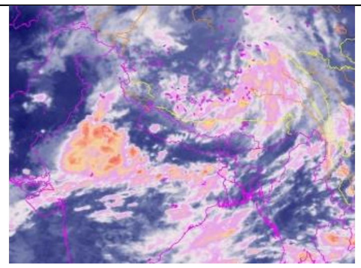 Fig 1.9 12:46 UTC, 17 July	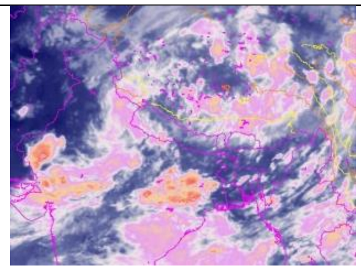 Fig 1.10 12:46 UTC, 18 July	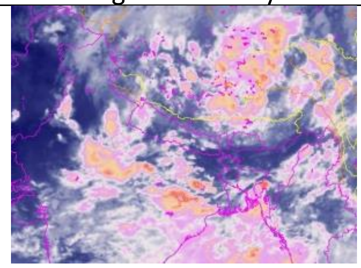 Fig 1.11 12:46 UTC, 19 July	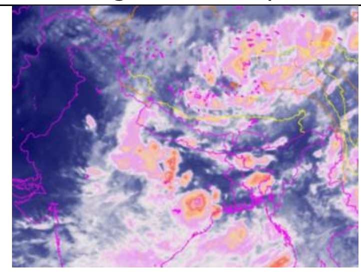 Fig 1.12 12:46 UTC, 20 July
Cape values **Unit : J/kg**	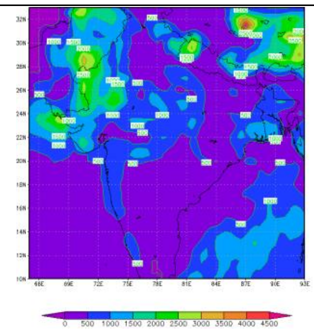 Fig 1.13 09 UTC, 17 July	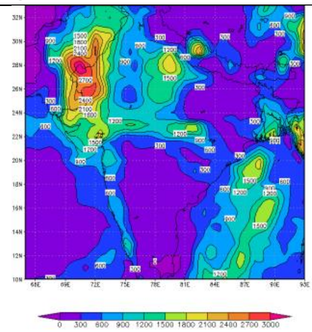 Fig 1.14 09 UTC, 18 July	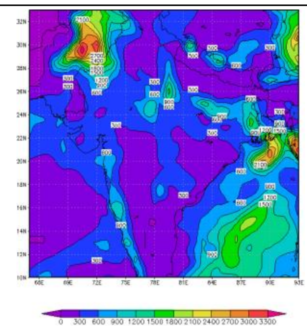 Fig 1.15 09 UTC, 19 July	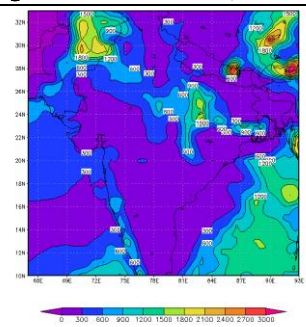 Fig 1.16 09 UTC, 20 July
MSLP **Unit: hpa**	**00 UTC, 17 July** 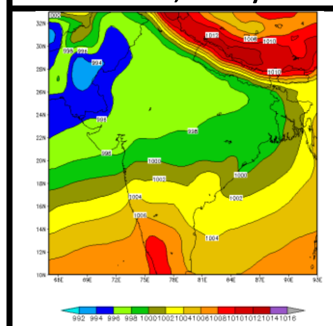 Fig 1.17 **12 UTC, 17 July** 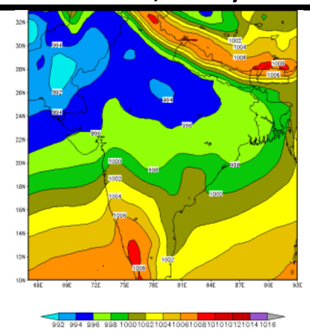 Fig 1.18	**00 UTC, 18 July** 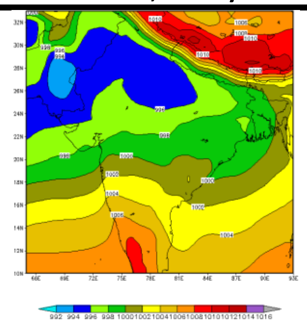 Fig 1.19 **12 UTC, 18 July** 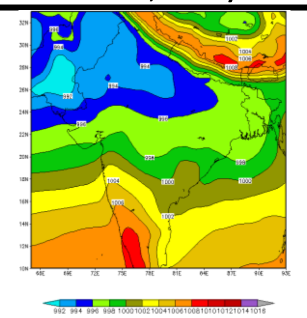 Fig 1.20	**00 UTC, 19 July** 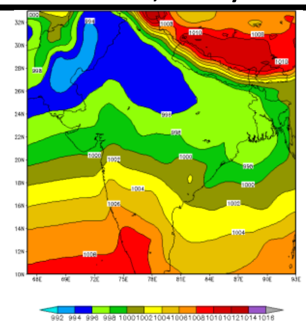 Fig 1.21 **12 UTC, 19 July** 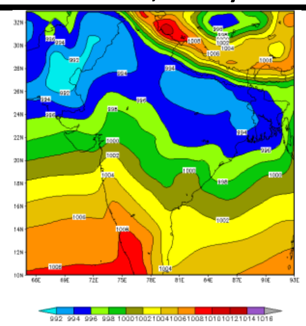 Fig 1.22	**00 UTC, 20 July** 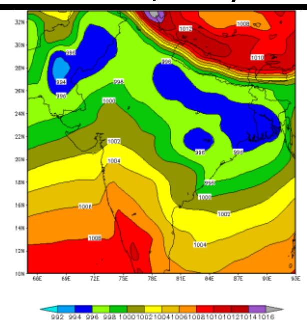 Fig 1.23 **12 UTC, 20 July** 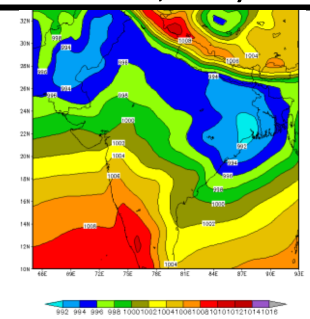 Fig 1.24

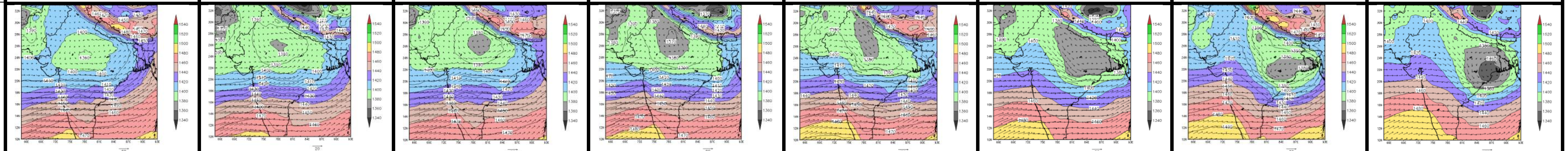

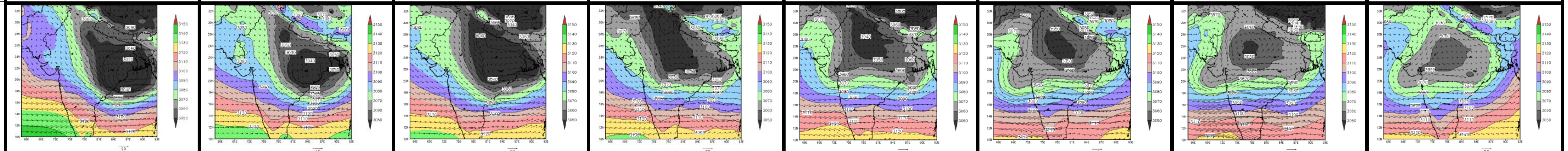

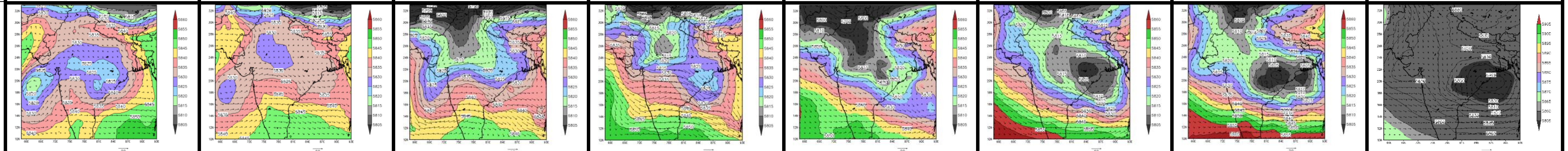

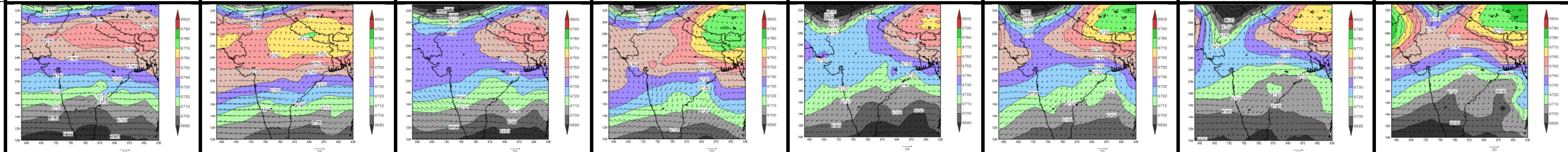

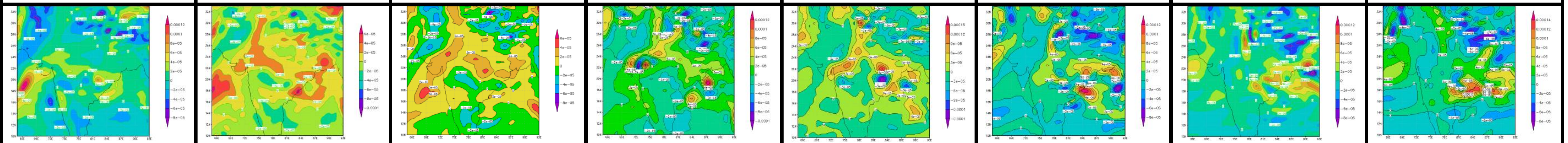

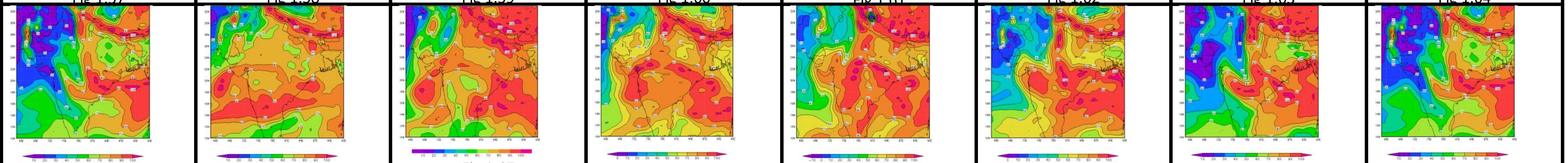

	00 UTC, 17 July	12 UTC, 17 July	00 UTC, 18 July	12 UTC, 18 July	00 UTC, 19 July	12 UTC, 19 July	00 UTC, 20 July	12 UTC, 20 July
Wind and gptm at 850 hpa **Unit: m/s and m**	Fig 1.25	Fig 1.26	Fig 1.27	Fig 1.28	Fig 1.29	Fig 1.30	Fig 1.31	Fig 1.32
Wind and gptm at 700 hpa **Unit: m/s and m**	Fig 1.33	Fig 1.34	Fig 1.35	Fig 1.36	Fig 1.37	Fig 1.38	Fig 1.39	Fig 1.40
Wind and gptm at 500 hpa **Unit: m/s and m**	Fig 1.41	Fig 1.42	Fig 1.43	Fig 1.44	Fig 1.45	Fig 1.46	Fig 1.47	Fig 1.48
Wind and gptm at 300 hpa **Unit: m/s and m**	Fig 1.49	Fig 1.50	Fig 1.51	Fig 1.52	Fig 1.53	Fig 1.54	Fig 1.55	Fig 1.56
Relative vorticity at 500 hpa **Unit: s^{-1}**	Fig 1.57	Fig 1.58	Fig 1.59	Fig 1.60	Fig 1.61	Fig 1.62	Fig 1.63	Fig 1.64
Relative humidity at 600 hpa **Unit: %**	Fig 1.65	Fig 1.66	Fig 1.67	Fig 1.68	Fig 1.69	Fig 1.70	Fig 1.71	Fig 1.72

Annex 2: Charts used for the study of MWE 2 (12-16 August 2014)

24 hour accumulated gauge rainfall ending at 03 UTC **Unit: mm**	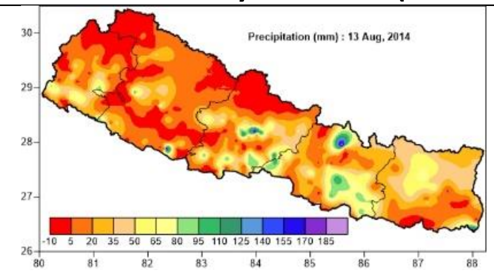 Fig 2.1 13 August		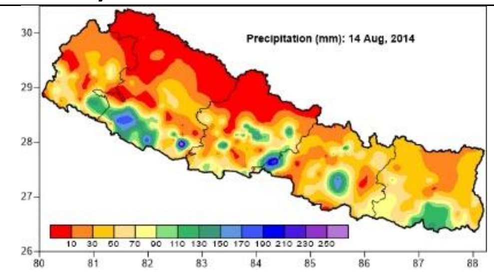 Fig 2.2 14 August		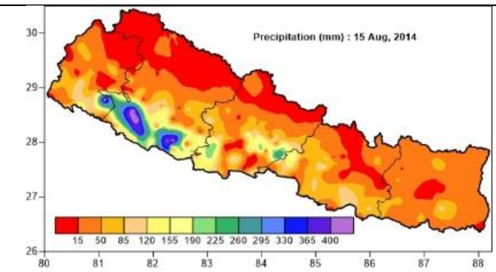 Fig 2.3 15 August		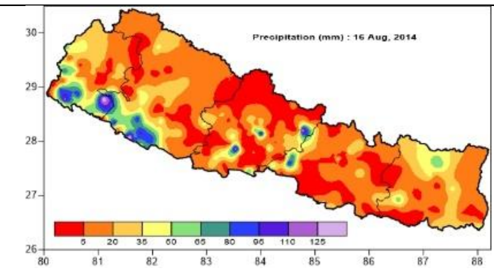 Fig 2.4 16 August		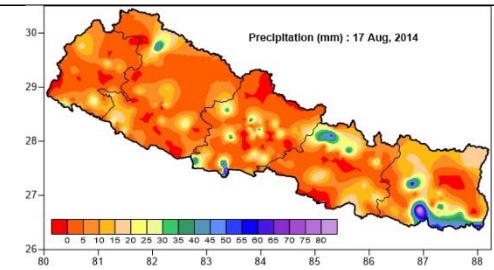 Fig 2.5 17 August	
24 hour accumulated estimated rainfall from GPM ending at 03 UTC **Unit: mm**	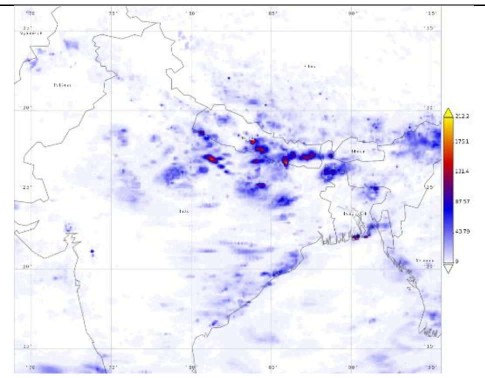 Fig 2.6 13 August		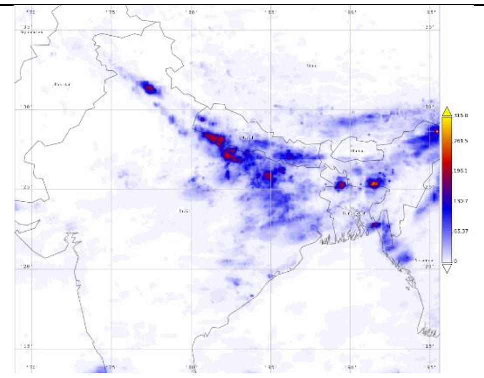 Fig 2.7 14 August		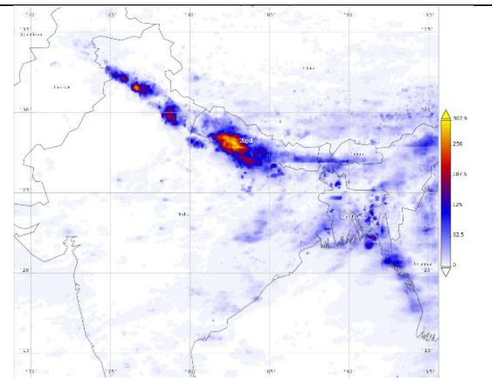 Fig 2.8 15 August		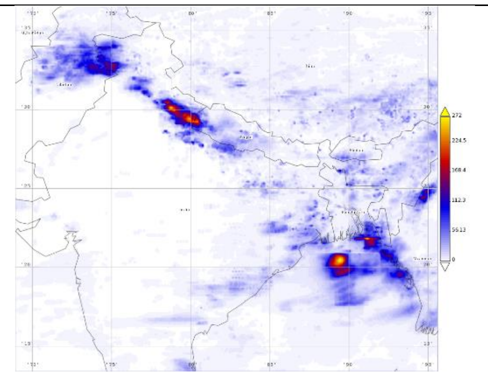 Fig 2.9 16 August		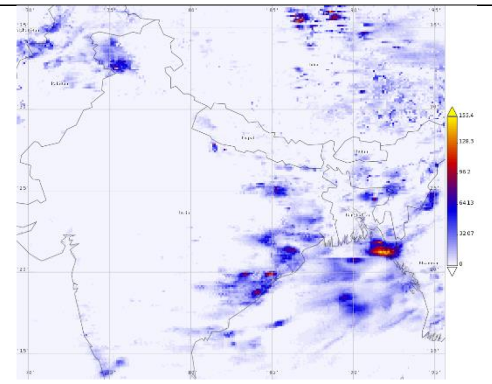 Fig 2.10 17 August	
Infra-red Satellite imageries **Unit: Unit less**	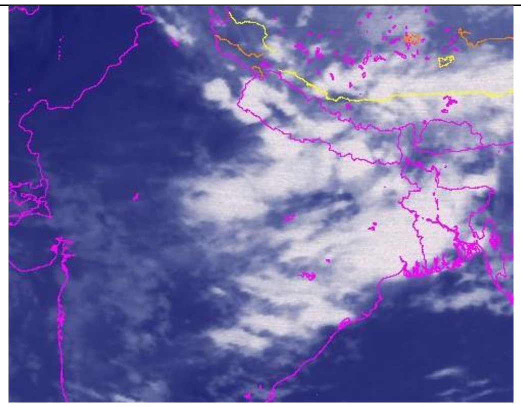 Fig 2.11 14:16 UTC, 13 August		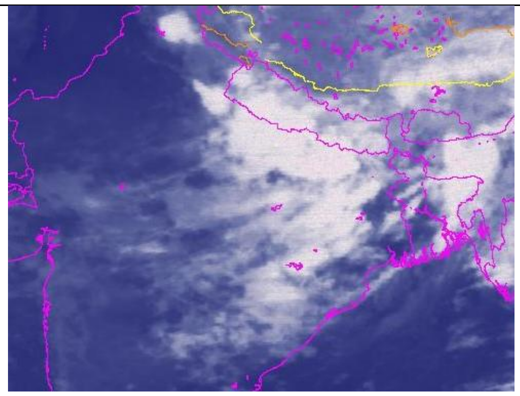 Fig 2.12 20:45 UTC, 13 August		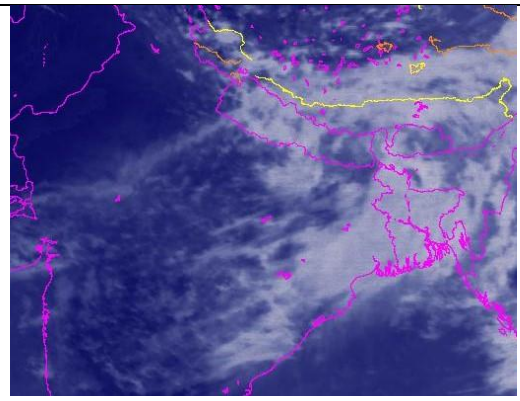 Fig 2.13 10:16 UTC, 14 August		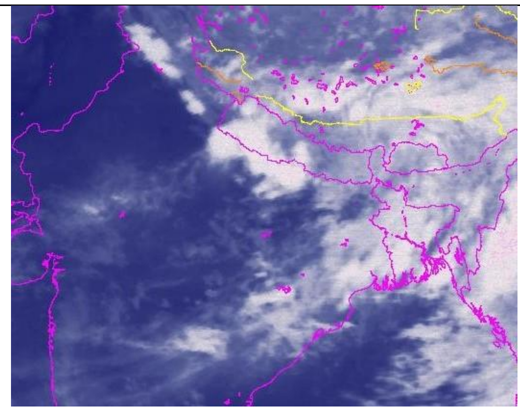 Fig 2.14 15:16 UTC, 14 August		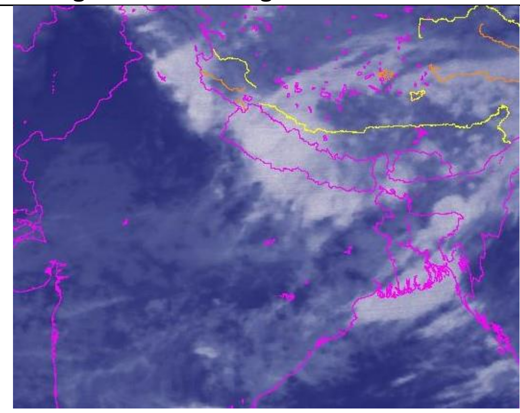 Fig 2.15 00:45 UTC, 15 August	
	00 UTC, 12 August	**12 UTC, 12 August**	**00 UTC, 13 August**	**12 UTC, 13 August**	**00 UTC, 14 August**	**12 UTC, 14 August**	**00 UTC, 15 August**	**12 UTC, 15 August**	**00 UTC, 16 August**	**12 UTC, 16 August**
MSLP **Unit: hpa**	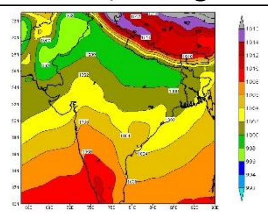 Fig 2.16	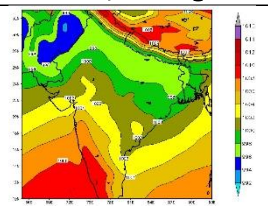 Fig 2.17	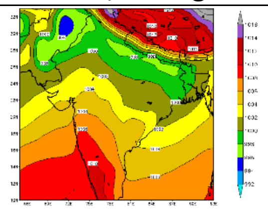 Fig 2.18	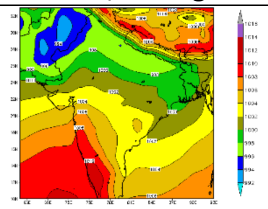 Fig 2.19	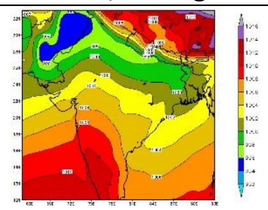 Fig 2.20	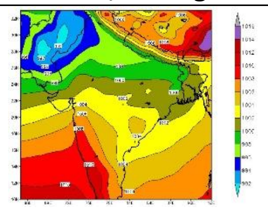 Fig 2.21	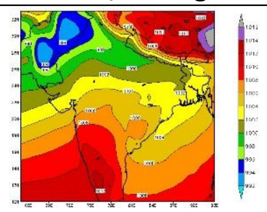 Fig 2.22	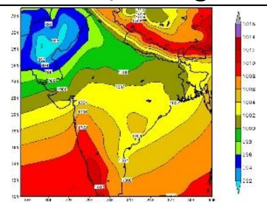 Fig 2.23	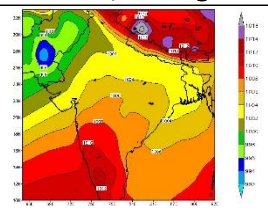 Fig 2.24	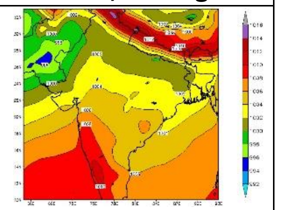 Fig 2.25
Wind and gptm at 850 hpa **Unit: m/s and m**	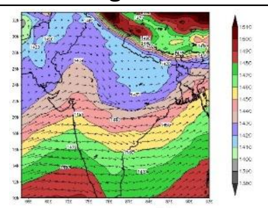 Fig 2.26	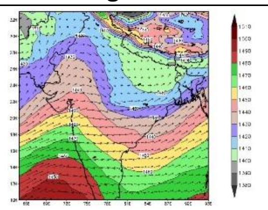 Fig 2.27	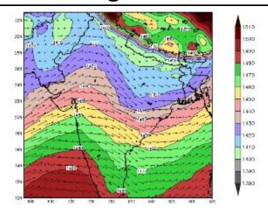 Fig 2.28	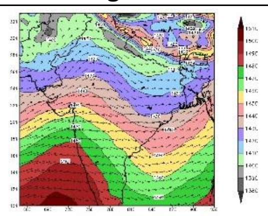 Fig 2.29	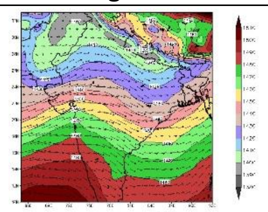 Fig 2.30	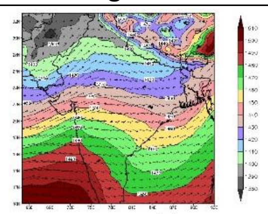 Fig 2.31	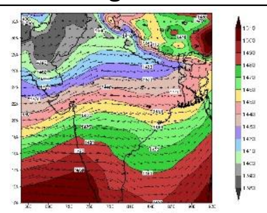 Fig 2.32	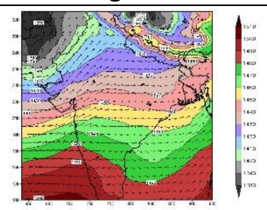 Fig 2.33	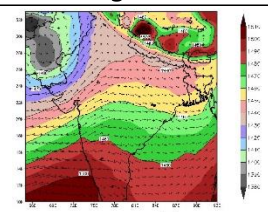 Fig 2.34	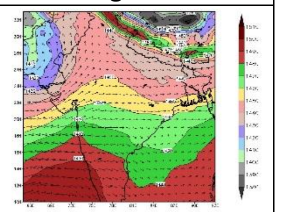 Fig 2.35

	00 UTC, 12 August	12 UTC, 12 August	00 UTC, 13 August	12 UTC, 13 August	00 UTC, 14 August	12 UTC, 14 August	00 UTC, 15 August	12 UTC, 15 August	00 UTC, 16 August	12 UTC, 16 August
Wind and gptm at 700 hpa **Unit: m/s and m**	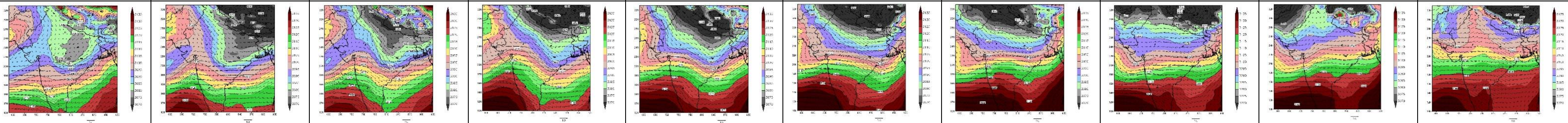 Fig 2.36	Fig 2.37	Fig 2.38	Fig 2.39	Fig 2.40	Fig 2.41	Fig 2.42	Fig 2.43	Fig 2.44	Fig 2.45
Wind and gptm at 500 hpa **Unit: m/s and m**	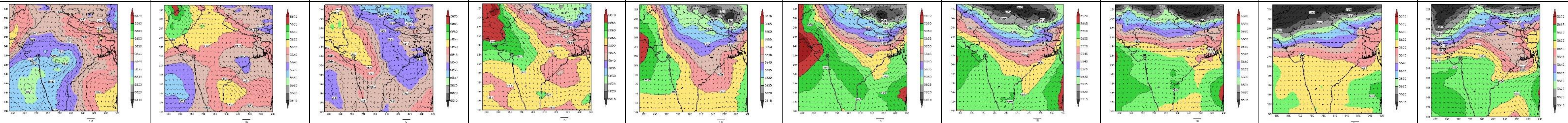 Fig 2.46	Fig 2.47	Fig 2.48	Fig 2.49	Fig 2.50	Fig 2.51	Fig 2.52	Fig 2.53	Fig 2.54	Fig 2.55
Wind and gptm at 300 hpa **Unit: m/s and m**	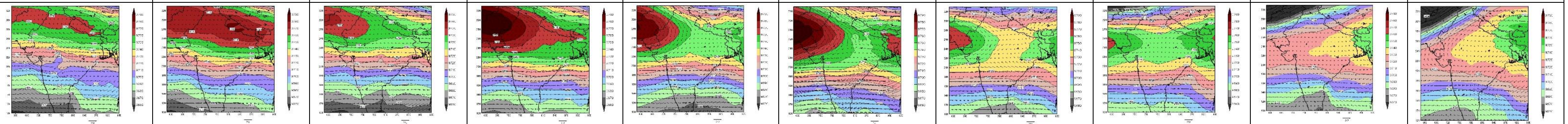 Fig 2.56	Fig 2.57	Fig 2.58	Fig 2.59	Fig 2.60	Fig 2.61	Fig 2.62	Fig 2.63	Fig 2.64	Fig 2.65
Relative Vorticity at 850 hpa **Unit: $X10^{-5}s^{-1}$**	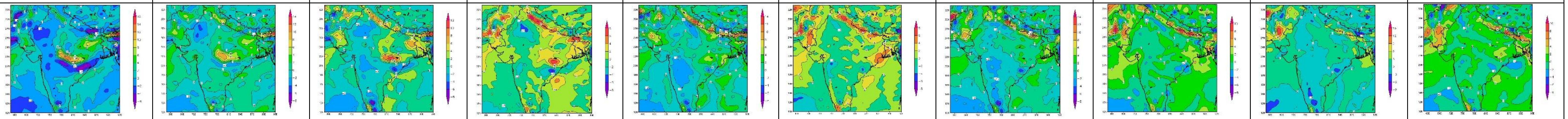 Fig 2.66	Fig 2.67	Fig 2.68	Fig 2.69	Fig 2.70	Fig 2.71	Fig 2.72	Fig 2.73	Fig 2.74	Fig 2.75
Relative humidity at 600 hpa **Unit: %**	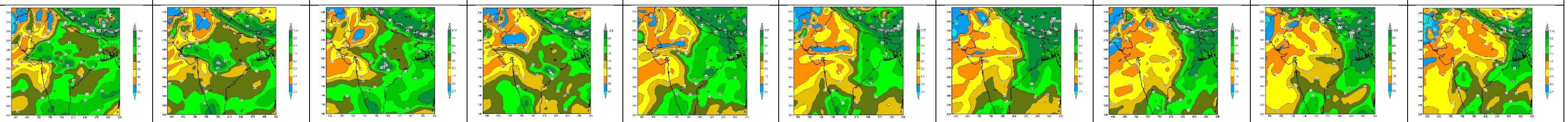 Fig 2.76	Fig 2.77	Fig 2.78	Fig 2.79	Fig 2.80	Fig 2.81	Fig 2.82	Fig 2.83	Fig 2.84	Fig 2.85

Annex 3: Charts Used for the study of MWE 3 (9-12 September 2014)

	9 September		10 September		11 September		12 September	
24 hour accumulated gauge rainfall ending at 03 UTC **Unit: mm**	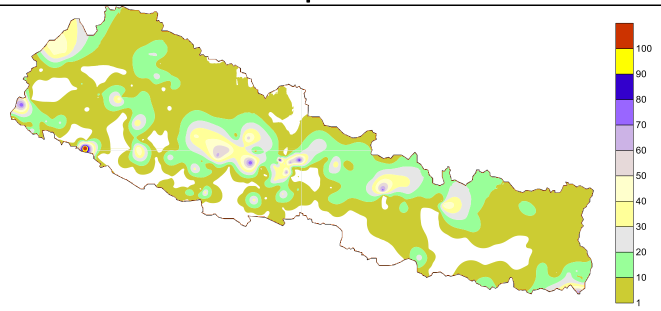 Fig 3.1		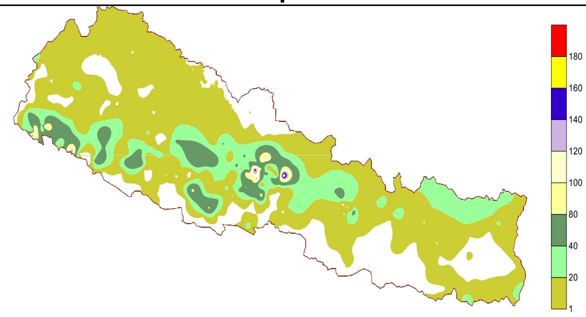 Fig 3.2		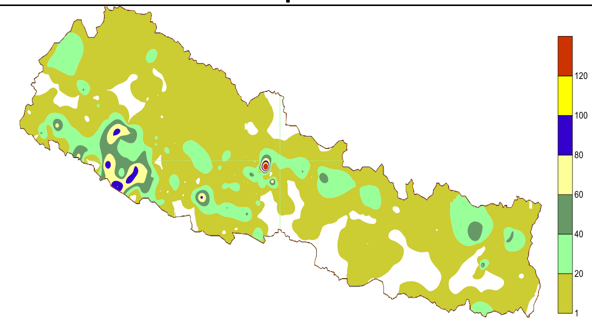 Fig 3.3		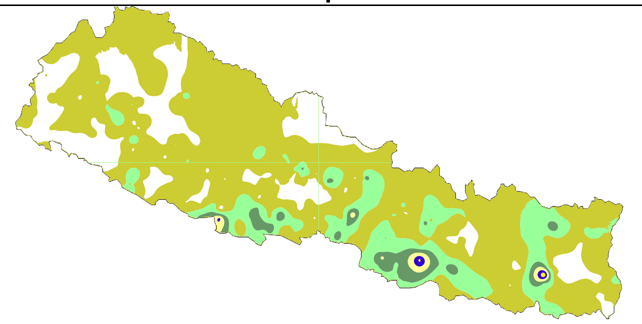 Fig 3.4	
24 hour accumulated estimated rainfall from GPM ending at 03 UTC **Unit: mm**	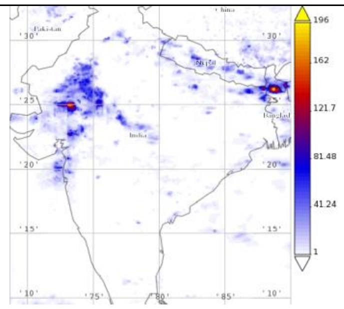 Fig 3.5		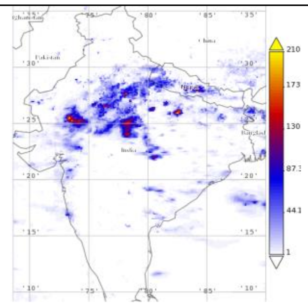 Fig 3.6		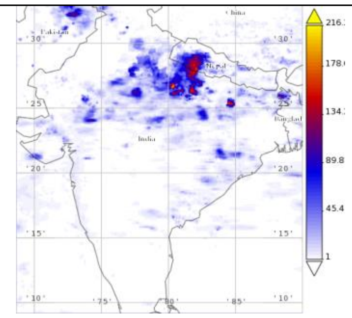 Fig 3.7		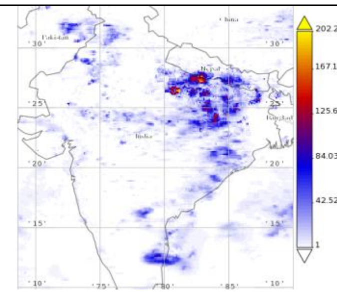 Fig 3.8	
Infra-Red Satellite images **Unit: unit less**	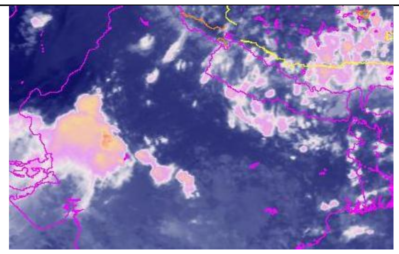 Fig 3.9 10:31 UTC		 Fig 3.10 21:31 UTC		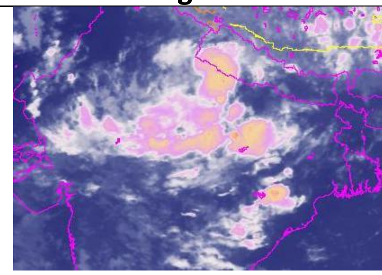 Fig 3.11 14:31 UTC		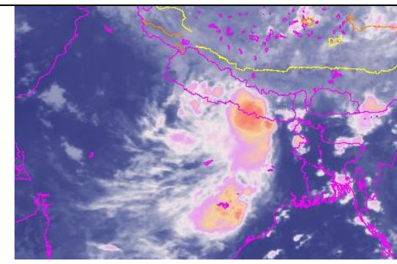 Fig 3.12 20:30 UTC	
	00 UTC, 9 September	12 UTC, 9 September	00 UTC , 10	12 UTC , 10 September	00 UTC, 11 September	12 UTC , 11 September	00 UTC, 12 September	12 UTC , 12 Septemb
MSLP **Unit: hpa**	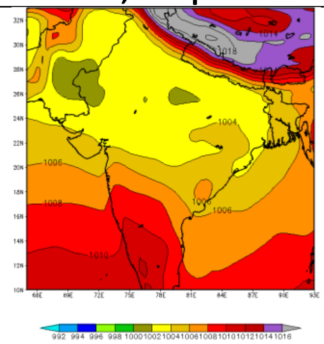 Fig 3.13	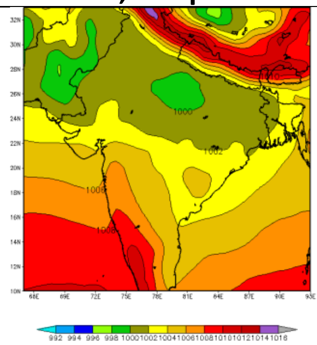 Fig 3.14	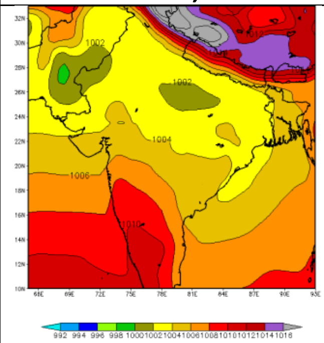 Fig 3.15	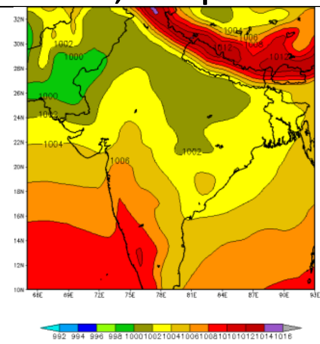 Fig 3.16	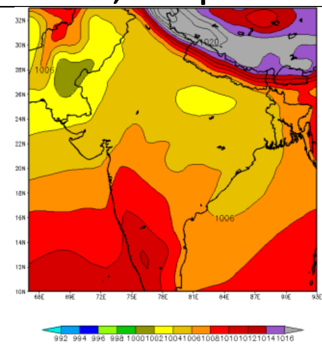 Fig 3.17	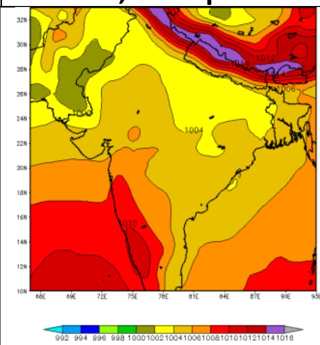 Fig 3.18	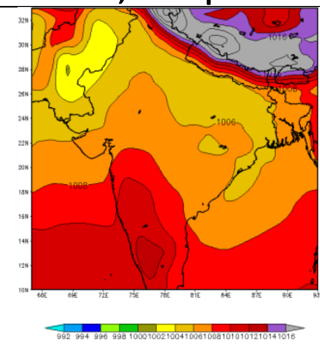 Fig 3.19	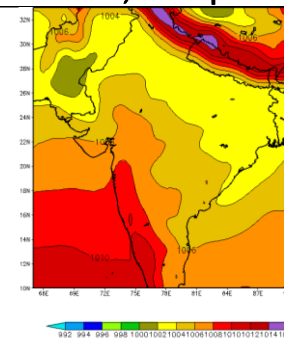 Fig 3.20
Wind and gptm at 850 hpa **Unit: m/s and m**	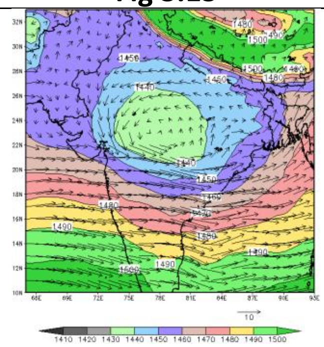 Fig 3.21	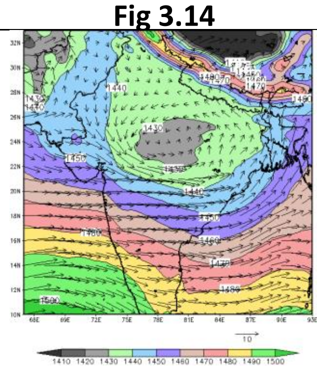 Fig 3.22	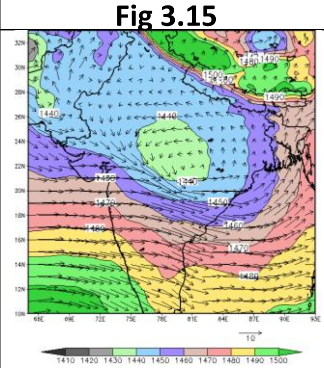 Fig 3.23	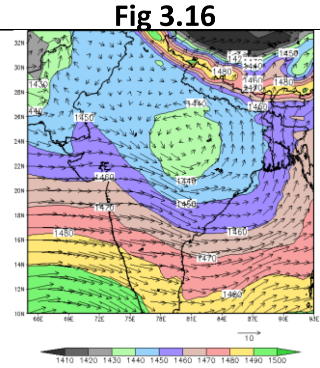 Fig 3.24	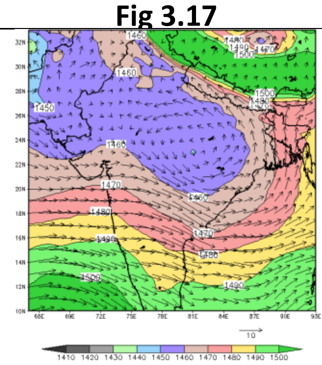 Fig 3.25	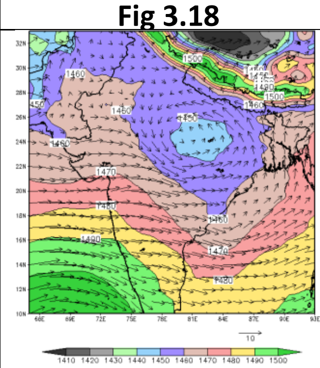 Fig 3.26	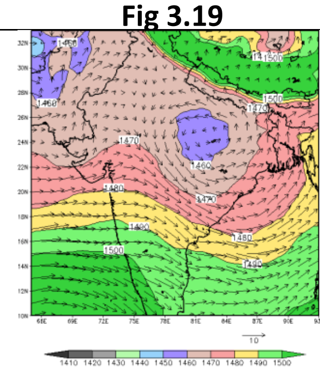 Fig 3.27	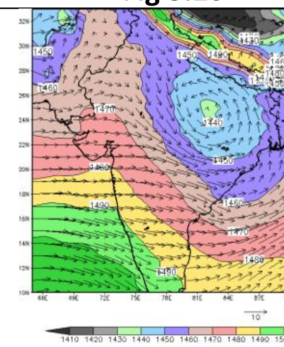 Fig 3.28

	00 UTC, 9 September	12 UTC, 9 September	00 UTC, 10 September	12 UTC, 10 September	00 UTC, 11 September	12 UTC, 11 September	00 UTC, 12 September	12 UTC, 12 September
Wind and gptm at 700 hpa **Unit: m/s and m**	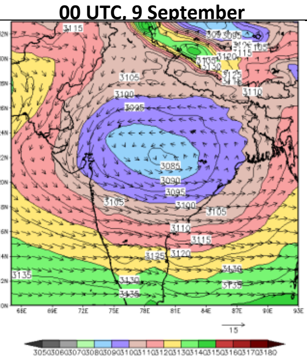 Fig 3.29	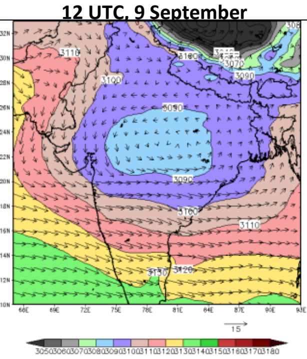 Fig 3.30	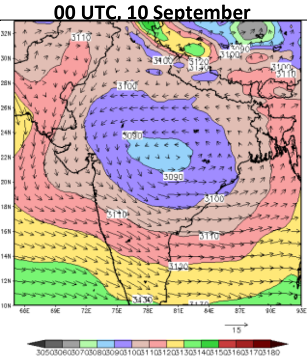 Fig 3.31	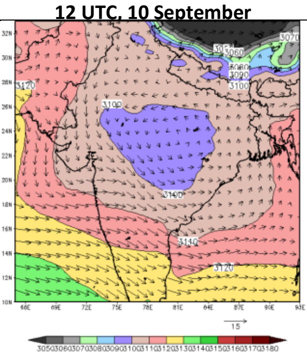 Fig 3.32	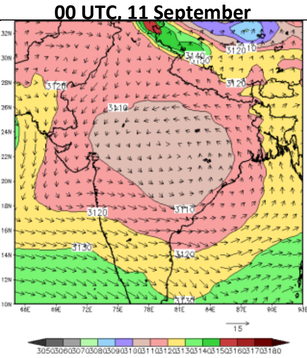 Fig 3.33	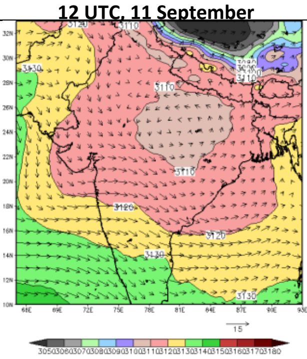 Fig 3.34	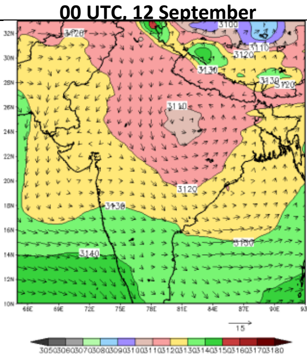 Fig 3.35	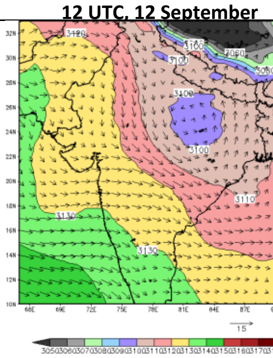 Fig 3.36
Wind and gptm at 500 hpa **Unit: m/s and m**	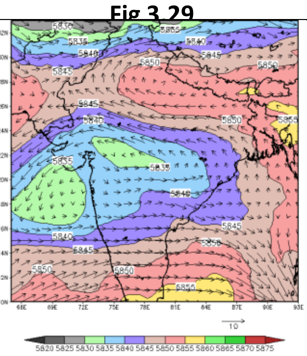 Fig 3.37	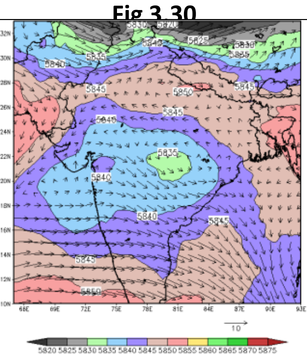 Fig 3.38	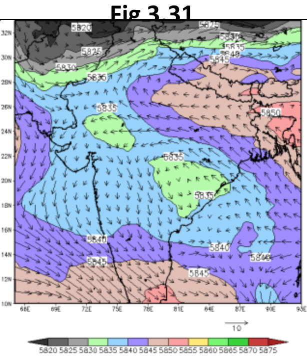 Fig 3.39	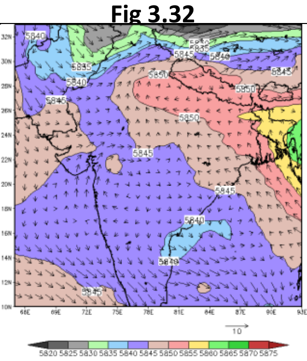 Fig 3.40	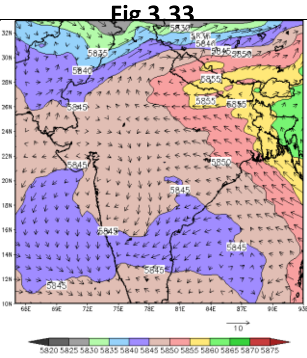 Fig 3.41	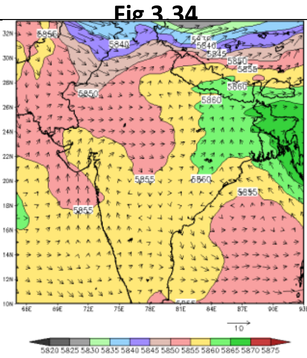 Fig 3.42	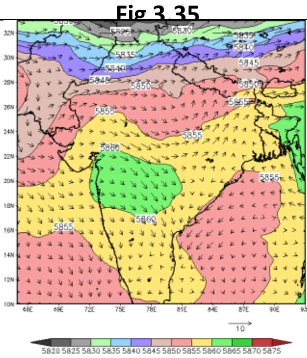 Fig 3.43	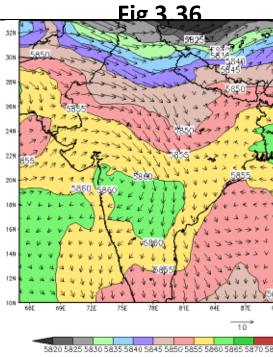 Fig 3.44
Wind and gptm at 300 hpa **Unit: m/s and m**	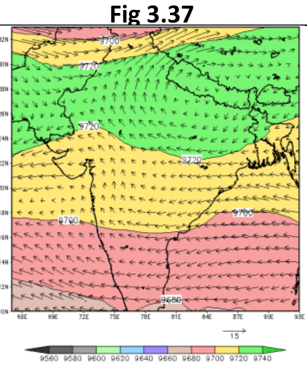 Fig 3.45	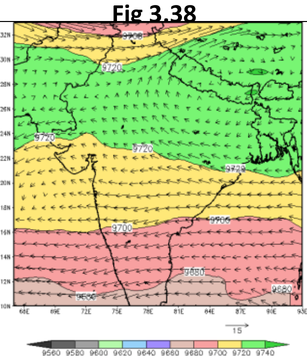 Fig 3.46	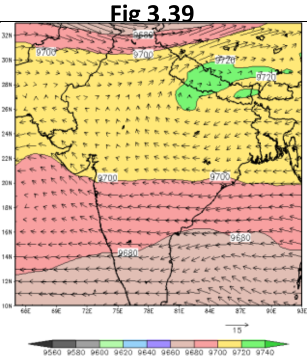 Fig 3.47	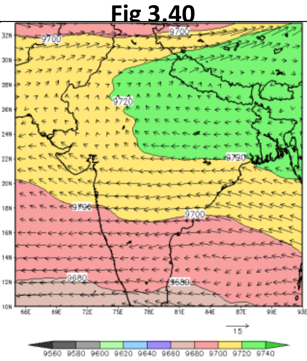 Fig 3.48	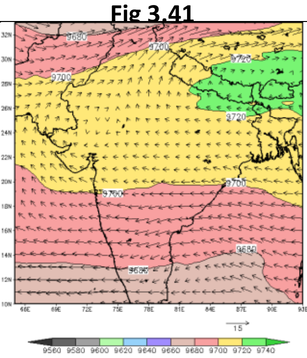 Fig 3.49	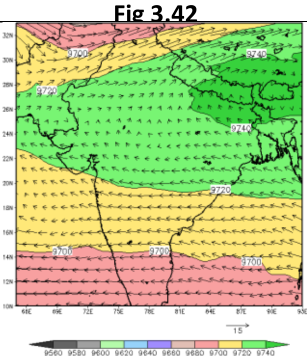 Fig 3.50	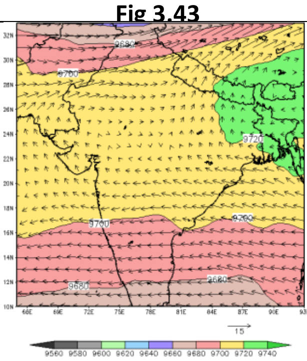 Fig 3.51	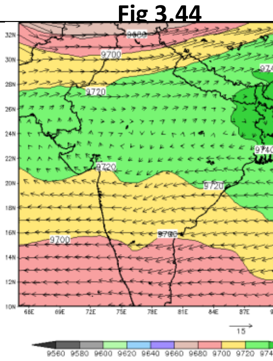 Fig 3.52
Relative Vorticity and streamline at 500 hpa **Unit:** **X10^{-5} s^{-1}**	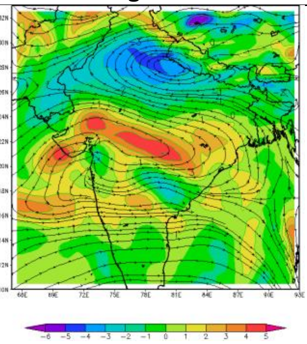 Fig 3.53	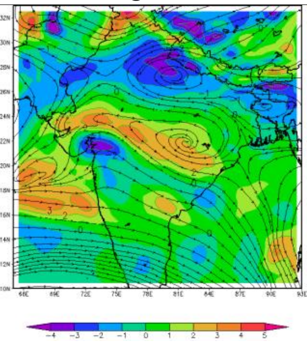 Fig 3.54	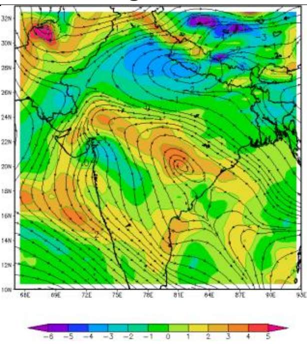 Fig 3.55	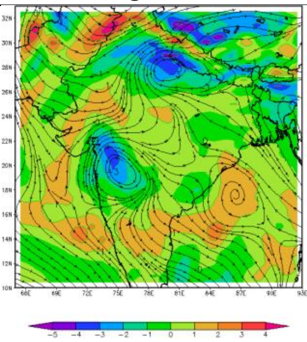 Fig 3.56	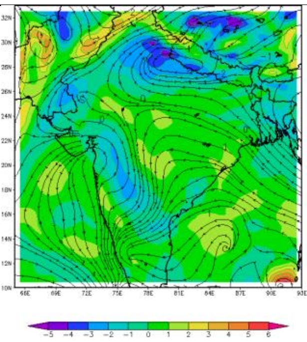 Fig 3.57	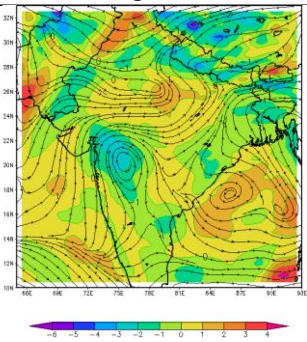 Fig 3.58	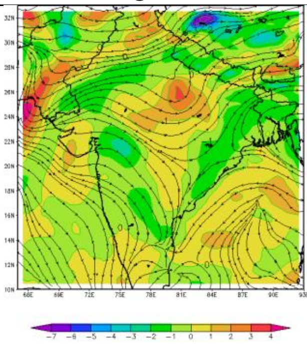 Fig 3.59	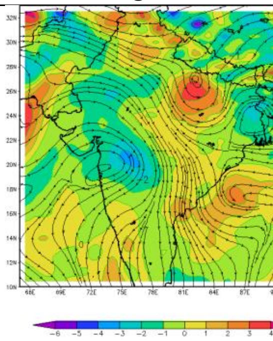 Fig 3.60
Relative humidity at 600 hpa **Unit: %**	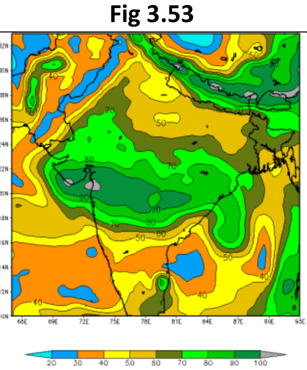	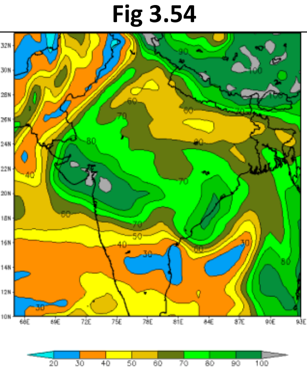	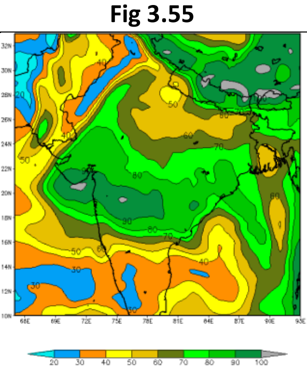	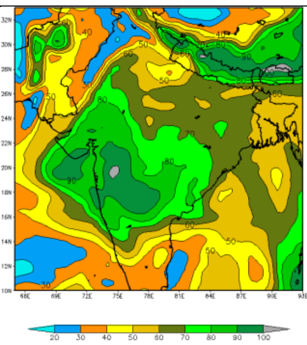	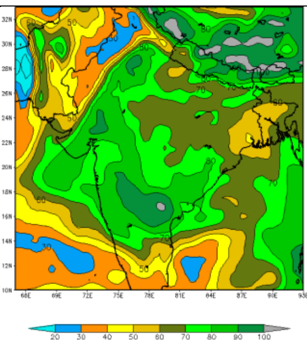	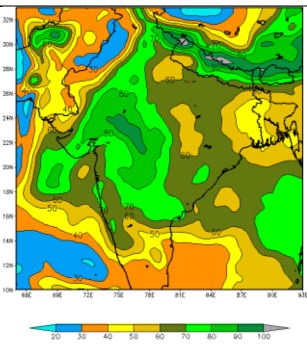	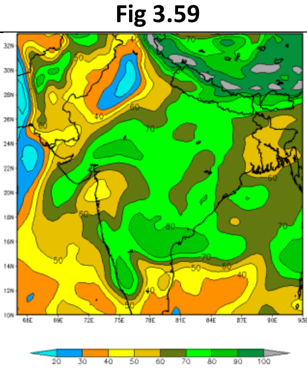	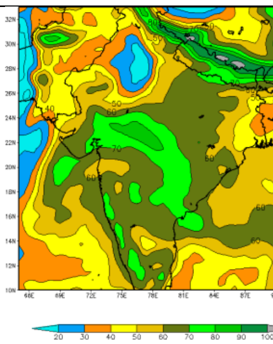

Annex 4: Charts Used for the MWE 4 (12-16 October 2014)

	12 October		13 October		14 October		15 October		16 October	
24 hour accumulated gauge rainfall ending at 03 UTC **Unit: mm**	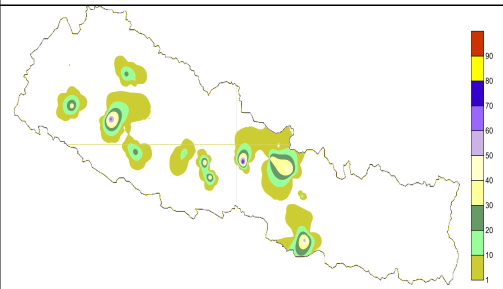 **Fig 4.1**		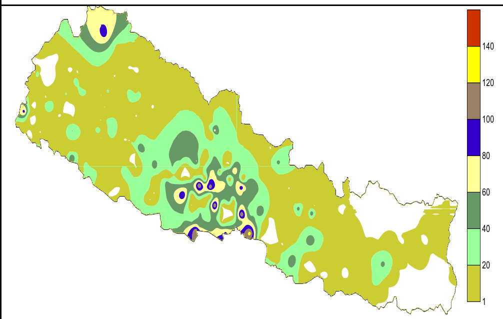 **Fig 4.2**		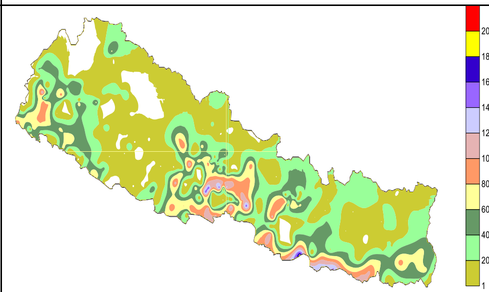 **Fig 4.3**		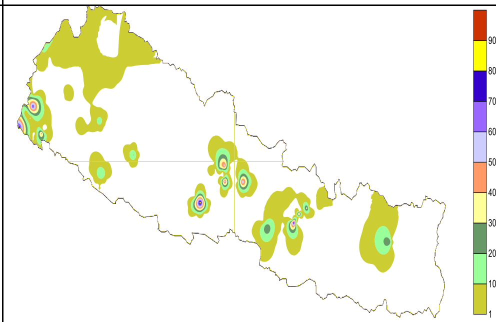 **Fig 4.4**		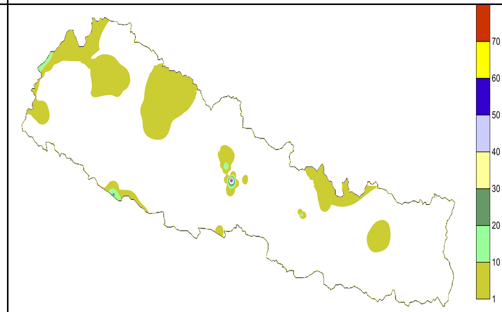 **Fig 4.5**	
24 hour accumulated estimated rainfall from GPM ending at 03 UTC **Unit: mm**	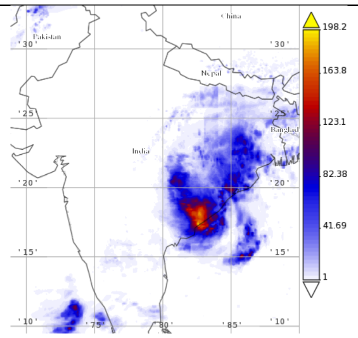 **Fig 4.6**		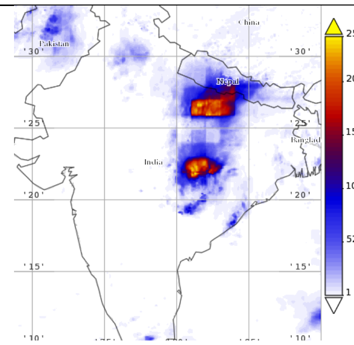 **Fig 4.7**		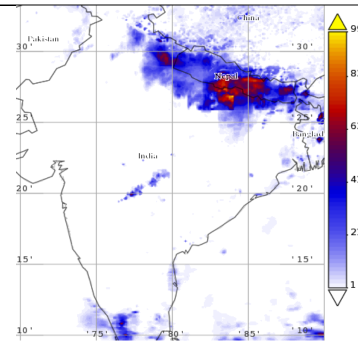 **Fig 4.8**		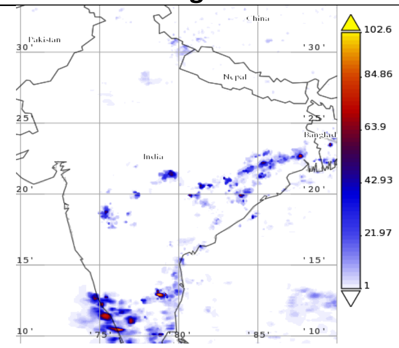 **Fig 4.9**		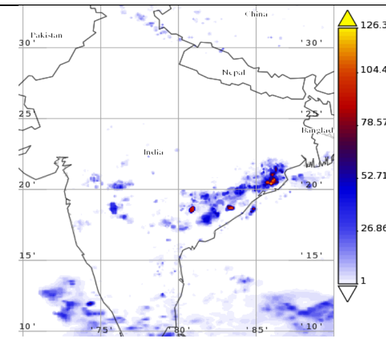 **Fig 4.10**	
Infra-red Satellite images **Unit: unit less**	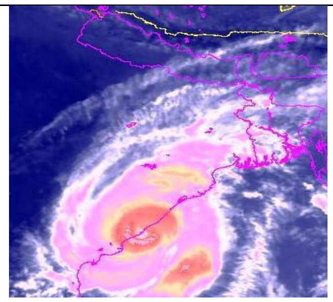 **Fig 4.11 05:32 UTC 12 October**		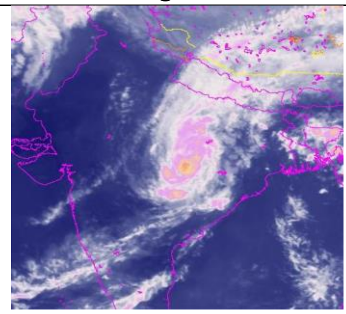 **Fig 4.12 12:02 UTC 13 October**		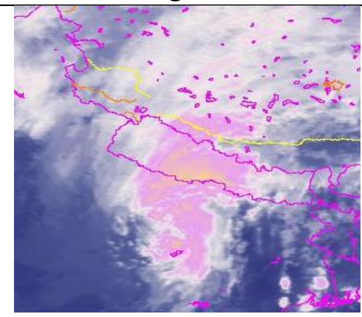 **Fig 4.13 02:02 UTC 14 October**		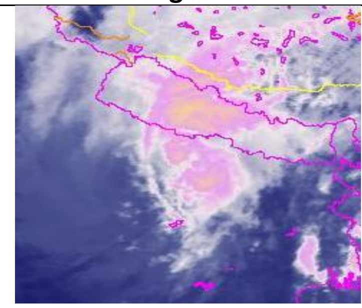 **Fig 4.14 5:32 UTC 14 October**		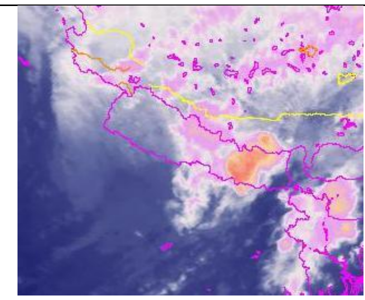 **Fig 4.15 11:32 UTC 14 October**	
	00 UTC, 12 October	**12 UTC, 12 October**	**00 UTC, 13 October**	**12 UTC, 13 October**	**00 UTC 14, October**	**12 UTC, 14 October**	**00 UTC, 15 October**	**12 UTC, 15 October**	**00 UTC, 16 October**	**12 UTC, 16 October**
MSLP **Unit: hpa**	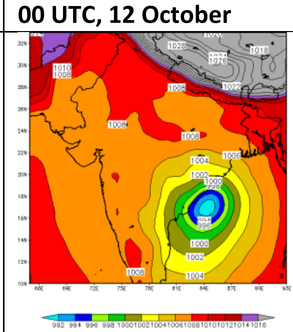 **Fig 4.16**	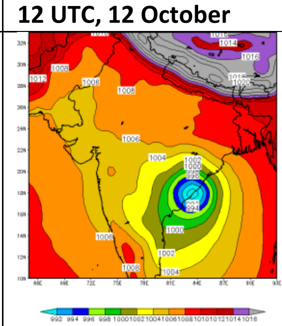 **Fig 4.17**	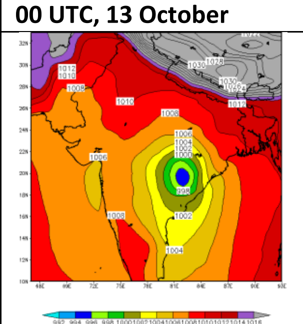 **Fig 4.18**	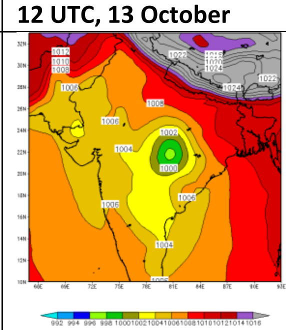 **Fig 4.19**	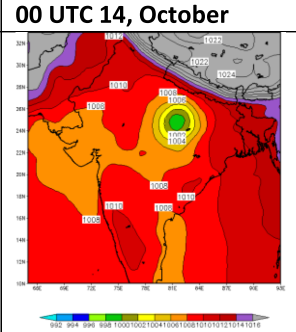 **Fig 4.20**	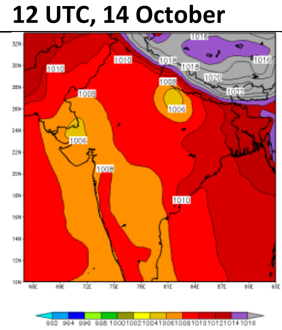 **Fig 4.21**	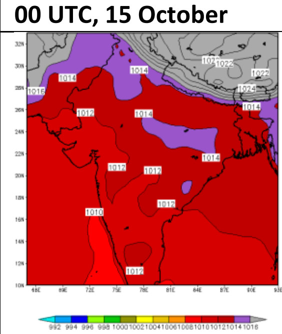 **Fig 4.22**	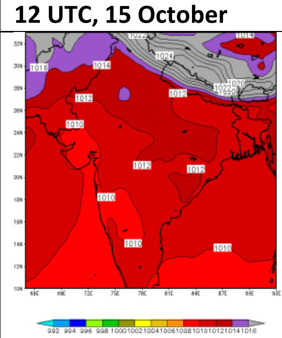 **Fig 4.23**	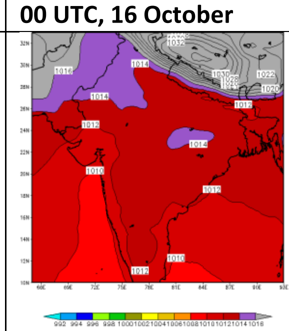 **Fig 4.24**	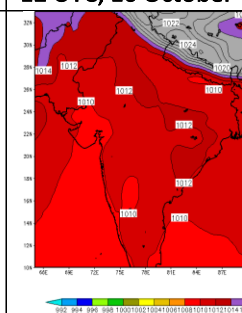 **Fig 4.25**
Wind and gptm at 850 hpa **Unit: m**	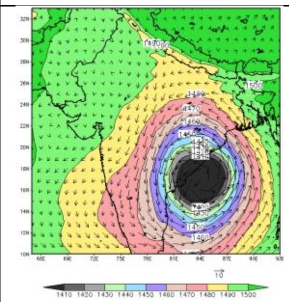 **Fig 4.26**	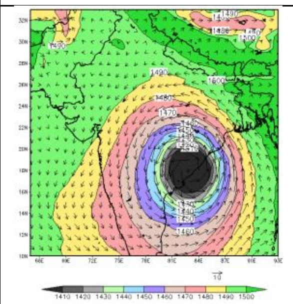 **Fig 4.27**	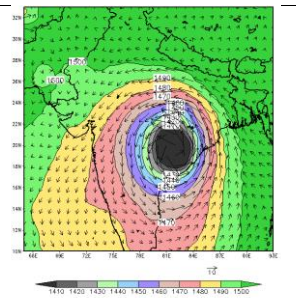 **Fig 4.28**	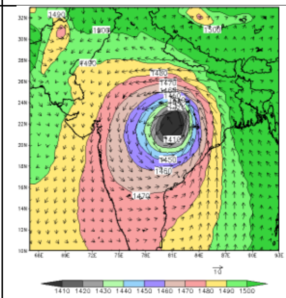 **Fig 4.29**	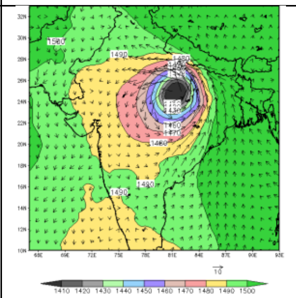 **Fig 4.30**	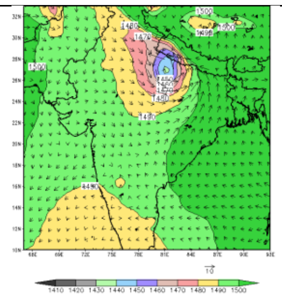 **Fig 4.31**	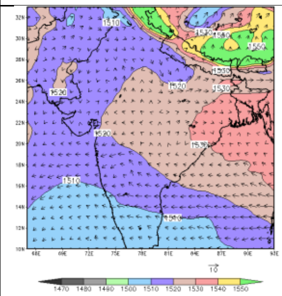 **Fig 4.32**	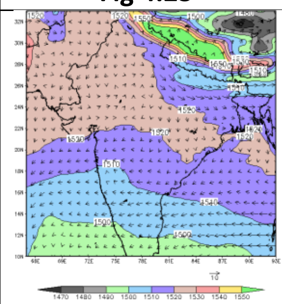 **Fig 4.33**	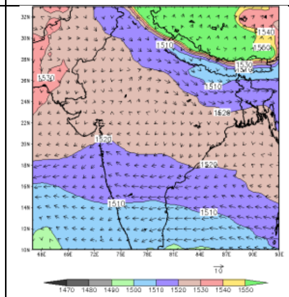 **Fig 4.34**	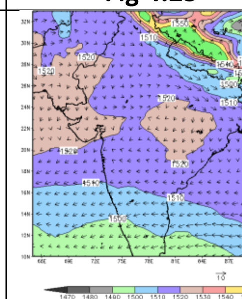 **Fig 4.35**

	00 UTC, 12 October	12 UTC, 12 October	00 UTC, 13 October	12 UTC, 13 October	00 UTC, 14 October	12 UTC, 14 October	00 UTC, 15 October	12 UTC, 15 October	00 UTC, 16 October	12 UTC, 16 October
Wind and gptm at 700 hpa Unit: m/s and m 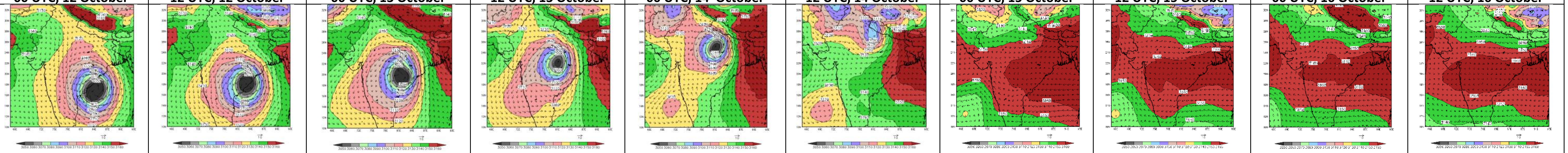	Fig 4.36	Fig 4.37	Fig 4.38	Fig 4.39	Fig 4.40	Fig 4.41	Fig 4.42	Fig 4.43	Fig 4.44	Fig 4.45
Wind and gptm at 500 hpa Unit: m/s and m 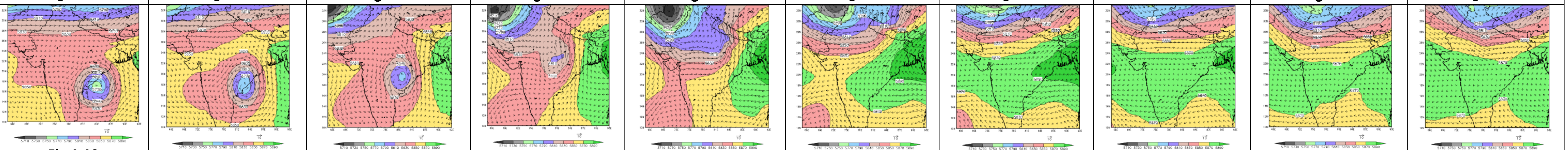	Fig 4.46	Fig 4.47	Fig 4.48	Fig 4.49	Fig 4.50	Fig 4.51	Fig 4.52	Fig 4.53	Fig 4.54	Fig 4.55
Wind and gptm at 300 hpa Unit: m/s and m 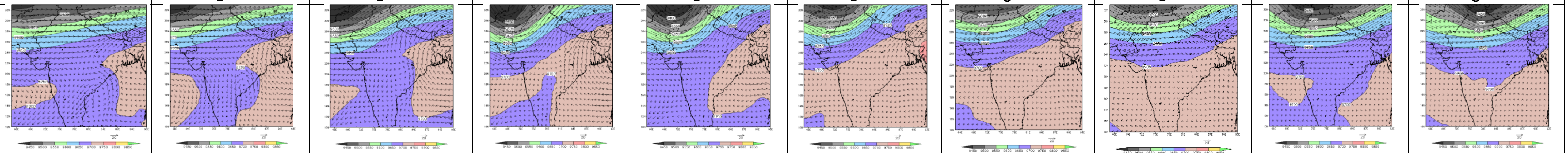	Fig 4.56	Fig 4.57	Figure 4.58	Fig 4.59	Fig 4.60	Fig 4.61	Fig 4.62	Fig 4.63	Fig 4.64	Fig 4.65
Relative Vorticity at 500 hpa Unit: s^{-1} 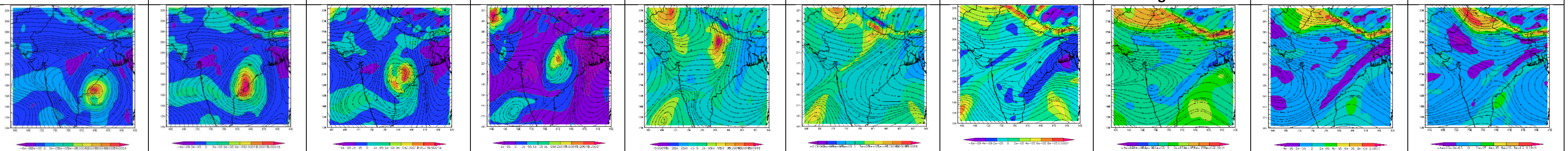	Fig 4.66	Fig 4.67	Fig 4.68	Fig 4.69	Fig 4.70	Fig 4.71	Fig 4.72	Fig 4.73	Fig 4.74	Fig 4.75
Relative humidity at 600 hpa Unit: % 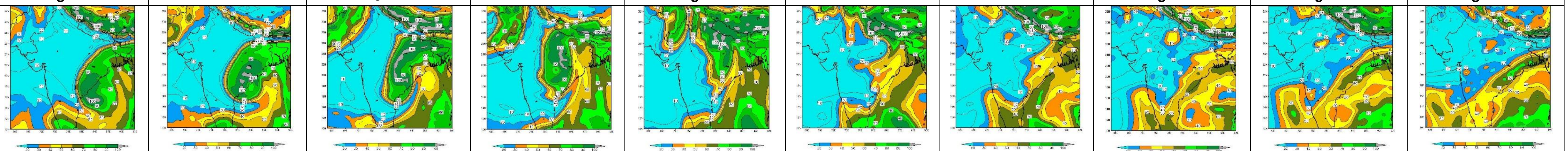	Fig 4.76	Fig 4.77	Fig 4.78	Fig 4.79	Fig 4.80	Fig 4.81	Fig 4.82	Fig 4.83	Fig 4.84	Fig 4.85

Annex 5: Charts Used for the MWE 5 (31 December-5anuary 2015)

	31 December, 2014	1 January, 2015	2 January	3 January	4 January	5 January
24 hour Accumulated gauge rainfall ending at 03 UTC Unit: mm	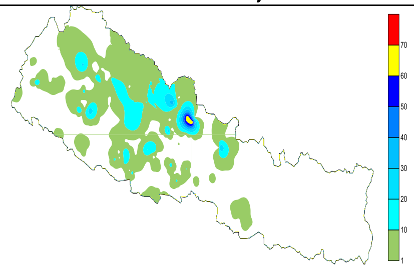 Fig 5.1	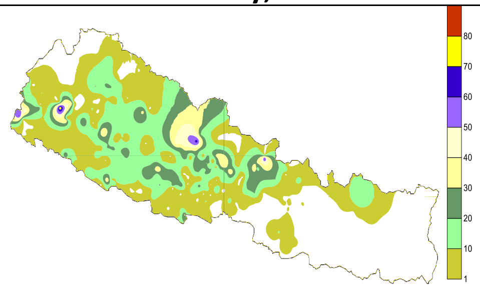 Fig 5.2	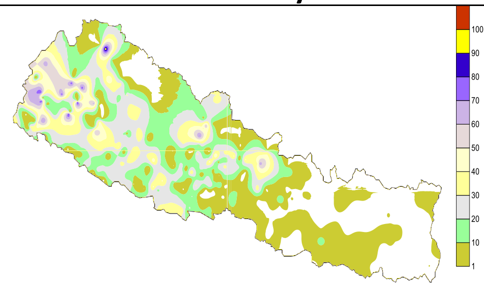 Fig 5.3	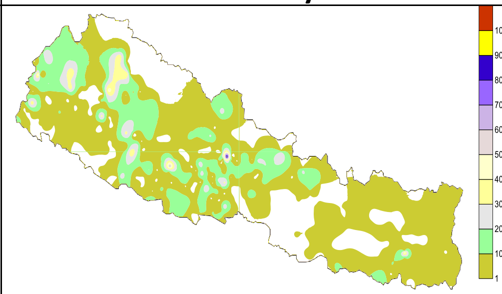 Fig 5.4	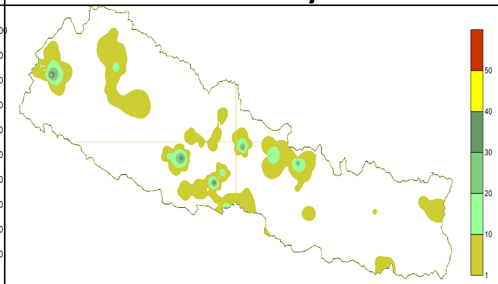 Fig 5.5	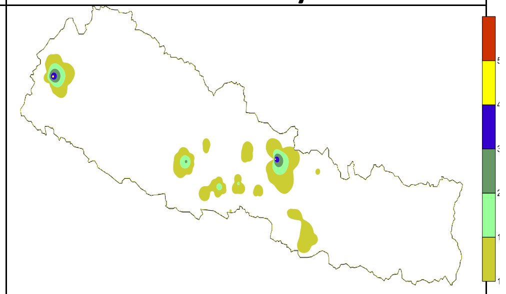 Fig 5.6
24 hour accumulated estimated rainfall from GPM ending at 03 UTC Unit: mm	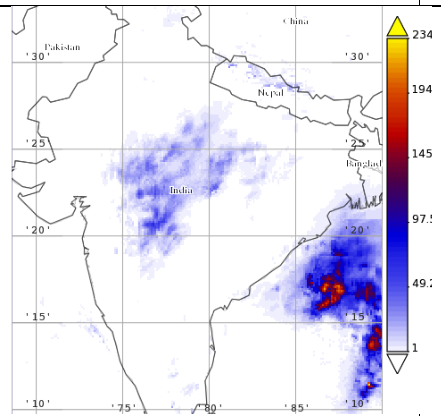 Fig 5.7	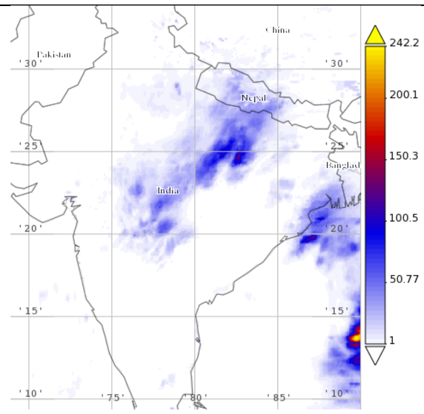 Fig 5.8	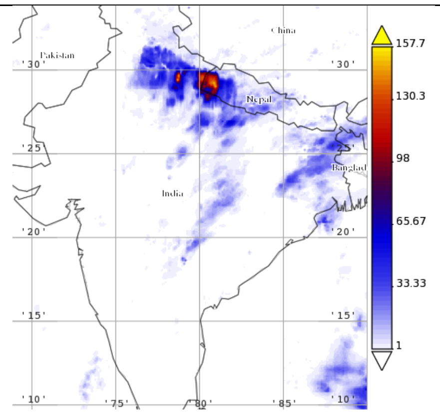 Fig 5.9	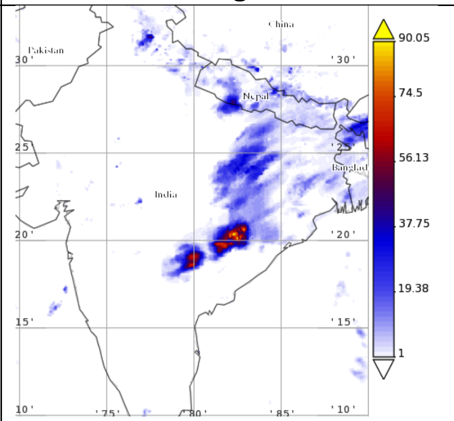 Fig 5.10	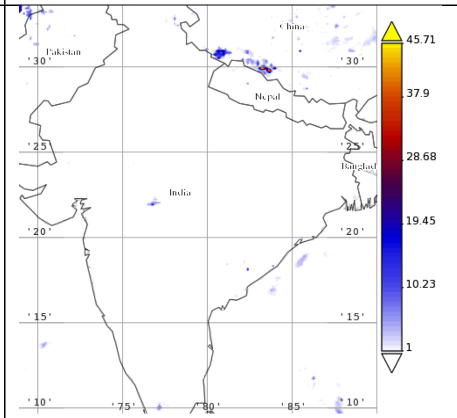 Fig 5.11	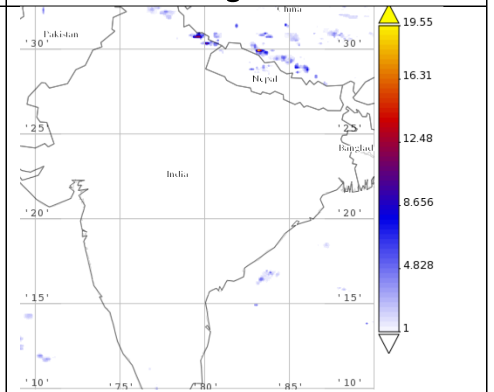 Fig 5.12
Infra-red Satellite images Unit: unit less	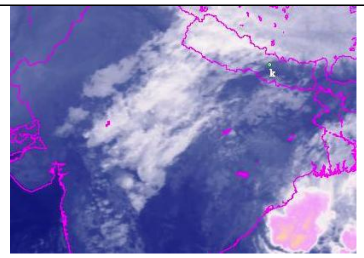 Fig 5.13 20:31 UTC	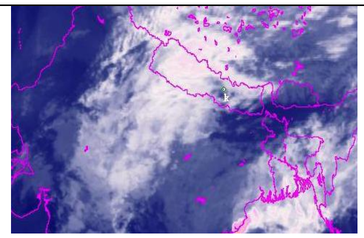 Fig 5.14 09:30 UTC	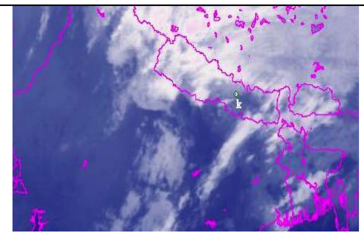 Fig 5.15 22:31 UTC	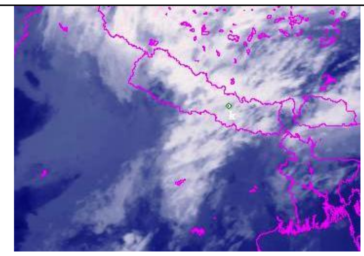 Fig 5.16 06:30 UTC	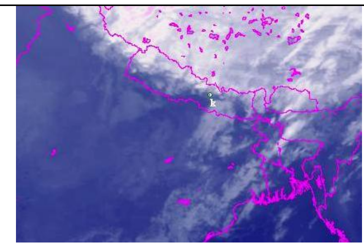 Fig 5.17 01:30 UTC	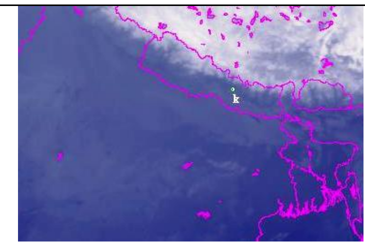 Fig 5.18 02:30 UTC

	12 UTC, 31 December	00 UTC, 1 January	12 UTC , 1 January	00 UTC , 2 January	12 UTC , 2 January	00 UTC , 3 January	12 UTC , 3 January	00 UTC , 4 January	12 UTC , 4 January	00 UTC , 5 January
MSLP Unit: hpa	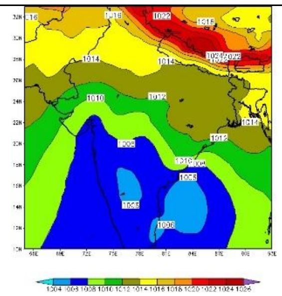 Fig 5.19	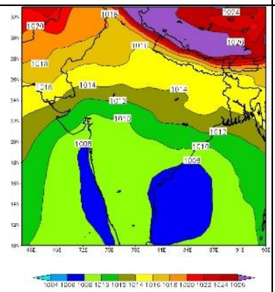 Fig 55.20	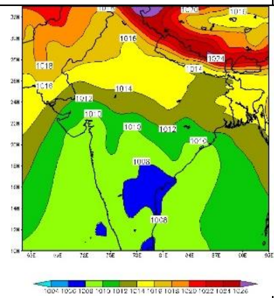 Fig 5.21	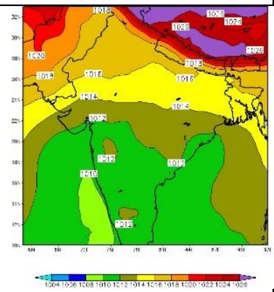 Fig 5.22	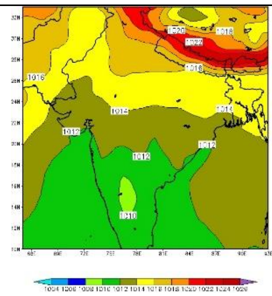 Fig 5.23	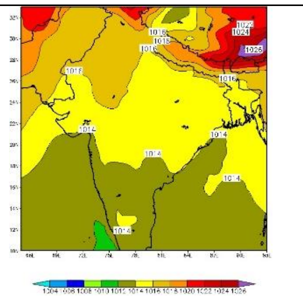 Fig 5.24	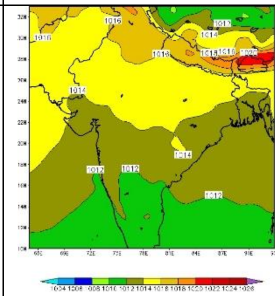 Fig 5.25	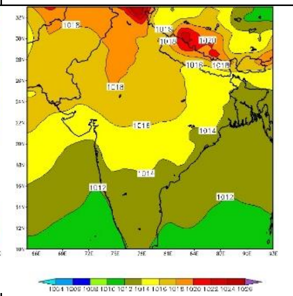 Fig 5.26	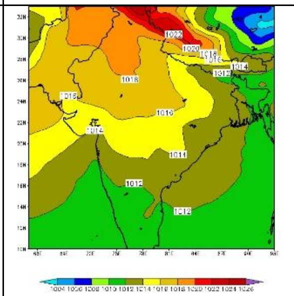 Fig 5.27	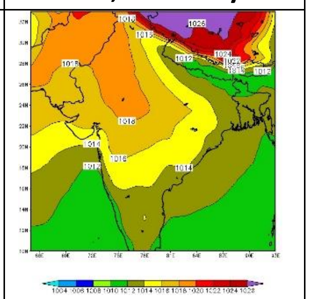 Fig 5.28
Wind and gptm at 850 hpa Unit: m/s and m	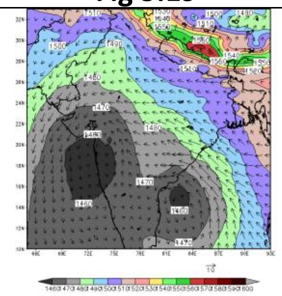 Fig 5.29	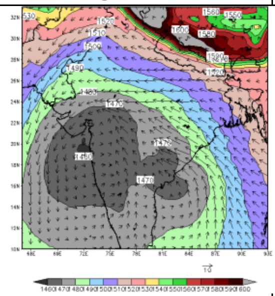 Fig 5.30	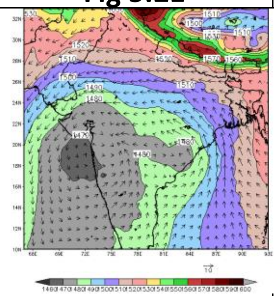 Fig 5.31	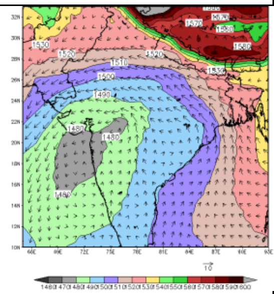 Fig 5.32	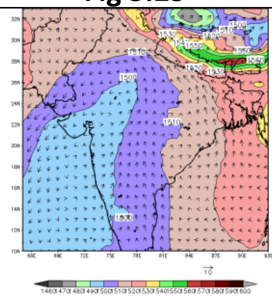 Fig 5.33	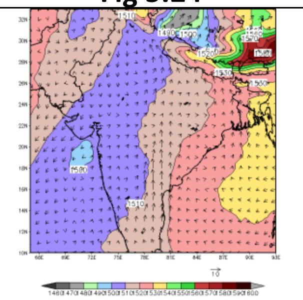 Fig 5.34	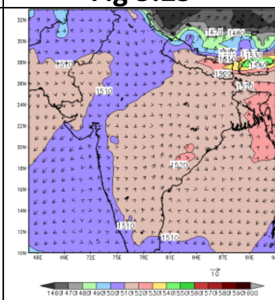 Fig 5.35	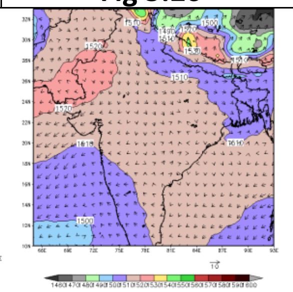 Fig 5.36	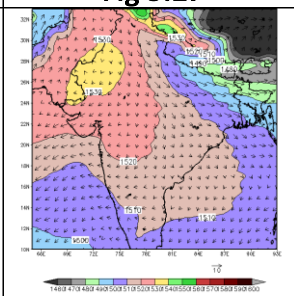 Fig 5.37	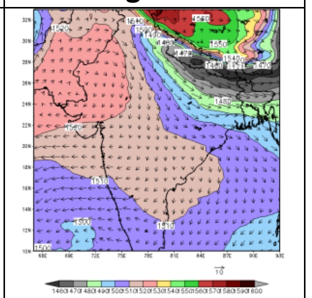 Fig 5.38

	12 UTC, 31 December	00 UTC, 1 January	12 UTC , 1 January	00 UTC, 2 January	12 UTC , 2 January	00 UTC, 3 January	12 UTC, 3 January	00 UTC, 4 January	12 UTC, 4 January	00 UTC, 5 January
Wind and gptm at 700 hpa **Unit: m/s and m** 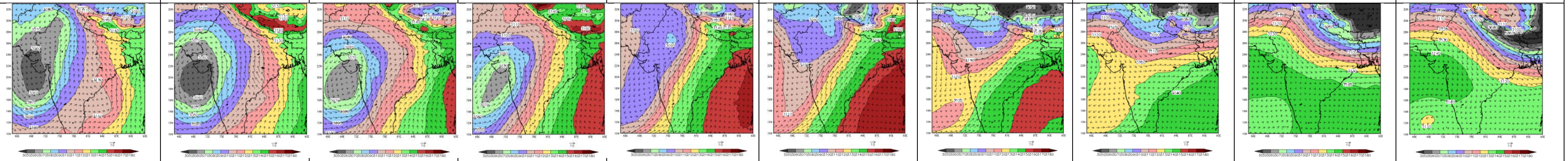	**Fig 5.39**	**Fig 5.40**	**Fig 5.41**	**Fig 5.42**	**Fig 5.43**	**Fig 5.44**	**Fig 5.45**	**Fig 5.46**	**Fig 5.47**	**Fig 5.48**
Wind and gptm at 500 hpa **Unit: m/s and m** 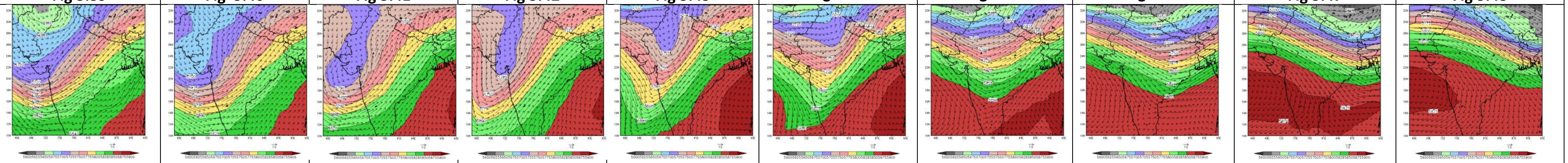	**Fig 5.49**	**Fig 5.50**	**Fig 5.51**	**Fig 5.52**	**Fig 5.53**	**Fig 5.54**	**Fig 5.55**	**Fig 5.56**	**Fig 5.57**	**Fig 5.58**
Wind and gptm at 300 hpa **Unit: m/s and m** 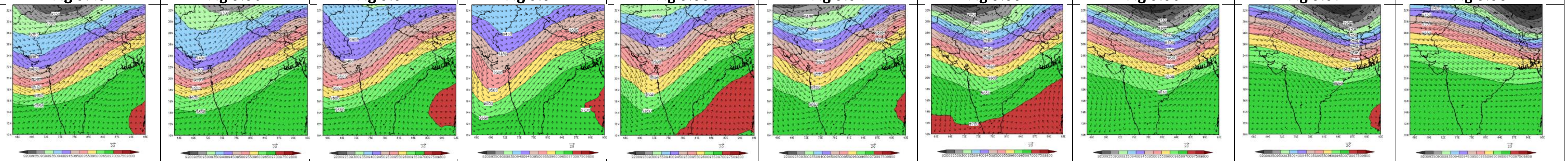	**Fig 5.59**	**Fig 5.60**	**Fig 5.61**	**Fig 5.62**	**Fig 5.63**	**Fig 5.64**	**Fig 5.65**	**Fig 5.66**	**Fig 5.67**	**Fig 5.68**
Relative Vorticity and streamline at 500 hpa **Unit: X10^{-5} s^{-1}** 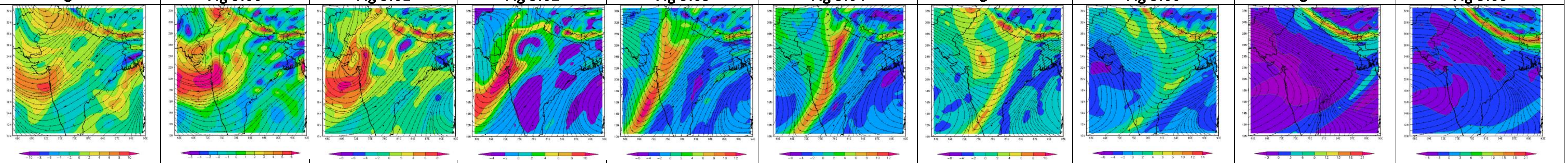	**Fig 5.69**	**Fig 5.70**	**Fig 5.71**	**Fig 5.72**	**Fig 5.73**	**Fig 5.74**	**Fig 5.75**	**Fig 5.76**	**Fig 5.77**	**Fig 5.78**
Relative humidity at 600 hpa **Unit: %** 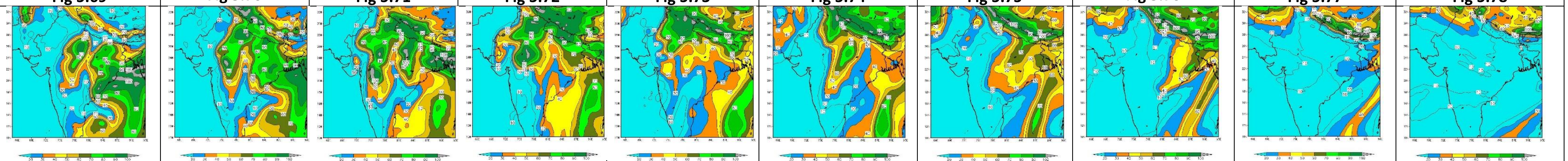	**Fig 5.79**	**Fig 5.80**	**Fig 5.81**	**Fig 5.83**	**Fig 5.84**	**Fig 5.85**	**Fig 5.86**	**Fig 5.87**	**Fig 5.88**	**Fig 5.89**

ANNEX 6: Charts used for the study of MWE 6 (25February-4 March)2015))

24 hour accumulated gauge rainfall ending at 03 UTC Unit: mm

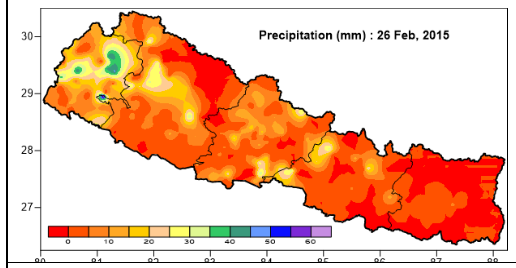

26 February Fig: 6.1

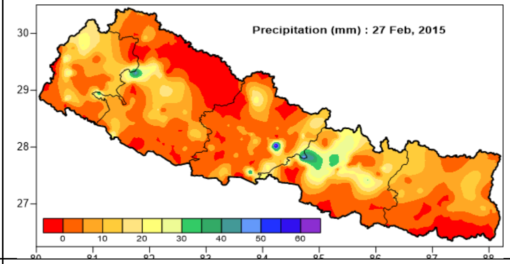

27 February Fig: 6.2

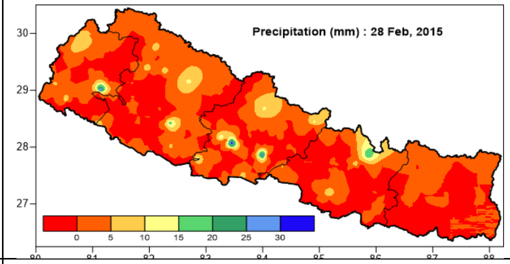

28 February Fig 6.3

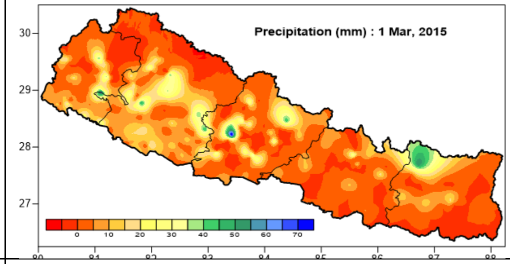

1 March Fig:6.4

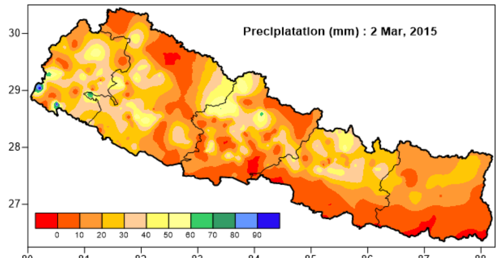

2 March Fig:6.5

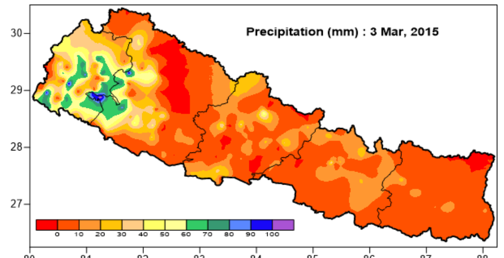

3 March Fig:6.6

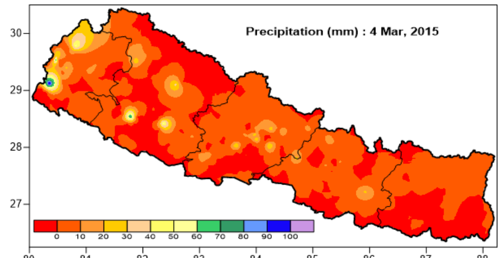

4 March Fig:6.7

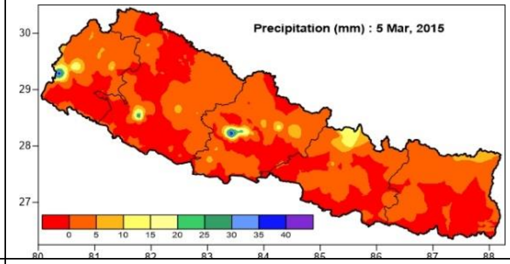

5 March Fig:6.8

24 hour accumulated estimated rainfall from GPM ending at 03 UTC Unit: mm

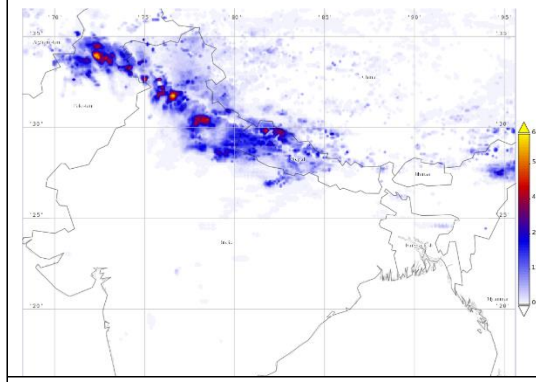
26 February Fig: 6.9

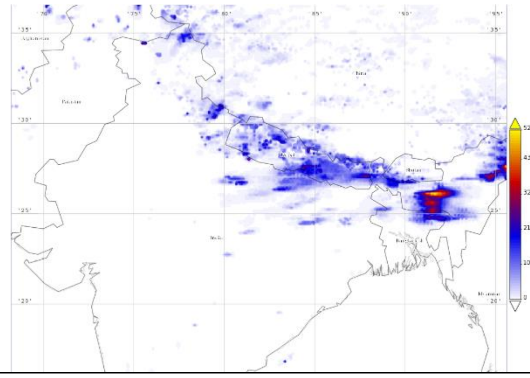
27 February Fig: 6.10

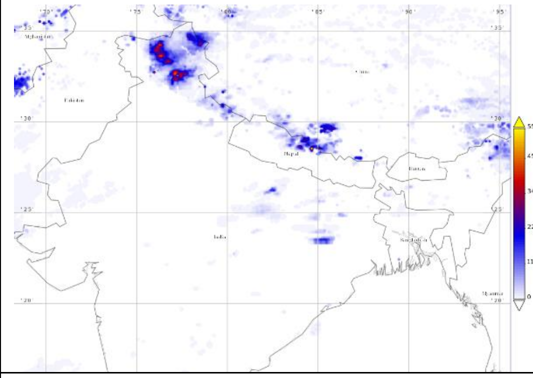
28 February Fig: 6.11

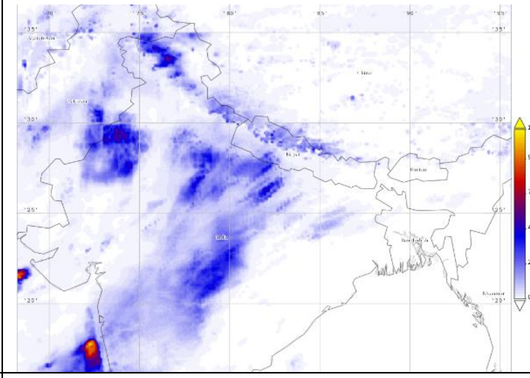
1 March Fig: 6.12

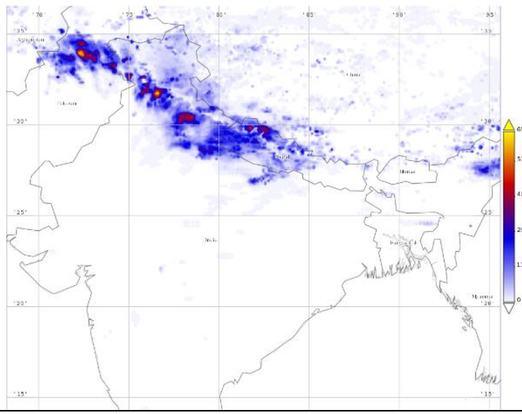
2 March Fig: 6.13

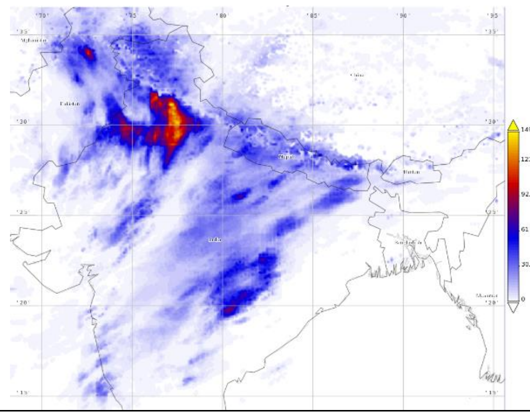
3 March Fig: 6.14

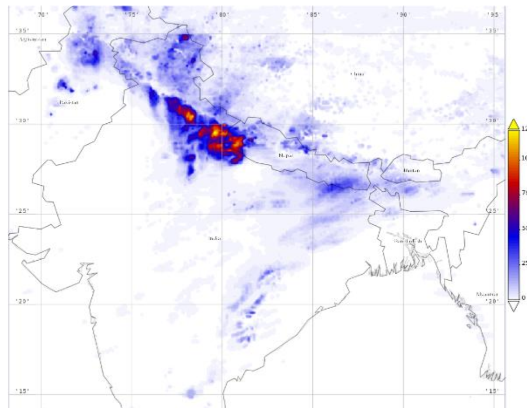
4 March Fig: 6.15

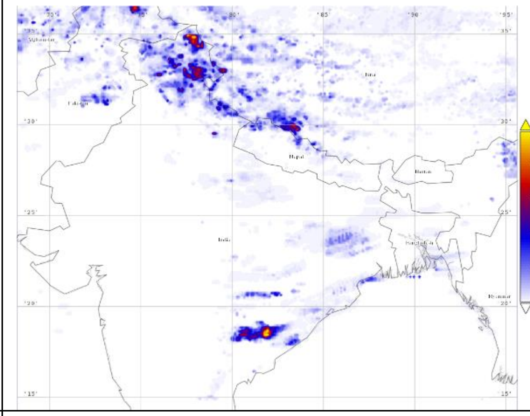
5 March Fig: 6.16

Infra-red Satellite imageries Unit: Unit less

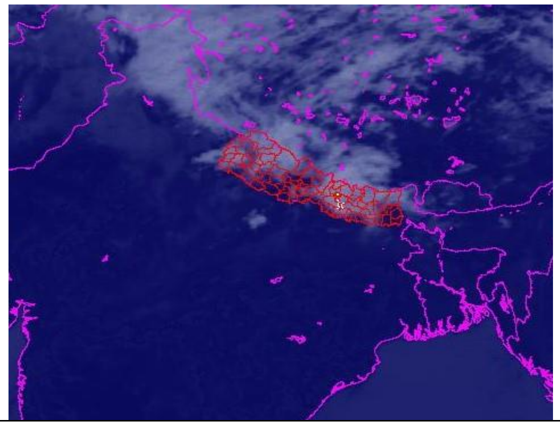
5:30 UTC, 26 February Fig: 6.17

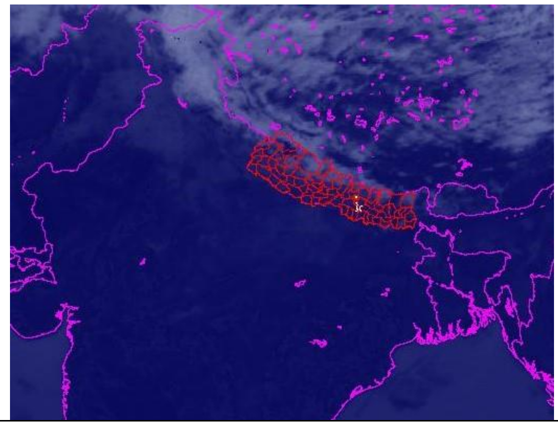
5:30 UTC,27 February Fig: 6.18

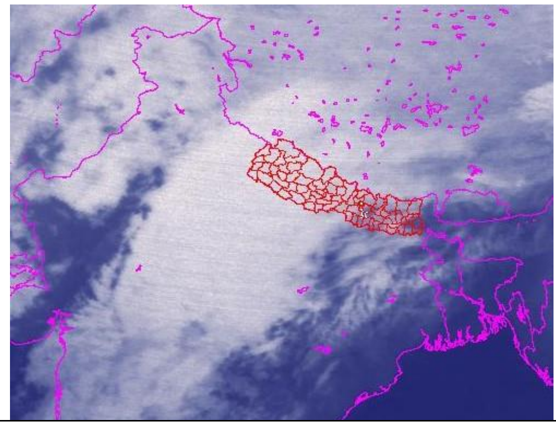
21:01 UTC, 28 February Fig: 6.19

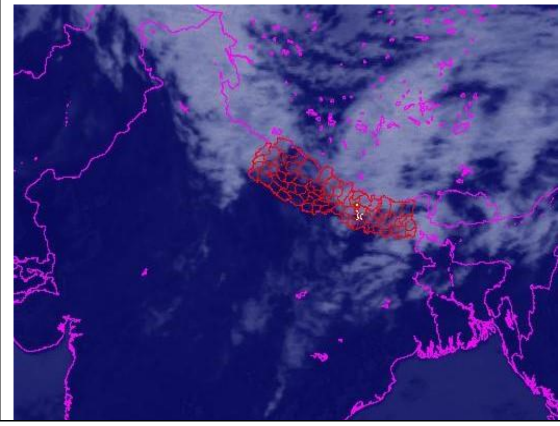
7:30 UTC, 2 March Fig: 6.20

MSLP

Unit: hpa

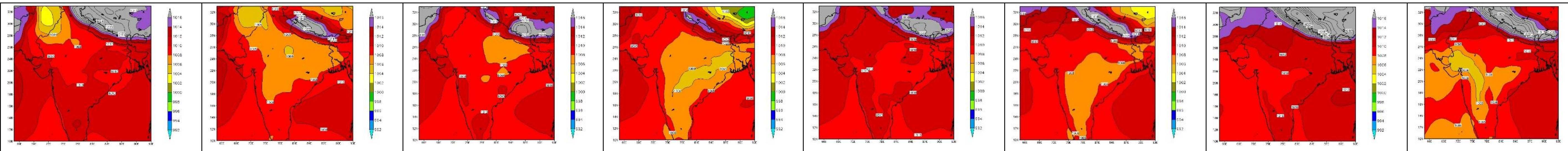

Fig 6.21 00 UTC,25 February | Fig 6.22 12 UTC ,25 February | Fig 6.23 00 UTC,26 February | Fig 6.24 12 UTC,26 February | Fig 6.25 00 UTC,27 February | Fig 6.26 12 UTC,27 February | Fig 6.27 00 UTC,28 February | Fig 6.28 12 UTC, 28 February

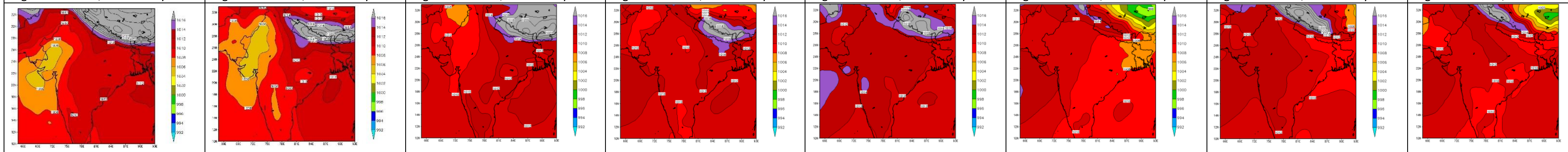

Fig 6.29 00 UTC,1 March | Fig 6.30 12 UTC,1 March | Fig 6.31 00 UTC,2 March | Fig 6.32 12 UTC,2 March | Fig 6.33 00 UTC,3 March | Fig 6.34 12 UTC,3 March | Fig 6.35 00 UTC,4 March | Fig 6.36 12 UTC ,4 March

Wind and gptm at 850 hpa

Unit: m/s and m

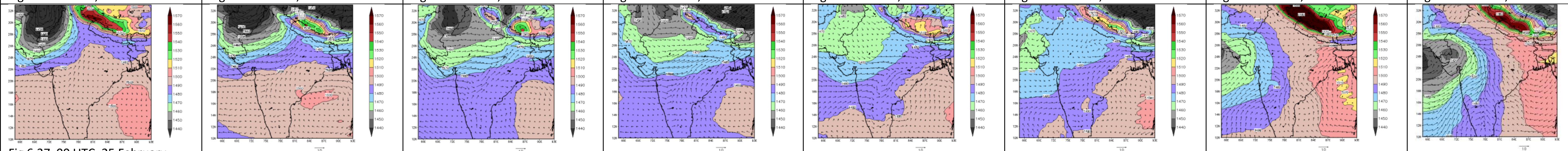

Fig 6.37 00 UTC ,25 February | Fig 6.38 12 UTC ,25 February | Fig 6.39 00 UTC 26 February | Fig 6.40 12 UTC , 26 February | Fig 6.41 00 UTC, 27 February | Fig 6.42 12 UTC, 27 February | Fig 6.43 00 UTC , 28 February | Fig 6.44 12 UTC , 28 February

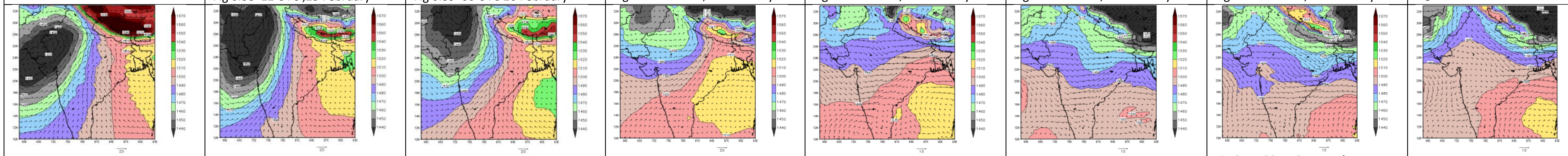

Fig 6.45 00 UTC,1 March | Fig 6.46 12 UTC,1 March | Fig 6.47 00 UTC,2 March | Fig 6.48 12 UTC,2 March | Fig 6.49 00 UTC,3 March | Fig 6.50 12 UTC,3 March | Fig 6.51 00 UTC,4 March | Fig 6.52 12 UTC,4 March

Wind and gptm at 700 hpa

Unit: m/s and m

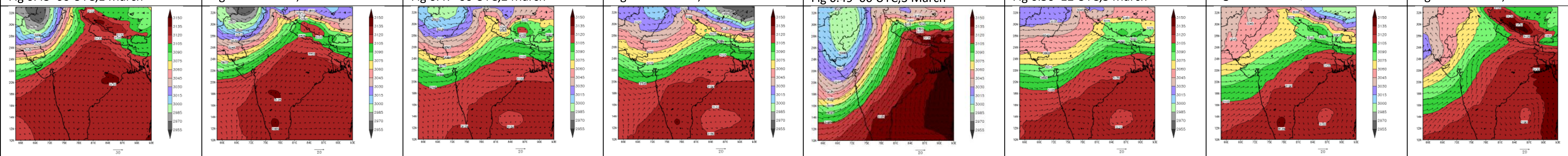

Fig 6.53 00 UTC, 25 February | Fig 6.54 12 UTC, 25 February | Fig 6.55 00 UTC, 26 February | Fig 6.56 12 UTC, 26 February | Fig 6.57 00 UTC, 27 February | Fig 6.58 12 UTC, 27 February | Fig 6.59 00 UTC, 28 February | Fig 6.60 12 UTC, 28 February

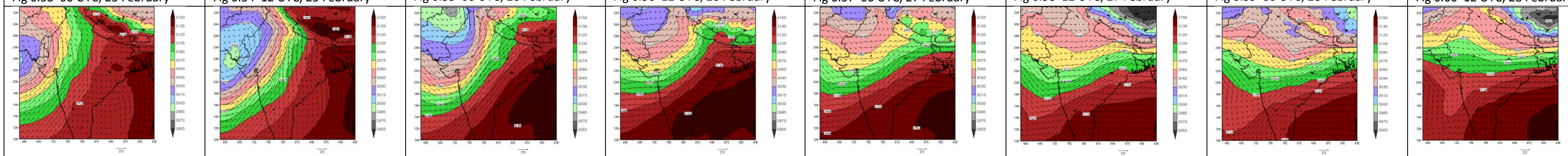

Fig 6.61 00 UTC,1 March | Fig 6.62 12 UTC,1 March | Fig 6.63 00 UTC,2 March | Fig 6.64 12 UTC,2 March | Fig 6.65 00 UTC,3 March | Fig 6.66 12 UTC,3 March | Fig 6.67 00 UTC,4 March | Fig 6.68 12 UTC,4 March

Wind and gptm at 500 hpa
Unit: m/s and m

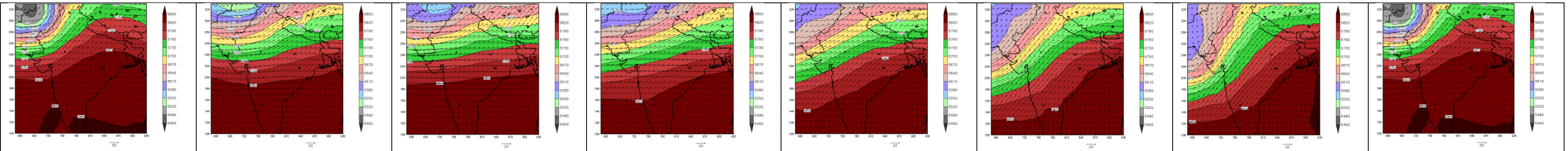

Fig 6.69 00 UTC, 25 February
Fig 6.70 12 UTC, 25 February
Fig 6.71 00 UTC, 26 February
Fig 6.72 12 UTC, 26 February
Fig 6.73 00 UTC, 27 February
Fig 6.74 12 UTC, 27 February
Fig 6.75 00 UTC, 28 February
Fig 6.76 12 UTC, 28 February

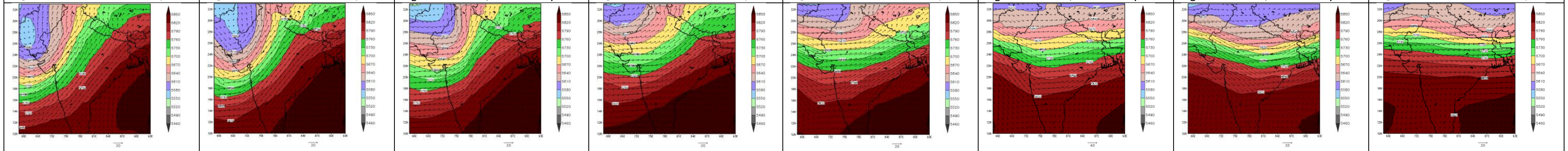

Fig 6.77 00 UTC,1 March
Fig 6.78 12 UTC,1 March
Fig 6.79 00 UTC,2 March
Fig 6.80 12 UTC,2 March
Fig 6.81 00 UTC,3 March
Fig 6.82 12 UTC,3 March
Fig 6.83 00 UTC,4 March
Fig 6.84 12 UTC,4 March

Wind and gptm at 300 hpa
Unit: m/s and m

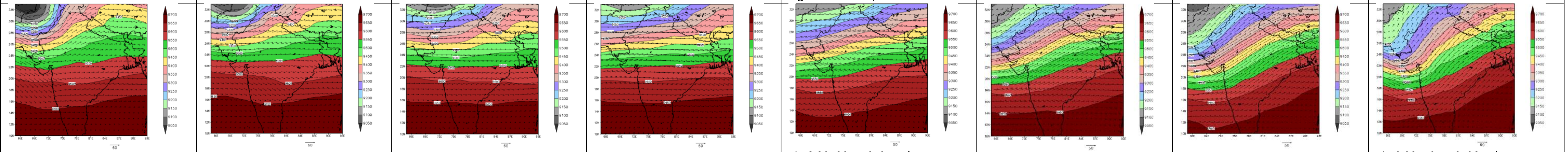

Fig 6.85 00 UTC, 25 February
Fig 6.86 12 UTC, 25 February
Fig 6.87 00 UTC, 26 February
Fig 6.88 12 UTC, 26 February
Fig 6.89 00 UTC, 27 February
Fig 6.90 12 UTC, 27 February
Fig 6.91 00 UTC, 28 February
Fig 6.92 12 UTC, 28 February

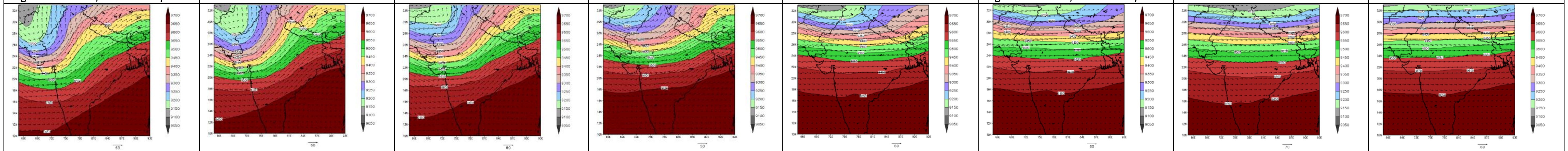

Fig 6.93 00 UTC, 1 March
Fig 6.94 12 UTC, 1 March
Fig 6.95 00 UTC, 2 March
Fig 6.96 12 UTC, 2 March
Fig 6.97 00 UTC,3 March
Fig 6.98 12 UTC,3 March
Fig 6.99 00 UTC,4 March
Fig 6.100 12 UTC,4 March

Relative Vorticity at 300 hpa
Unit: X10^{-5}s^{-1}

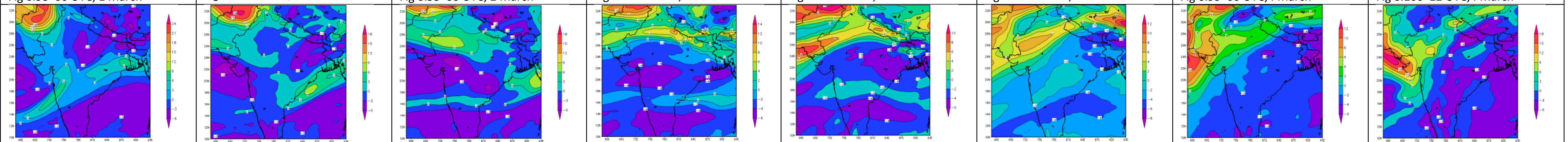

Fig 6.101 00 UTC, 25 February
Fig 6.102 12 UTC,25 February
Fig 6.103 00 UTC,26 February
Fig 6.104 12 UTC,26 February
Fig 6.105 00 UTC,27 February
Fig 6.106 12 UTC,27 February
Fig 6.107 00 UTC,28 February
Fig 6.108 12 UTC,28 February

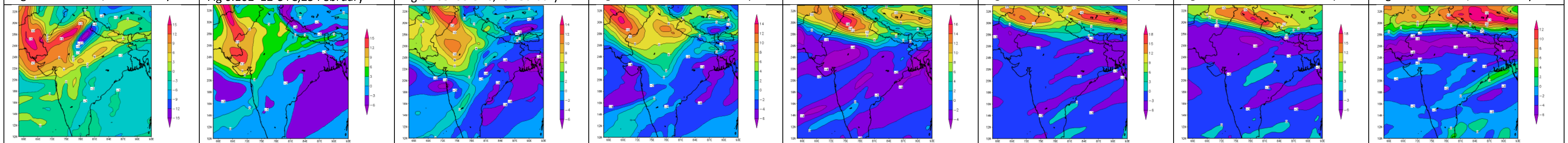

Fig 6.109 00 UTC, 1 March
Fig 6.110 12 UTC, 1 March
Fig 6.111 00 UTC, 2 March
Fig 6.112 12 UTC, 2 March
Fig 6.113 00 UTC, 3 March
Fig 6.114 12 UTC, 3 March
Fig 6.115 00 UTC , 4 March
Fig 6.116 12 UTC, 4 March

Relative humidity at 600 hpa **Unit: %**	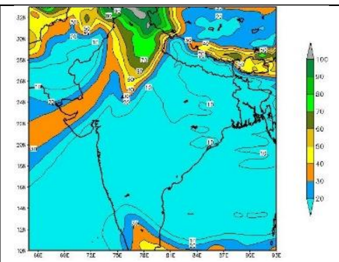 Fig 6.117 00 UTC,25 February	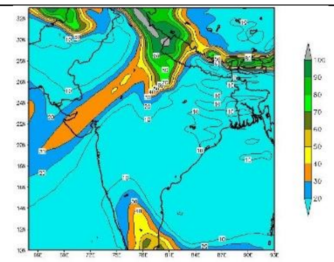 Fig 6.118 12 UTC,25 February	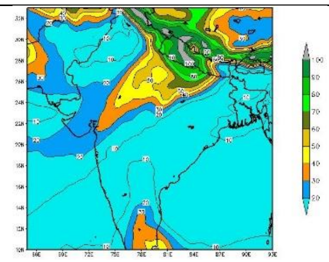 Fig 6.119 00 UTC,26 February	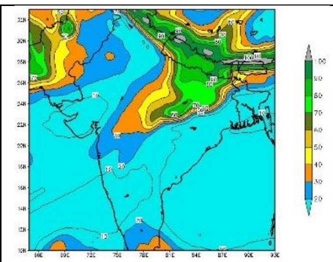 Fig 6.120 12 UTC,26 February	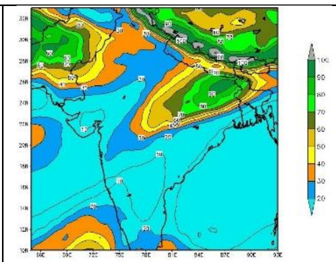 Fig 6.121 00 UTC,27 February	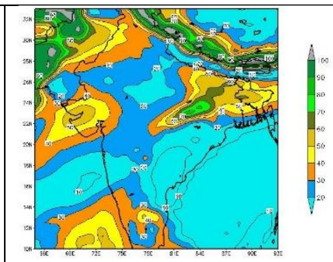 Fig 6.122 12 UTC,27 February	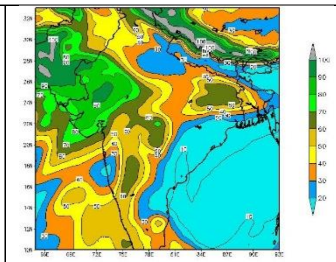 Fig 6.123 00 UTC,28 February	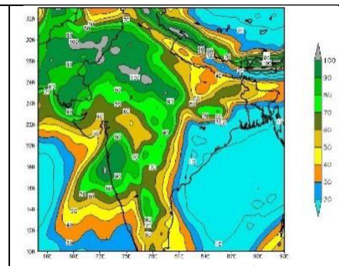 Fig 6.124 12 UTC,28 February
	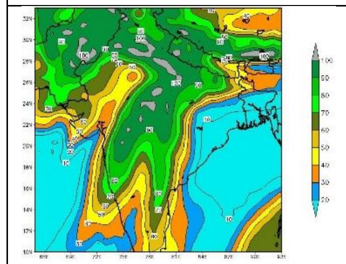 Fig 6.125 00 UTC, 1 March	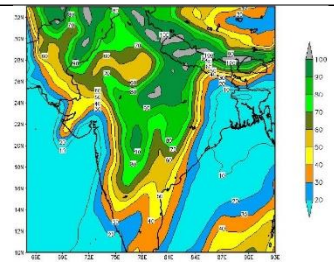 Fig 6.126 12 UTC, 1 March	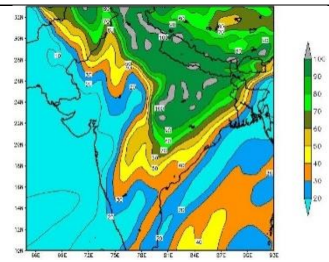 Fig 6.127 00 UTC, 2 March	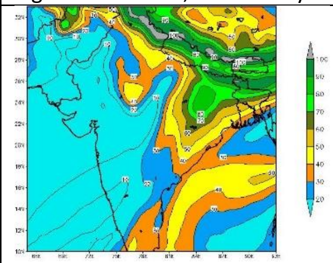 Fig 6.128 12 UTC, 2 March	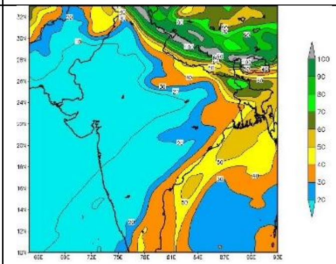 Fig 6.129 00 UTC, 3 March	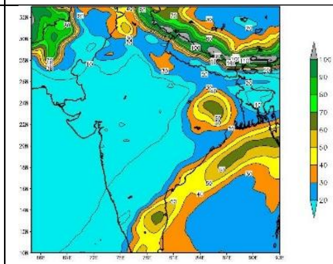 Fig 6.130 12 UTC, 3 March	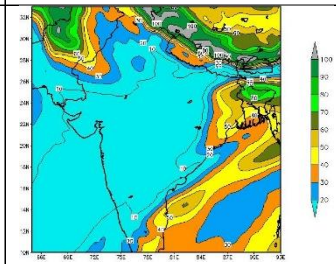 Fig 6.131 00 UTC, 4 March	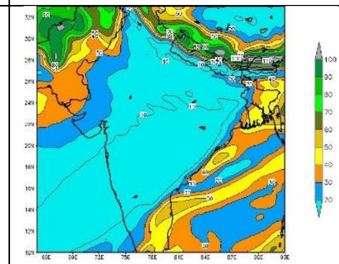 Fig 6.132 12 UTC, 1 March

Annex 7: Charts used for the study of MWE 7 (29 March-01 April 2015)

24 hour accumulated gauge rainfall ending at 03 UTC **Unit: mm**	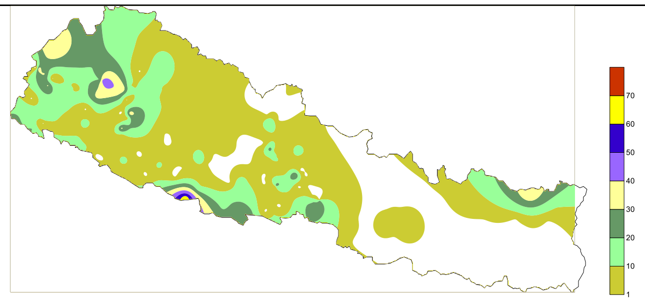 Fig 7.1 30 March	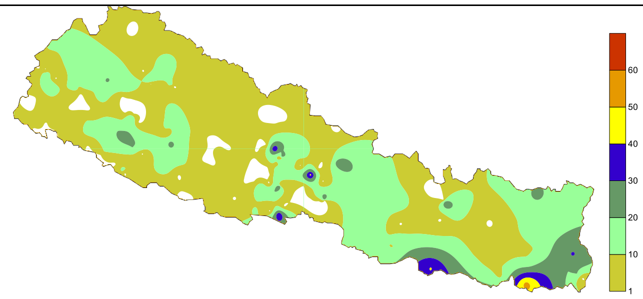 Fig 7.2 31 March	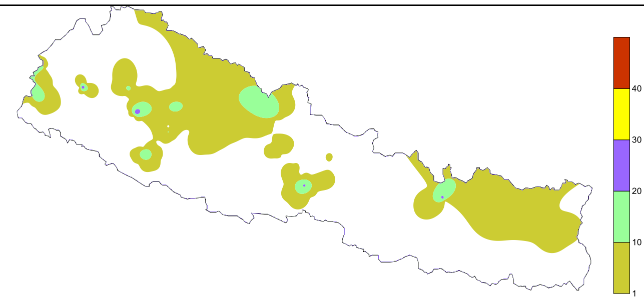 Fig 7.3 01 April	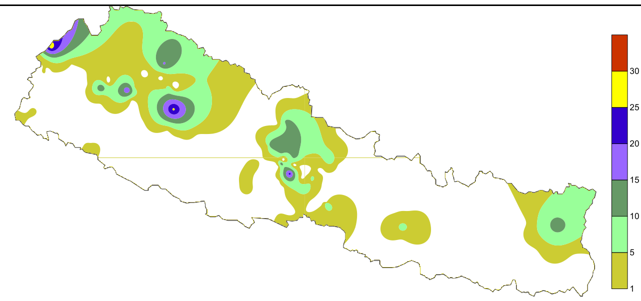 Fig 7.4 02 April
24 hour accumulated estimated rainfall from GPM ending at 03 UTC **Unit: mm**	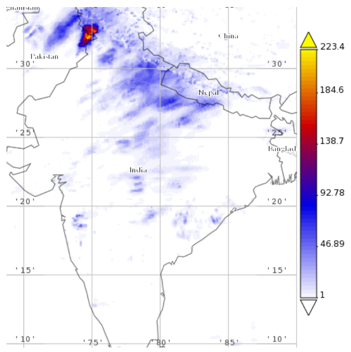 Fig 7.5 30 March	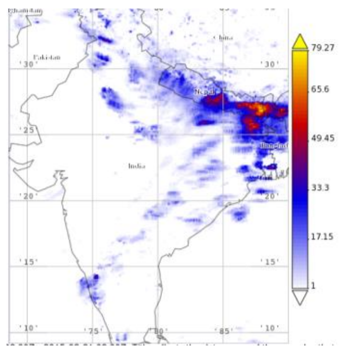 Fig 7.6 31 March	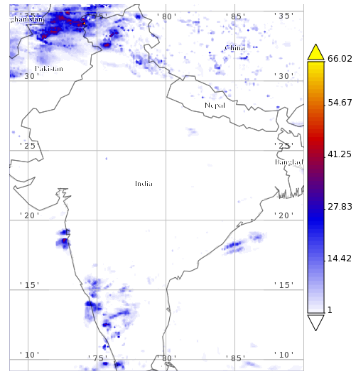 Fig 7.7 01 April	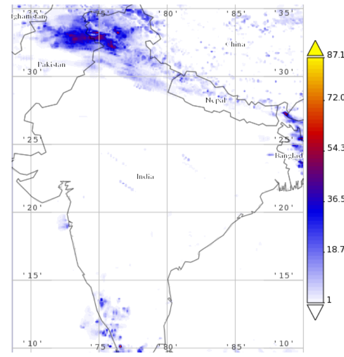 Fig 7.8 02 April
IR Satellite images **Unit:** **unit less**	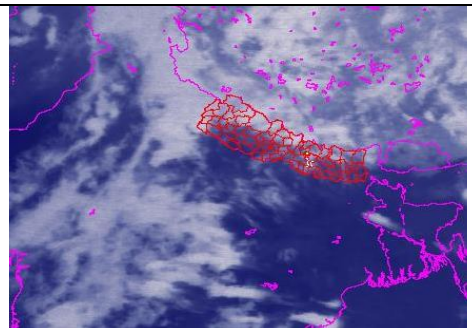 Fig 7.9 12.46 UTC, 29 March	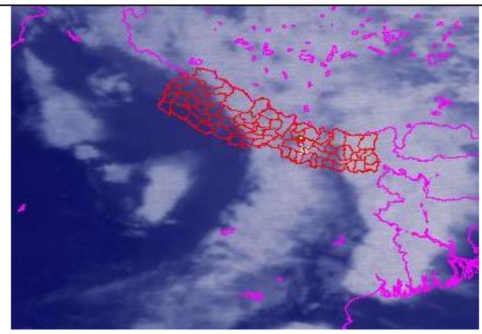 Fig 7.10 11.46 UTC, 30 March	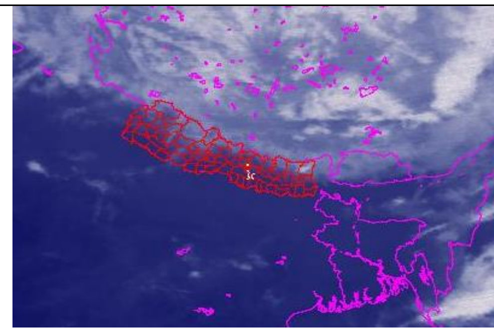 Fig 7.11 12.46 UTC, 31 March	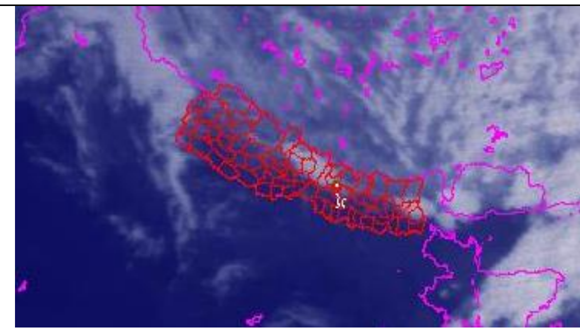 Fig 7.12 11.46 UTC, 01 April

	00 UTC, 29 March	12 UTC, 29 March	00 UTC, 30 March	12 UTC, 30 March	00 UTC, 31 March	12 UTC, 31 March	00 UTC, 01 April	12 UTC, 01 April
MSLP **Unit: hpa**	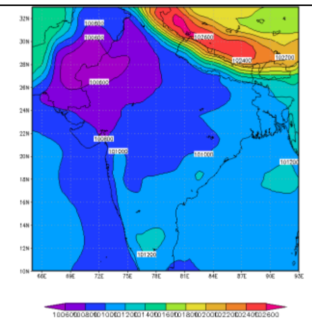 Fig 7.13	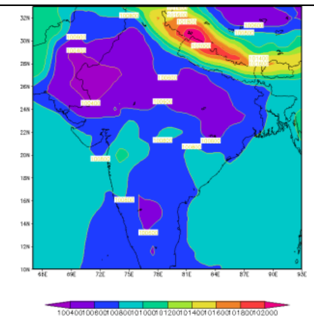 Fig 7.14	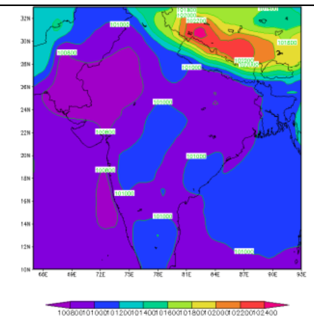 Fig 7.15	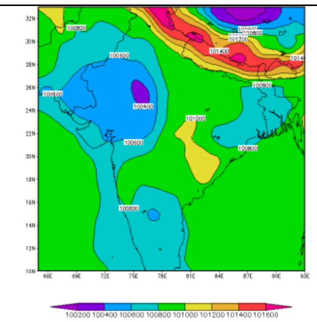 Fig 7.16	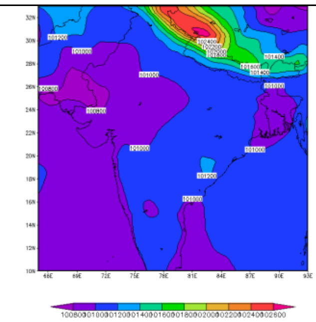 Fig 7.17	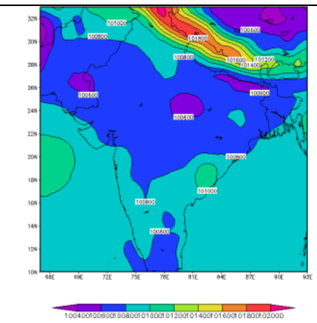 Fig 7.18	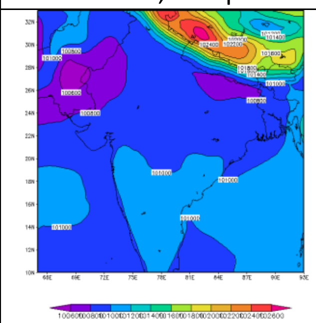 Fig 7.19	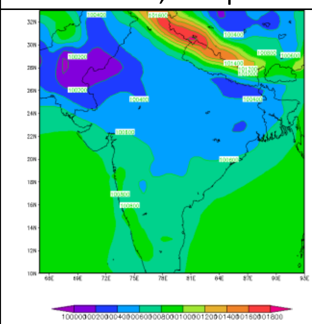 Fig 7.20
Wind and gptm at 850 hpa **Unit: m/s and m**	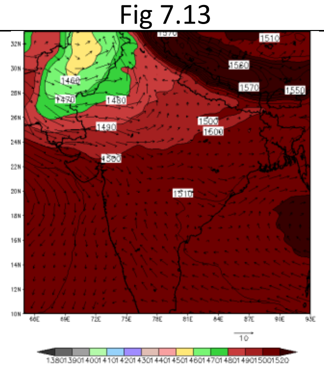 Fig 7.21	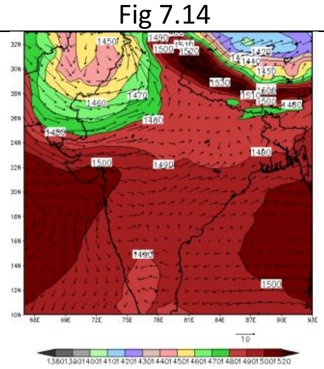 Fig 7.22	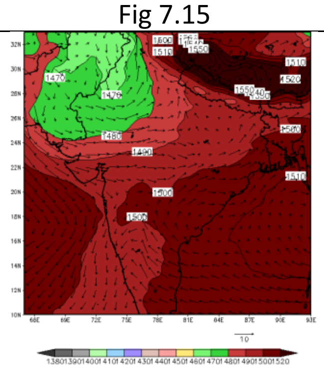 Fig 7.23	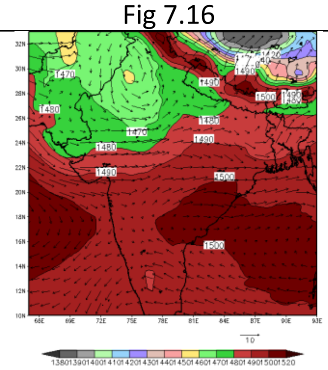 Fig 7.24	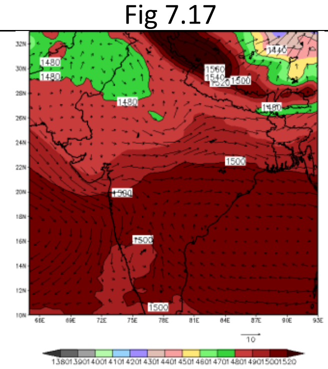 Fig 7.25	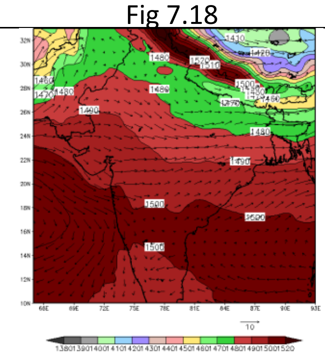 Fig 7.26	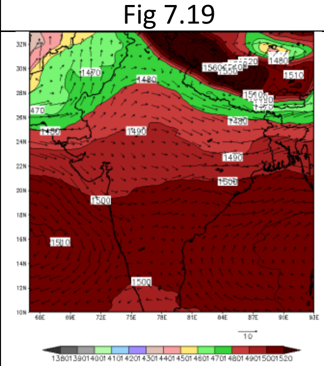 Fig 7.27	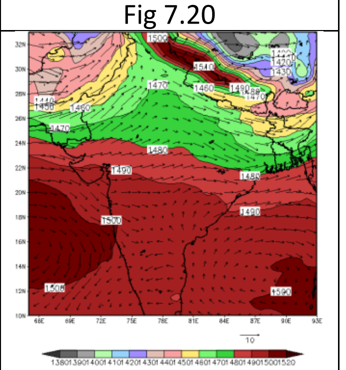 Fig 7.28

	00 UTC, 29 March	12 UTC, 29 March	00 UTC, 30 March	12 UTC, 30 March	00 UTC, 31 March	12 UTC,31 March	00 UTC, 01 April	12 UTC,01 April
Wind and gptm at 700 hpa **Unit: m/s and m**	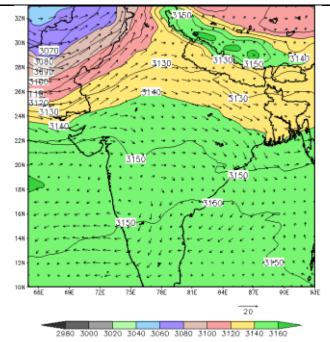 Fig 7.29	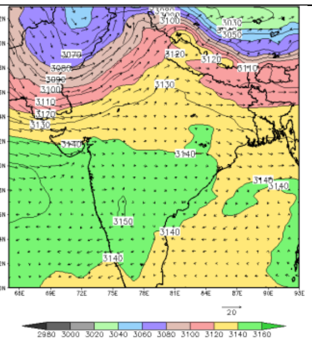 Fig 7.30	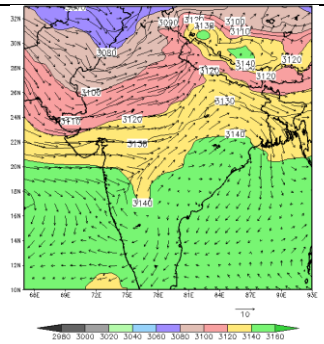 Fig 7.31	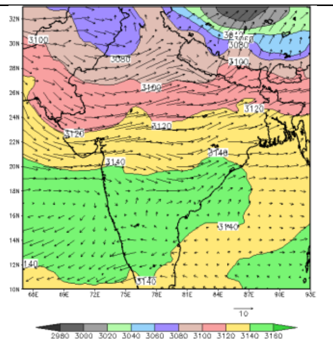 Fig 7.32	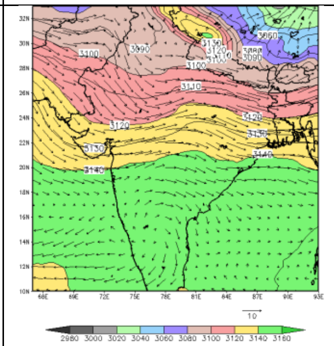 Fig 7.33	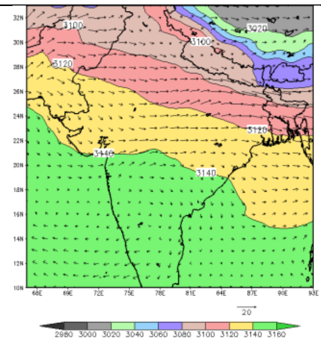 Fig 7.34	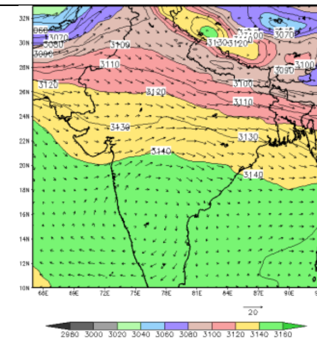 Fig 7.35	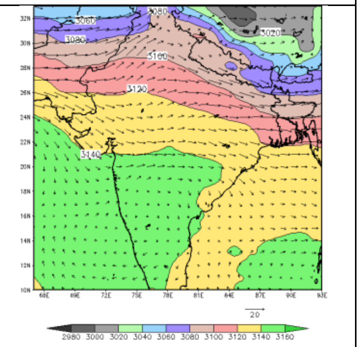 Fig 7.36
Wind and gptm at 500 hpa **Unit: m/s and m**	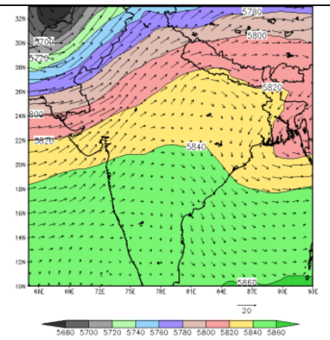 Fig 7.37	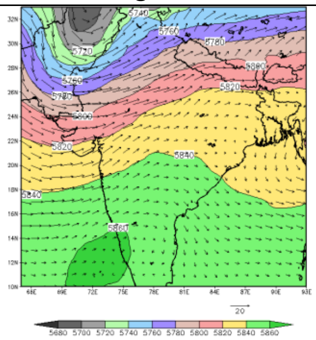 Fig 7.38	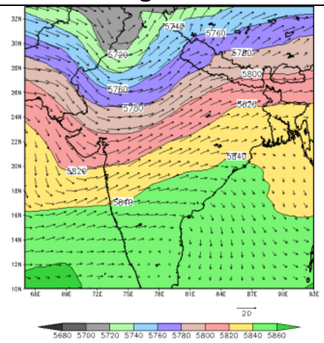 Fig 7.39	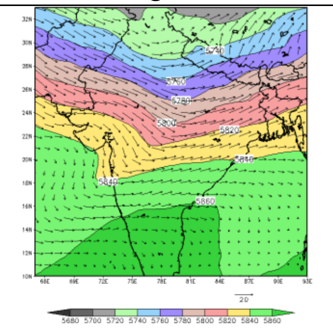 Fig 7.40	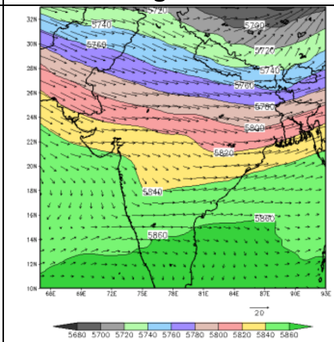 Fig 7.41	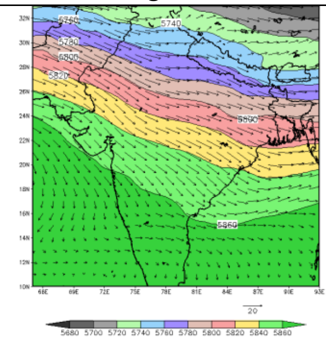 Fig 7.42	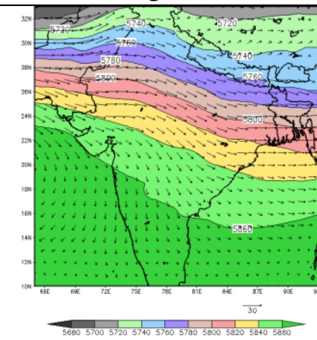 Fig 7.43	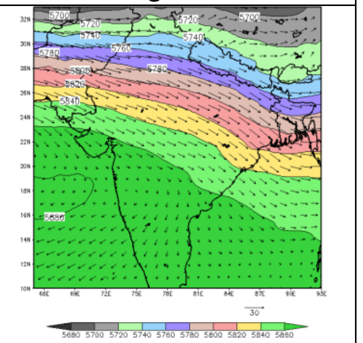 Fig 7.44
Wind and gptm at 300 hpa **Unit: m/s and m**	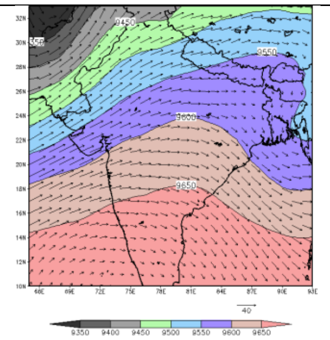 Fig 7.45	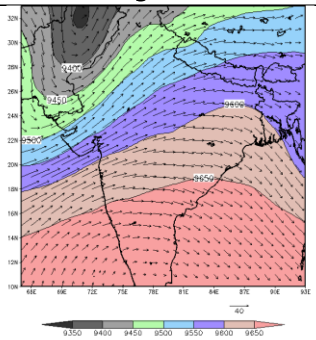 Fig 7.46	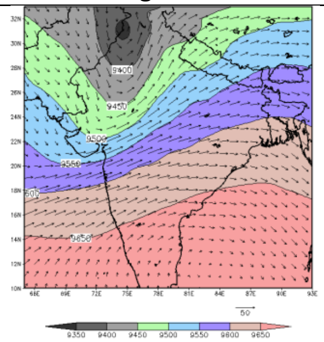 Fig 7.47	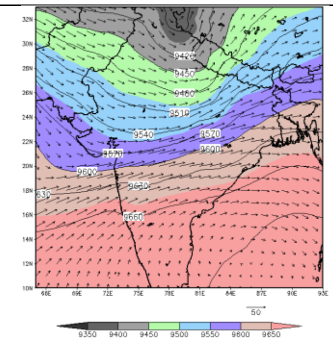 Fig 7.48	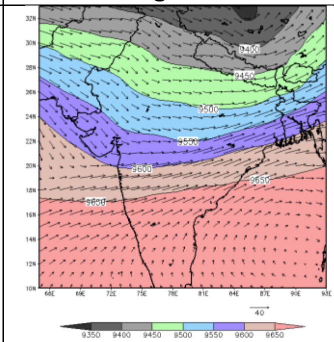 Fig 7.49	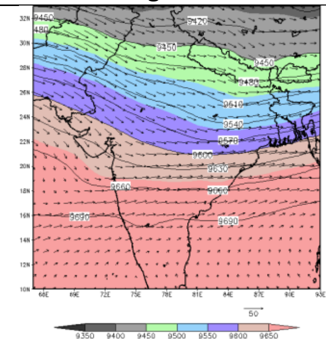 Fig 7.50	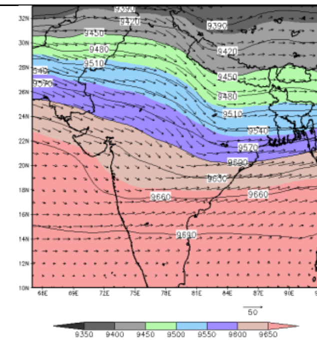 Fig 7.51	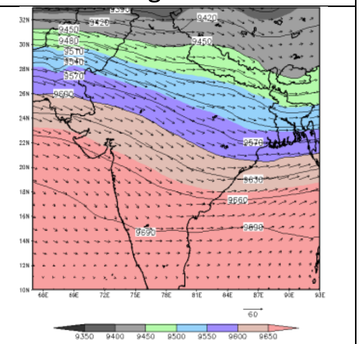 Fig 7.52
Relative Vorticity at 500 hpa **Unit:s^{-1}**	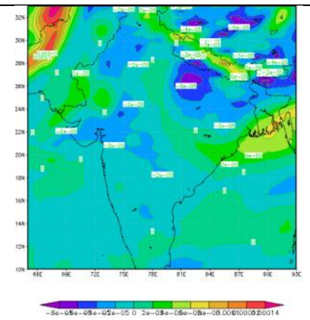 Fig 7.53	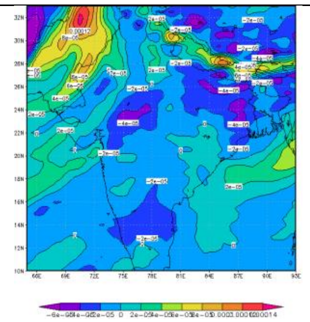 Fig 7.54	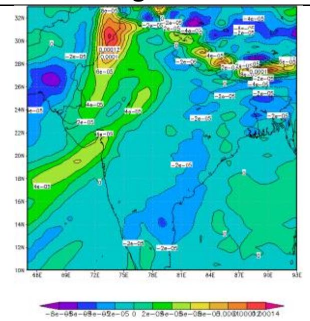 Fig 7.55	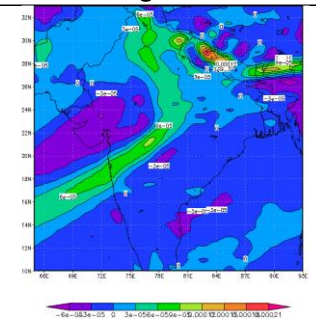 Fig 7.56	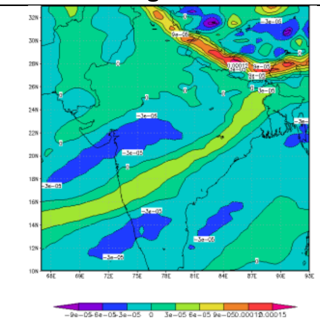 Fig 7.57	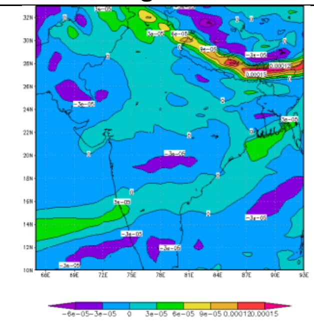 Fig 7. 58	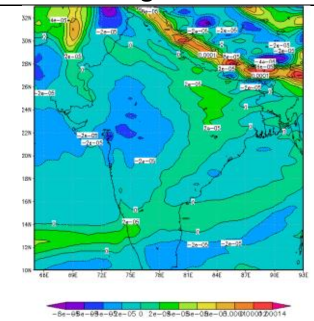 Fig 7.59	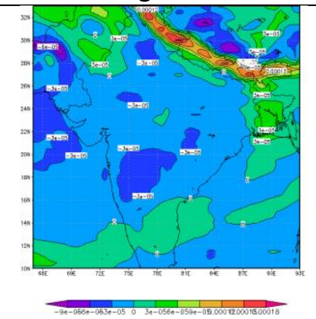 Fig 7.60
Relative Humidity at 600 hpa **Unit: %**	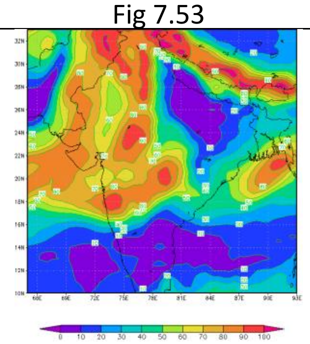 Fig 7.61	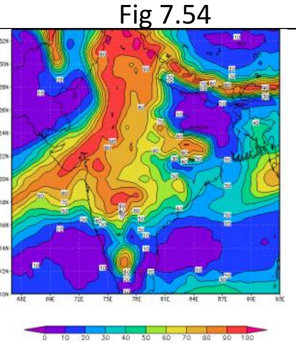 Fig 7.62	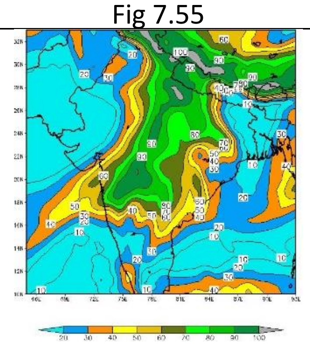 Fig 7.63	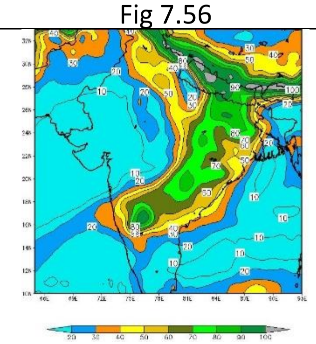 Fig 7.64	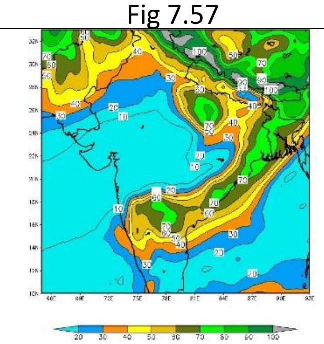 Fig 7.65	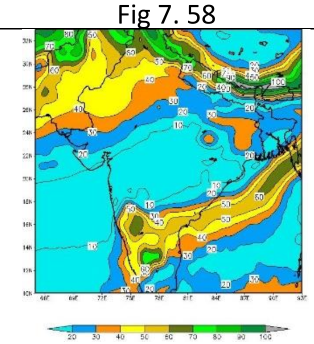 Fig 7.66	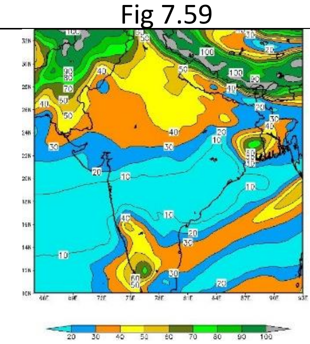 Fig 7.67	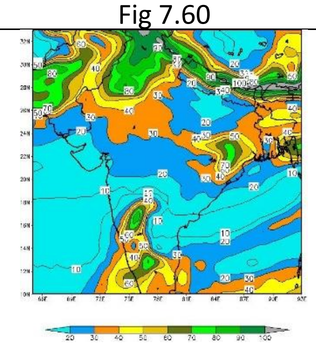 Fig 7.68

ANNEX 8: Charts used for the study of MWE 8 (10-13) May 2015)

24 hour accumulated gauge rainfall ending at 03 UTC Unit: mm	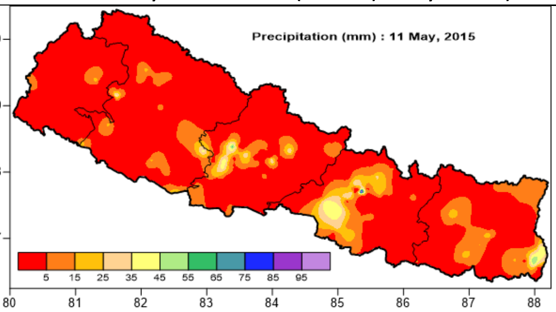 Fig 8.1 11 May	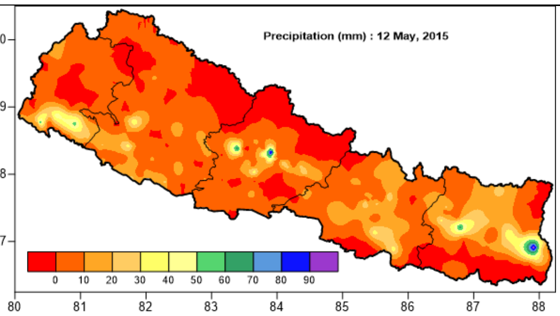 Fig 8.2 12 May	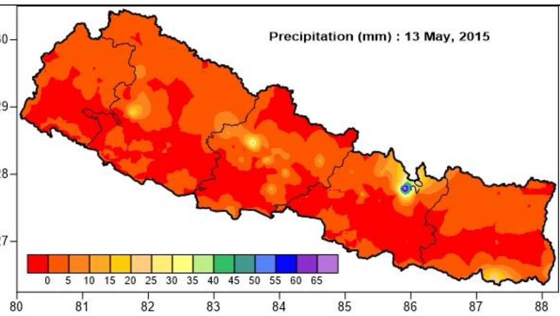 Fig 8.3 13 May	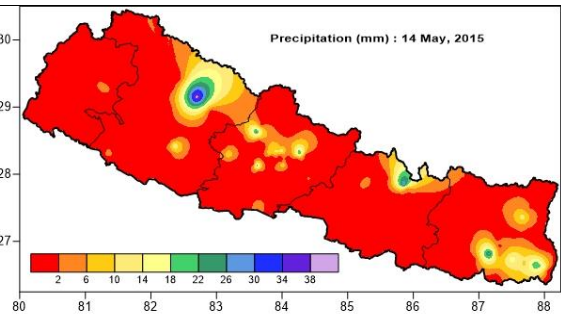 Fig 8.4 14 May
24 hour accumulated estimated rainfall from GPM ending at 03 UTC Unit: mm	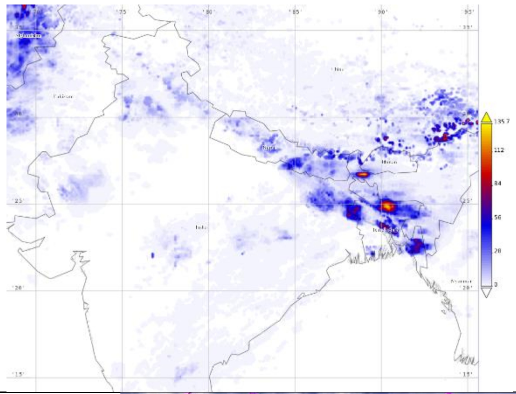 11 May Fig 8.5	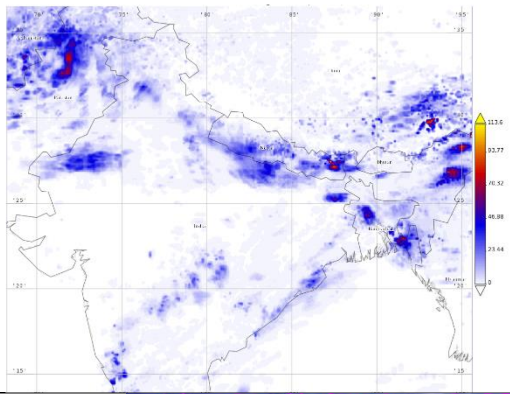 12 May Fig 8.6	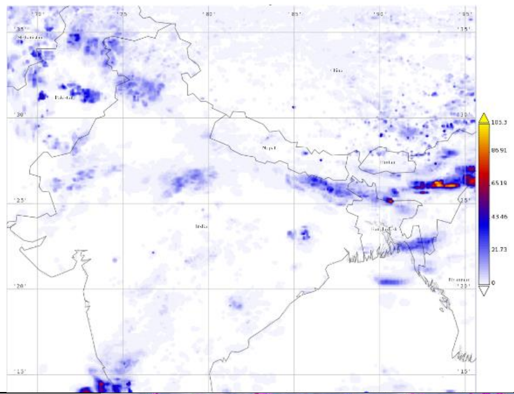 13 May Fig 8.7	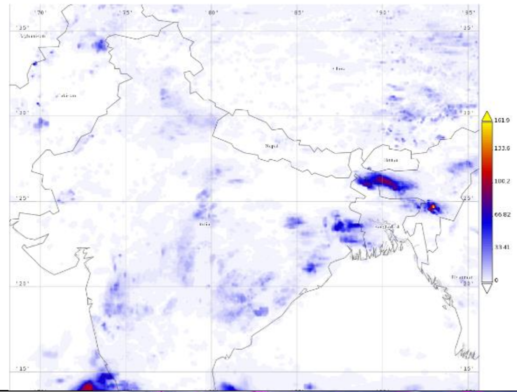 14 May Fig 8.8
Infra-red Satellite imageries Unit: Unit less	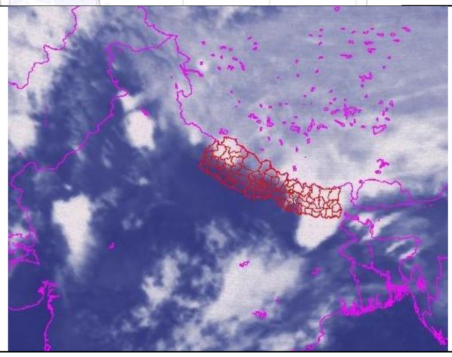 Fig 8.9 20:31 UTC,10 May	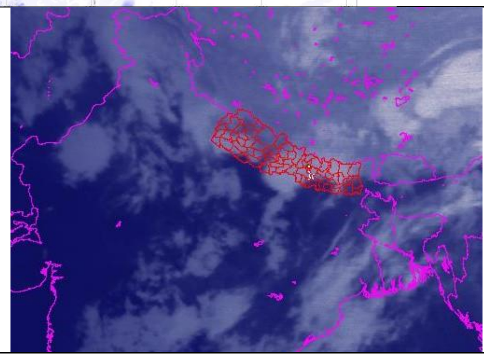 Fig 8.10 17:31UTC ,11 May	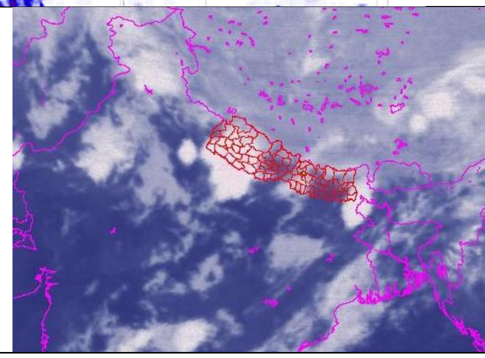 Fig 8.11 ,20:31Z 11 May	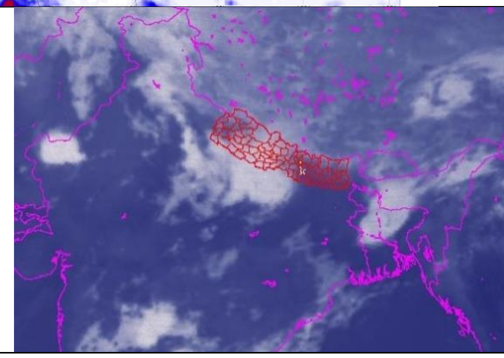 Fig 8.12 00:30UTC,12 May
CAPE values at 09 UTC Unit: J/kg	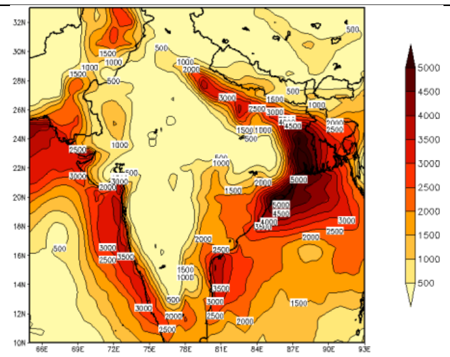 Fig 8.13 10 May	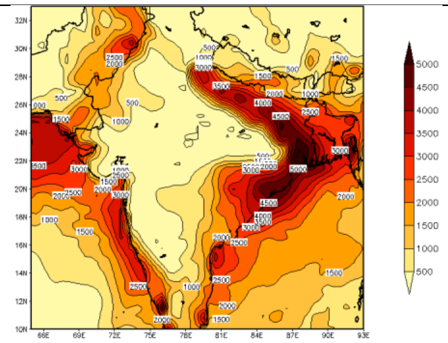 Fig 8.14 11 May	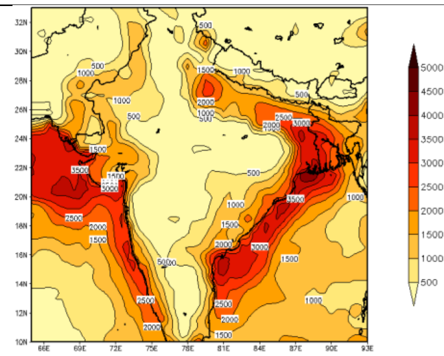 Fig 8.15 12 May	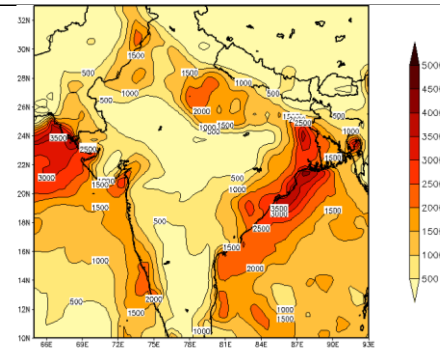 Fig 8.16 13 May
	00 UTC, 10 May / 12 UTC, 10 May	00 UTC,11 May / 12 UTC , 11 May	00 UTC, 12 May / 12 UTC, 12 May	00 UTC, 13 May / 12 UTC, 13 May
MSLP Unit: hpa	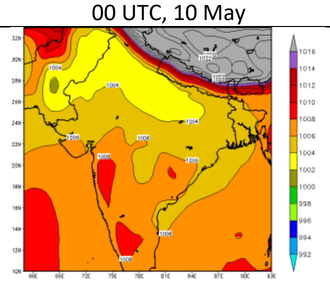 Fig 8.17 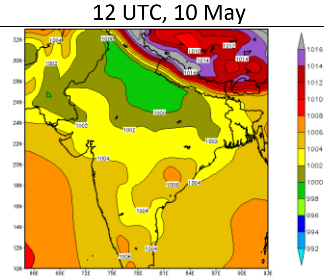 Fig 8.18	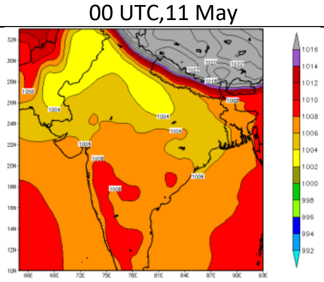 Fig 8.19 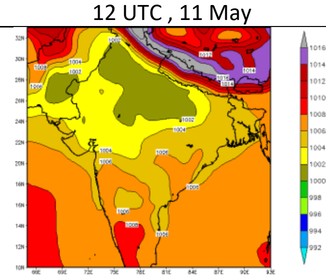 Fig 8.20	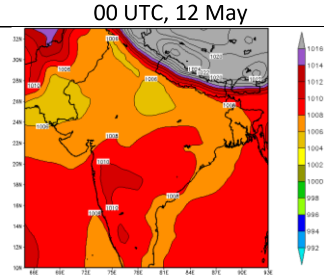 Fig 8.21 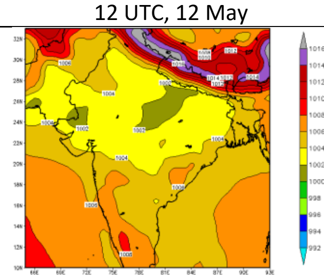 Fig 8.22	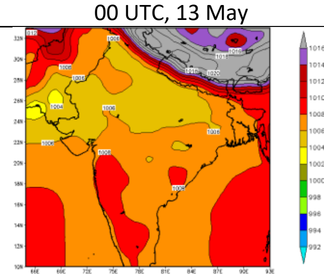 Fig 8.23 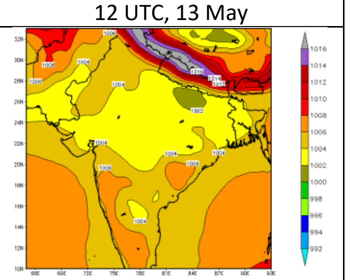 Fig 8.24

	00 UTC, 10 May	12 UTC, 10 May	00 UTC,11 May	12 UTC , 11 May	00 UTC, 12 May	12 UTC, 12 May	00 UTC, 13 May	12 UTC, 13 May
Wind and gptm at 850 hpa **Unit: m/s and m**	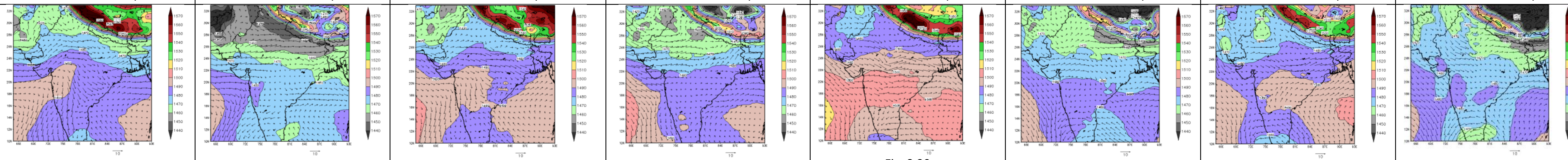 Fig 8.25	Fig 8.26	Fig 8.27	Fig 8.28	Fig 8.29	Fig 8.30	Fig 8.31	Fig 8.32
Wind and gptm at 700 hpa **Unit: m/s and m**	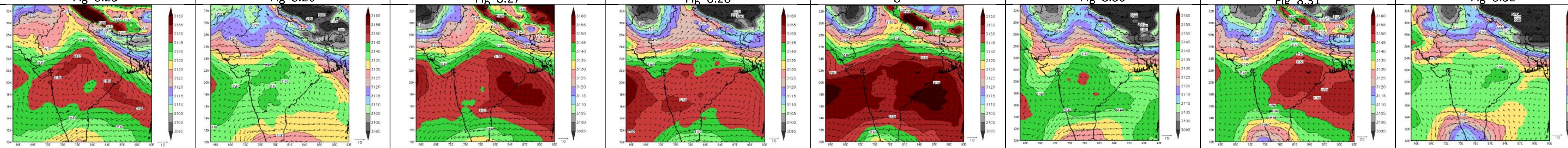 Fig 8.33	Fig 8.34	Fig 8.35	Fig 8.36	Fig 8.37	Fig 8.38	Fig 8.39	Fig 8.40
Wind and gptm at 500 hpa **Unit: m/s and m**	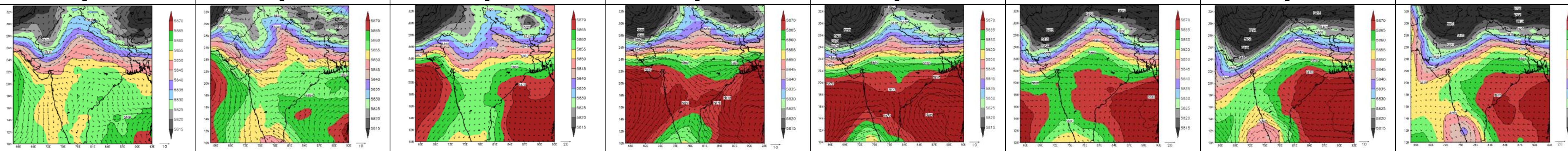 Fig 8.41	Fig 8.42	Fig 8.43	Fig 8.44	Fig 8.45	Fig 8.46	Fig 8.47	Fig 8.48
Wind and gptm at 300 hpa **Unit: m/s and m**	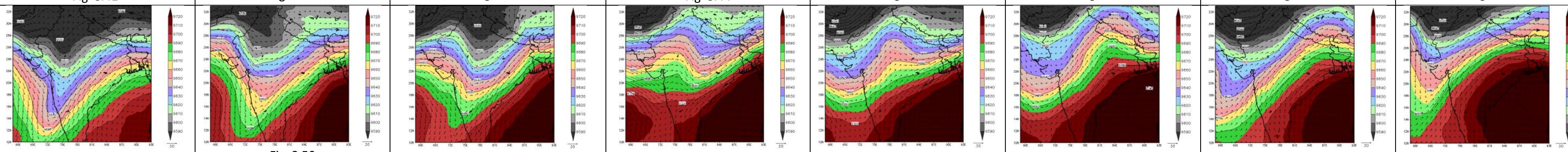 Fig 8.59	Fig 8.50	Fig 8.51	Fig 8.52	Fig 8.53	Fig 8.54	Fig 8.55	Fig 8.56
Relative Vorticity at 500 hpa **Unit: X10^{-5} s^{-1}**	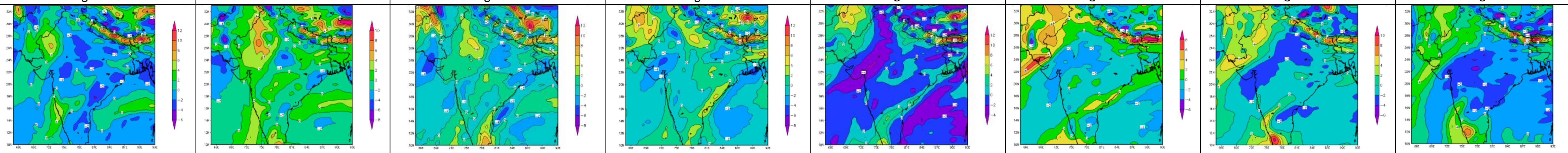 Fig 8.57	Fig 8.58	Fig 8.59	Fig 8.60	Fig 8.61	Fig 8.62	Fig 8.63	Fig 8.64
Relative humidity at 600 hpa **Unit: %**	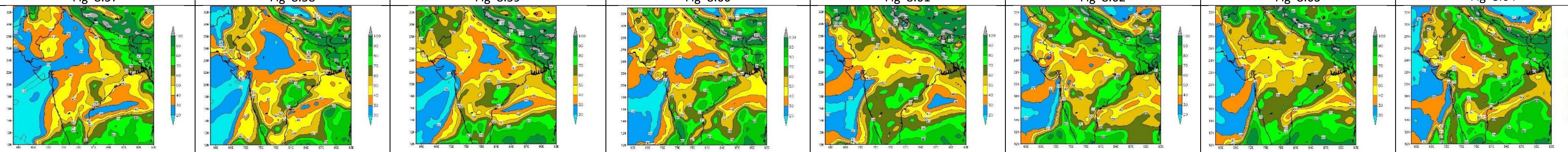 Fig: 8.65	Fig: 8.66	Fig: 8.67	Fig: 8.68	Fig: 8.69	Fig: 8.70	Fig: 8.71	Fig: 8.72